CAPITAL UNIVERSITY OF SCIENCE AND TECHNOLOGY, ISLAMABAD

Effect of Inclined Magnetic Field and Higher Order Chemical Reaction on Stagnation Point Nanofluid Flow

by

Saba Jabeen

A thesis submitted in partial fulfillment for the degree of Master of Philosophy

in the

Faculty of Computing
Department of Mathematics

2020

DEDICATION

All dedications in the memory of my dearest father

Muhammad Azram (Late)

(May Allah gives him higher place in jannah. Aameen)

who always believed in me to be successful whatever the situation and his well wishes will remain with me throughout my life.

CERTIFICATE OF APPROVAL

Effect of Inclined Magnetic Field and Higher Order Chemical Reaction on Stagnation Point Nanofluid Flow

by

Saba Jabeen

(MMT173018)

THESIS EXAMINING COMMITTEE

S. No.	Examiner	Name	Organization
(a)	External Examiner	Dr. Muhammad Sabeel Khan	IBA University Sukkur
(b)	Internal Examiner	Dr. Muhammad Afzal	CUST, Islamabad
(c)	Supervisor	Dr. Shafqat Hussain	CUST, Islamabad

Supervisor Name
Dr. Shafqat Hussain
September, 2020

Dr. Muhammad Sagheer
Head
Dept. of Mathematics
September, 2020

Dr. Muhammad Abdul Qadir
Dean
Faculty of Computing
September, 2020

Author's Declaration

I, **Saba Jabeen** hereby state that my M.Phil thesis titled "**Effect of Inclined Magnetic Field and Higher Order Chemical Reaction on Stagnation Point Nanofluid Flow**" is my own work and has not been submitted previously by me for taking any degree from Capital University of Science and Technology, Islamabad or anywhere else in the country/abroad.

At any time if my statement is found to be incorrect even after my graduation, the University has the right to withdraw my M.Phil Degree.

(Saba Jabeen)

Registration No: MMT173018

Plagiarism Undertaking

I solemnly declare that research work presented in this thesis titled "**Effect of Inclined Magnetic Field and Higher Order Chemical Reaction on Stagnation Point Nanofluid Flow**" is solely my research work with no significant contribution from any other person. Small contribution/help wherever taken has been duly acknowledged and that complete thesis has been written by me.

I understand the zero tolerance policy of the HEC and Capital University of Science and Technology towards plagiarism. Therefore, I as an author of the above titled thesis declare that no portion of my thesis has been plagiarized and any material used as reference is properly referred/cited.

I undertake that if I am found guilty of any formal plagiarism in the above titled thesis even after award of M.Phil Degree, the University reserves the right to withdraw/revoke my M.Phil degree and that HEC and the University have the right to publish my name on the HEC/University website on which names of students are placed who submitted plagiarized work.

(Saba Jabeen)

Registration No: MMT173018

Acknowledgements

In the name of **Allah**, the Most Gracious and the Most Merciful Alhamdulillah, all praises to Creator and Sustainer of the universe for the strengths and His blessing in completing this thesis. This study is nothing, but an effort to understand and articulate the principles of one of the several hundred thousand phenomena, with a tool, the brain, a precious gift from Almighty.

I would like to express my sincerest appreciation to my enthusiastic supervisor, **Dr. Shafqat Hussain** for his supervision, assistance, and immense knowledge. I am sincerely thankful to him for his constant support, motivation, and patience. His invaluable help of constructive comments and suggestions throughout the thesis work have contributed to the success of this research. It has been an amazing experience and I thank him wholeheartedly, not only for his tremendous support, but also for introducing me to the world of research.

I am truly thankful to my teachers at Capital University of Science and Technology, **Dr. Muhammad Sagheer**, **Dr. Rashid Ali**, **Dr. Abdul Rehman Kashif**, **Dr. M.Afzal**, **Dr. Samina Rashid** and **Dr. Dur e Shehwar**. They are excellent teachers and I learnt alot from them throughout the course of my M.Phil study.

My deepest gratitude goes to my beloved parents and siblings for tolerating my mood swings and being patient with me. A special thanks to my father for believing in me, for giving me the determination to overcome many trying moments to pursue my dreams. Heartily thanks to my mother for her love and moral support. I would like to thanks to my brothers **Muhammad Sajjad Azram**, **Muhammad Shahzad Azram**, **Masood Akhtar** and **Rauf Akhtar** for their support in completing my degree program.

Finally, I am grateful to the management staff of Capital University of Science and Technology, Islamabad for providing a friendly environment for studies.

(Saba Jabeen)

Registration No: MMT173018

Abstract

The main objective of this dissertation is to focus on a numerical study of inclined magnetic field and higher order chemical reaction on the stagnation point nanofluid flow past a porous surface with convective boundary condition. Impact of Joule heating has also been incorporated. A mathematical model which resembles the physical flow problem has been developed. Similarity transformations are used to convert the partial differential equations (PDEs) into a system of nonlinear ordinary differential equations (ODEs). Shooting method has been used to obtain the numerical results with the help of the computational software MATLAB. Effects of various physical parameters on the dimensionless velocity, temprature, and concntration profiles are analyzed in the form of graphs. Numerical values of skin friction coefficient, Nusselt number (heat transfer rate) and Sherwood number (mass transfer rate) are also computed and discussed in detail.

Contents

List of Figures

List of Tables

Abbreviations

MHD	Magnetohydrodynamic
ODEs	Ordinary differential equations
PDEs	Partial differential equations
RK	Runge-Kutta

Symbols

t	Time
p	Pressure
$\mathbf{V}$	Velocity
F	Force
B	Magnetic Field
ρ	Fluid Density
μ	Viscosity
ν	Kinematic Viscosity
τ	Stress Tensor
k	Thermal Conductivity
α	Thermal Diffusivity
τ_w	Wall Shear Stress
η	Dimensionless Similarity Variable
ψ	Stream Function
$f'(\eta)$	Dimensionless Velocity
$\theta(\eta)$	Dimensionless Temperature
$h(\eta)$	Dimensionless Concentration
ϵ	Thermal Conductivity Parameter
a	Constant
h	Convective Heat Flux
D	Species Diffusivity
L	Reference Length
R	Radiation Parameter

M	Magnetic Parameter
P	Permeability Parameter
γ	Chemical Reaction Parameter
k^*	Absorption Coefficient
A	Temperature Dependent Viscosity
C_p	Specific Heat
R_e	Reynolds Number
P_r	Prandtl Number
N_u	Nusselt Number
Sh_x	Sherwood Number
Sc	Schmidt Number
Ec	Eckert Number
C_{fx}	Skin Friction Coefficient
T	Temperature
T_∞	Free Stream Temperature
T_w	Wall Temperature
U_∞	Free Stream Velocity
C_∞	Ambient Concentration
σ^*	Stefan-Boltzmann Constant
$(\rho c_p)_f$	Heat Capacity of the Fluid
q_r	Radiative Heat Flux
(u, v)	Velocity Components
(x, y)	Cartesian Coordinates

Chapter 1

Introduction

In this chapter few important aspect of mass transfer, fluid flow and heat conduction are explained.

1.1 Nanofluid

The applications of nanotechnology have attracted the attention of scientists and mathematicians towards the nanoscale material as these materials retain remarkable chemical, optical and electrical aspects. Current studies made it possible to diffuse nanoparticles in the conventional heat transport liquids comprising machine oil, ethylene glycol and water to generate another class of heat transport liquids with improved efficiency. Nanofluids can be termed as a colloidal fusion contains of a base liquid and nanoparticles of magnitude 1–100 nm. Enhanced application of nanoparticles boosts the thermo-physical aspects of the base liquid, i.e, the heat transport raises with an increment in the heat conduction of liquid. Choi [1] was the first who presented the theory of term nanofluid. Later, Buongiorno [2] established widespread study of nanofluids and developed the preservation equations of a non-homogeneous constancy model of a nanofluid. Hashmi *et al.* [3] investigated magneto Oldroyd-B nanofluid considering the mixed convection effect in double unrestrained isothermal stretching disks. These consequences have shown that on temperature and concentration fields, the influence of buoyancy and Brownian parameter are significant. The multiple slip influence on magnetite Al_2O_3-Cu and Al_2O_3-Cu nanofluids with chemical reaction was studied by Tlili *et al.* [4]. In this area various studies are reported in Refs. [5–7].

1.2 Stagnation Point

In modern world the concept of stagnation point flows has potential applications in numerous regions of aerospace equipment and mechanical industries. In the flow a point with zero local velocity is represented by stagnation point flow. Initially, the theory of stagnation point in 2D viscous fluid model was presented by Hiemenz [8]. He reported that the velocity field at various situations is same by attaining exact solution. Homann [9] increased this idea for axisymmetric motion. The stagnation point flows have a variety of industrial uses and numerous mechanical devotions, mostly in metallurgy and polymer diligence. For example, the slow chilling of an uninterrupted stretching metal or malleable tiles can be revealed which have numerous uses in material fabrication by Lok *et al.* [10]. Markin and Pop [11] reported the concept of stagnation point focused on Arrhenius kinetics to stretched surface. Hiemenz stagnation-point flow for unvaryingly rotational plate was analyzed by Weidman [12]. It was noted that when angular velocity intensifies the centrifugal influence becomes enhancing predominant. Presently, Mahapatra and Sidui [13] examined Homann stagnation-point flow for non-axisymmetric viscoelastic liquid numerically.

1.3 Thermal Radiation

Recently, the thermal radiation has essential influence on heat transport properties in the region of dynamics and manufacturing, interstellar technology, developments at high temperature. Thermal radiation characterize the thermal heat arise form the surface and diffusing in all direction. Moreover, it has important involvement in enhancement of heat transport features in polymer dispensation industry. Nanofluid is proposed quite worthwhile in this trend and numerous performances for improvement of radiation have been wanted [14–16]. Waqas *et al.* [17] considered the influence of radiation and MHD for revised nanofluid relation numerically.

1.4 Magnetohydrodynamics

In modern industry the theory of MHD has various real-world applications due to the influence of magnetic fields on the flow controller and on the enactment of several structures exhausting electrically conducting liquids for instance, liquid metals and water assortment with small acid and others. Furthermore, in the gesture of the earth' score, optimization of solidification procedures of alloys and metals, waste atomic dispensation, diffusion mechanism of compound waste and chemicals, solar astronomy, geo-physics and polymer engineering are variety of MHD. Chamkha and Al-Mudhaf [18] considered the aspects of MHD in mixed convection flow in an ambient fluid with angular velocity subject to heat sink/-source. Chatterjee *et al.* [19] reported numerically, the impact of mixed convective in vertical lid-driven four-sided enclosure packed with an electrically-conducting liquid. Recently, in this area numerous researchers are engaged to study the aspects of MHD in different geometries [20–22].

1.5 Viscous Dissipation

The transport of heat subject to viscous dissipation is significant precisely for the extremely viscous flows regardless of reasonable velocities. It transforms the energy (kinetic to internal) i.e., warming of liquid caused by viscosity and therefore increases the fluid movement. Numerous devices are assembled in stream-beds to falloff flowing water kinetic energy to reduce their erosive potential at stream and banks extremities. The non-dimensional influence (Eckert number) is designated as liquid motion modifiable variable. Limited studies related to viscous dissipation are reported in Refs. [23–25].

1.6 Chemical Reaction

Without any uncertainty the influence of chemical reaction has a critical part of heat and mass transport in diverse branches of industries and science. Applications of this form of flow can be established in diverse manufacturing and built-up uses for instance ignition structures, metallurgy, fissionable devices, solar antenna and chemical trade. Numerous beneficial diffusive progressions comprise the species molecular dispersion with chemical reaction inside or on the boundary. The properties of chemical reaction concerning a horizontal plate were considered by Anjalidevi and Kandasamy [26]. Thermo-solutal Marangoni convection with magnetic impact and chemical reaction were established by Zhang and Zheng [27]. Bhattacharyya and Layek [28] scrutinized the performance of chemical reaction with slip impact considering suction/blowing cases caused by vertical stretched surface. A number of investigators described their studies in this trend [29–31].

1.7 Porous Media

The porous media has many applications in biochemical catalytic vessels, energy diligences, transport development in human lungs and kidneys, thermal isolation, strategy of dense medium heat exchangers and geothermal processes, etc. Further, building material, mineral, leakage of water in stream beds and timber are few specimens of naturally obtainable porous medium. Usually the established Darcy's law has been engaged even for the flow of non-Newtonian liquids. This concern is not truthful since conflict for non-Newtonian liquids are dissimilar than viscous liquids. Therefore, reformed Darcy's law execution is deliberated more realistic. The study of [32–35] were absorbed on Darcy law to include the porous medium in diverse geometries.

1.8 Inclined Magnetic Field

Magnetic sensing techniques exploit a wide range of ideas and phenomena from the fields of physics and materials science. These include search coils, fluxgate, optical pumping, nuclear prefix, squid, hole effect, asymmetric magnetic resistance, giant magnetic resistance, magnetic tunnel junctions, giant magnetic components, magnetic / piezoelectric installations, dual magnets, transistors, optical fibers, electromagnetic, exact electromagnetic systems and existing magnetic sensors [36]. Gilbert studied [37] the difference of the angle of inclination (or magnetic slope) over a broken foundation stone in the form of a sphere, perhaps one of the greatest experiments of models made in Earth sciences. The angle that a magnetic needle makes with the horizontal plane at any specific location. The magnetic inclination is 0^0 at the magnetic equator and 90^0 at each of the magnetic poles. Sugunamma and Sandeep observed the alignment magnetic field and chemical reaction effects on the flow over a vertical seesaw plate past over a permeable surface [38]. The magnetic effect over a free thermal conductivity of electricity and mass transfer from a inclined plate with heat generation / absorption were studied by Chamkha *et al.* [39]. Yih [40] discussed the effects of suction / blowing on mixed convection around sloping surfaces in porous media that digitally show that with an increase in suction and decrease with blowing increases the Sherwood and Nusselt number.

1.9 Joule Heating

The passage of an electric current produces heat that phenomena is known as Joule heating. Joule heating is also acknowledged as Ohmic heating. Joule heating has a collection of standard in built-up and scientific progressions for instance, electric fires, electric heaters, radiant light bulb, electrical fuses, electronic fag, ther-mistor and some others. For the concept of Joule heating some studied are presented here [41–44].

1.10 nth Order Chemical Reaction

In modern existence, the nth order chemical reaction problem with mass transfer phenomenon has been a theme of unlimited devotion in the former few spans. Quite a lot of investigators on account of its completed uses in various industrial developments, which comprises energy transmission in a damp chilling tower, ventilation disappearance at the shallow of a water body, engendering electric power, plantations of fruit plants, salting of plastics, biochemical dispensation of ingredients, and harvests destruction owing to chilly etc. A number of authors has conceded out their examination to explore the impact of nth order chemical reaction on heat-mass transmission flow problems [45–47].

Layout of Thesis

A brief overview of the contents of the thesis is provided below.

Chapter 2 demonstrates the basics of fluid dynamics. A brief discussion about the basic definitions, governing laws for fluid motion and governing equations have been illustrated. The solution methodology has also been demonstrated. Dimensionless physical quantities of interest are also mentioned briefly related to the problems.

Chapter 3 interprets a review analysis of the study which has been performed by Mabood *et al.* [48]. This work has covered the scope related to a numerical study of viscous dissipation, radiation and chemical reaction of MHD stagnation point flow of nanofluids in porous medium. Heat and mass exchange of nanofluid past through a flat plate in permeable surface is analyzed. The system of dimensionless ODEs is solved numerically by shooting method. The behaviour of different physical parameters is explained through tables and graphs. The result achieved are also compared with the published results of Ref [48] found an excellent agreement between them.

Chapter 4 presents the extension to the forgoing work of Mabood *et al.* [48] by adding the effects of Joule heating, inclined magnetic field and nth order chemical reaction. By utilizing similarity transformations we transform the set of governing nonlinear PDEs into the set of nonlinear ODEs. Results for various parameters are discussed through graphs and tables.

Chapter 5 summarizes the whole study with concluding remarks.

All the references used in the research work are listed in **Biblography**.

Chapter 2

Preliminaries

In this chapter, some basic definition governing laws and dimensionless quantities are presented, which will be used in the next chapters. Dimensionless quantities are also discussed which have been used in subsequent chapters. Furthermore, a brief discussion has been done for the shooting method which has been used to find the numerical results.

2.1 Some Important Definitions

Definition 2.1.1. (**Fluid**) [49]

"A substance exists in three primary phases. solid, liquid and gas. (At very high temperatures, it also exists as plasma) A substance in the liquid or gas phase is referred to as a fluid. Distinction between a solid and fluid is made on the basis of substances ability to resist an applied shear or (tangential) stress that tends to change its shape."

Definition 2.1.2. (**Flow**) [50]

"A material that undergoes deformation when certain forces act upon it and continuously increases without limit then such phenomenon is called flow."

Definition 2.1.3. (**Fluid Mechanics**) [51]
"Fluid mechanics deals with the behaviour of fluids at rest or in motion. There are two branches of fluid mechanics."

Definition 2.1.4. (**Fluid Statics**) [51]
"Fluid static is the part of fluid mechanics, that deals with the fluid and its characteristics at the constant position."

Definition 2.1.5. (**Fluid Dynamics**) [51]
"The branch of fluid mechanics that covers the properties of the fluid in the state of progression from one place to another is called fluid dynamics."

Definition 2.1.6. (**Hydrodynamics**) [52]
"The study of the motion of fluids that are practically incompressible such as liquids, especially water and gases at low speeds is usually referred to as hydrodynamics."

Definition 2.1.7. (**Magnetohydrodynamics**) [53]
"Magnetohydrodynamics (MHD) is concerned with the flow of electrically conducting fluids in the presence of magnetic fields, either externally applied or generated within the fluid by inductive action."

Definition 2.1.8. (**Newton's Law of Viscosity**) [54]
"In a Newtonian fluid the stress is directly proportional to the velocity gradient. If τ^* be the force per unit area, then for one-dimensional flow $u(y)$ it can be expressed as

$$\tau^* = \mu \left(\frac{du}{dy} \right).$$

In the above relation τ^* and μ are stress and dynamic viscosity, respectively."

2.2 Classification of Fluids

Fluids are basically divided into two main classes that are: Ideal or Perfect fluids and Real fluids.

Definition 2.2.1. (Ideal Fluids) [49]

"Ideal or perfect fluids are those fluids having viscosity equal to 0, i.e., $\mu = 0$. Such fluids do not have shear forces and are fictitious in nature. These are incompressible and also known as inviscid fluids."

Definition 2.2.2. (Real Fluids) [49]

"Real or viscous fluids have non-zero viscosity, i.e., $\mu \neq 0$. These fluids always possess non-zero viscosity and are either compressible or incompressible in nature. Major real fluid classes are termed as Newtonian and non-Newtonian fluids."

2.3 Types of Flow

Definition 2.3.1. (Compressible and incompressible flows) [52]

"A flow is classified as being compressible or incompressible, depending on the level of variation of density during flow. Incompressibility is an approximation, and a flow is said to be incompressible if the density remains nearly constant throughout. Therefore, the volume of every portion of fluid remains unchanged over the course of its motion when the flow (or the fluid) is incompressible. The densities of liquids are essentially constant, and thus the flow of liquids is typically incompressible. Therefore, liquids are usually referred to as incompressible substances. A pressureof 210 atm, for example, causes the density of liquid water at 1 atm to change by just 1 percent. Gases, on the other hand, are highly compressible. A pressure change of just 0:01 atm, for example, causes a change of 1 percent in the density of atmospheric air."

Definition 2.3.2. (Steady versus unsteady flow) [52]

"The terms steady and uniform are used frequently in engineering, and thus it is important to have a clear understanding of their meanings. The term steady implies no change at a point with time. The opposite of steady is unsteady. The term uniform implies no change with location over a specified region. These meanings are consistent with their everyday use (steady girlfriend, uniform distribution, etc.). The terms unsteady and transient are often used interchangeably, but these terms are not synonyms. In fluid mechanics, unsteady is the most general term that applies to any flow that is not steady, but transient is typically used for developing flows. When a rocket engine is fired up, for example, there are transient effects (the pressure builds up inside the rocket engine, the flow accelerates, etc.) until the engine settles down and operates steadily. The term periodic refers to the kind of unsteady flow in which the flow oscillates about a steady mean."

Definition 2.3.3. (**Laminar versus turbulent flow**) [52]
"Some flows are smooth and orderly while others are rather chaotic. The highly ordered fluid motion characterized by smooth layers of fluid is called laminar. The word laminar comes from the movement of adjacent fluid particles together in laminates. The flow of high-viscosity fluids such as oils at low velocities is typically laminar. The highly disordered fluid motion that typically occurs at high velocities and is characterized by velocity fluctuations is called turbulent. The flow of low-viscosity fluids such as air at high velocities is typically turbulent. The flow regime greatly influences the required power for pumping. A flow that alternates between being laminar and turbulent is called transitional."

Definition 2.3.4. (**Viscous and inviscid flow**) [52]
"When two fluid layers move relative to each other, a friction force develops between them and the slower layer tries to slow down the faster layer. This internal resistance to flow is quantified by the fluid property viscosity, which is a measure of internal stickiness of the fluid. Viscosity is caused by cohesive forces between the molecules in liquids and by molecular collisions in gases. There is no fluid with zero viscosity, and thus all fluid flows involve viscous effects to some degree. Flows in which the frictional effects are significant are called viscous flows. However, in many flows of practical interest, there are regions (typically regions not close to solid surfaces) where viscous forces are negligibly small compared to inertial or pressure forces. Neglecting the viscous terms in such inviscid flow regions greatly simplifies the analysis without much loss in accuracy."

Definition 2.3.5. (**Newtonian and non-Newtonian fluids**) [52]
"Fluids for which the viscosity is not independent of the rate of shear are referred

as non-Newtonian and the liquids for which the viscosity is independent of the rate of shear are called Newtonian fluids."

2.4 Fluid Properties

Definition 2.4.1. (**Heat Transfer**) [51]
"It is the energy transfer due to temperature difference. At the point when there is a temperature contrast in a medium or between media, heat transfer must take place. Heat transfer is normally conducted from a high temperature region to a low temperature."

Definition 2.4.2. (**Mass Transfer**) [51]
"Mass exchange is the total movement of mass from one place to another."

Definition 2.4.3. (**Stagnation Point**) [51]
"It is a point in a flow field where the fluid velocity is zero. It exists at the surface of objects in the field where fluid is rest by the object. Static pressure is the example of stagnation point."

Definition 2.4.4. (**Viscous Dissipation**) [51]
"The process in which the work done by fluid is converted into heat is called viscous dissipation."

Definition 2.4.5. (**Radiation**) [51]
"Radiation is the energy transfer due to the release of photons or electromagnetic waves from a surface volume. Radiation doesn't require any medium to transfer heat. The energy produced by radiation is transformed by electromagnetic waves."

Definition 2.4.6. (**Boundary Layer**) [55]
"Viscous effects are particularly important near the solid surfaces, where the strong interaction of the molecules of the fluid with molecules of the solid causes the relative velocity between the fluid and the solid to become almost exactly zero for a stationary surface. Therefore, the fluid velocity in the region near the wall must reduce to zero. This is called no slip condition. In that condition there is no

relative motion between the fluid and the solid surface at their point of contact. It follows that the flow velocity varies with distance from the wall; from zero at the wall to its full value some distance away, so that significant velocity gradients are established close to the wall. In most cases this region is thin (compared to the typical body dimension), and it is called a boundary layer."

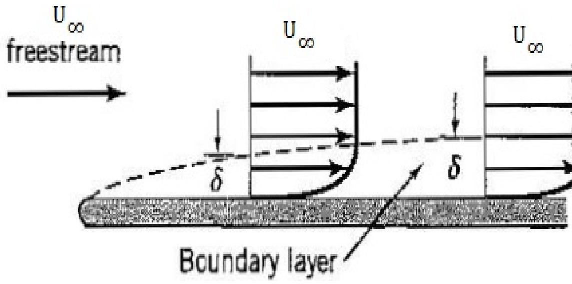

FIGURE 2.1: Figure of Boundary Layer.

Definition 2.4.7. (**Density**) [56]

"Density is defined as mass per unit volume. It is represented by ρ. Let m be the mass of fluid and V be the volume, then density is given by

$$\rho = \frac{m}{V}."$$

Definition 2.4.8. (**Pressure**) [56]

"A normal force $\mathbf{F}$ exerted by a fluid per unit area A is called pressure. It is formulated as

$$p = \frac{\mathbf{F}}{A}."$$

Definition 2.4.9. (**Velocity Field**) [49]

"It is the representation of net motion of molecules of fluid from one point in space to another point as a function of time. It is expressed as

$$\mathbf{V} = u(x, y, z, t)\hat{i} + v(x, y, z, t)\hat{j} + w(x, y, z, t)\hat{k},$$

where $\mathbf{V}$ represents three-dimensional velocity field with respective components u, v and w.

Definition 2.4.10. (Streamlines) [49]

"A streamline is a line that is every where tangent to velocity field of fluid. Streamlines show pictorial representation of flow. For a three-dimensional velocity field it can be written as

$$\frac{dx}{u} = \frac{dy}{v} = \frac{dz}{w}."$$

Definition 2.4.11. (Substantial or Material Derivative) [49]

"If ξ represent any property of fluid, with dx, dy, dz and dt are arbitrary changes of four independent variables, then total differential change in ξ is given by

$$\frac{d\xi}{dt} = u\frac{d\xi}{dx} + v\frac{d\xi}{dy} + w\frac{d\xi}{dz} + \frac{d\xi}{dt}.$$

The above mathematical relation is called substantial derivative or material derivative."

Definition 2.4.12. (Acceleration of Flow Field) [49]

"Acceleration is the rate of change of velocity of fluid with respect to time. Acceleration a of fluid is mathematically given by

$$\mathbf{a} = \frac{d\mathbf{V}}{dt},$$

similarly by definition 2.4.11, acceleration for a three-dimensional velocity flow field is written below

$$\mathbf{a} = u\frac{\partial \mathbf{V}}{\partial x} + v\frac{\partial \mathbf{V}}{\partial y} + w\frac{\partial \mathbf{V}}{\partial z} + \frac{\partial \mathbf{V}}{\partial t}."$$

Definition 2.4.13. (Enthalpy) [49]

"It is the combination of internal energy of fluid $\widetilde{E}$ and pressure energy $\left(\frac{p}{\rho}\right)$. This fluid property is called enthalpy which is represented by $\hat{h}$.

$$\hat{h} = \left(\widetilde{E} + \frac{p}{\rho}\right)."$$

2.5 Some Basic Definitions of Heat Transfer

Definition 2.5.1. (**Conduction**) [51]

"Conduction is the process in which heat is transferred through the material between the objects that are in physical contact. For example: picking up a hot cup of tea."

Definition 2.5.2. (**Convection**) [51]

"Convection is a mechanism in which heat is transferred through fluids (gases or liquids) from a hot place to a cool place. For example: Macaroni rising and falling in a pot of boiling water."

Definition 2.5.3. (**Forced Convection**) [51]

"Forced convection is a process in which fluid motion is produced by an external source. It is a special type of heat transfer in which fluid moves in order to increase the heat transfer. In other words, a method of heat transfer in which heat transfer is caused by dependent source like a fan and pump etc, is called forced convection. For example: Gas convection heaters have a gas burner to generate the heat, and a fan to force the heated air to circulate around the room."

Definition 2.5.4. (**Natural Convection**) [51]

"Natural convection is a heat transport process, in which the heat transfer is not caused by an external source, like pump, fan and suction. It happens due to the temperature differences which affect the density of the fluid. It is also called free convection. Example: Daily weather."

Definition 2.5.5. (**Mixed Convection**) [51]

"It is a combination of both forced convection and natural convection. For example if fluid is moving upward along the moment of the vertical stretching sheet is forced between while in the same phenomena fluid is freely falling due to the gravity which is forced convection. When these two phenomena appear in the same model then such kind of flow is mixed convection."

Definition 2.5.6. (**Thermal Conductivity**) [49]

"According to Fourier's law: The heat transfer rate q^{**} in any direction $\bar{\mathbf{n}}$ per unit area is measured normal to $\bar{\mathbf{n}}$. It is given by

$$q^{**} = -k\left(\frac{\partial T}{\partial \bar{\mathbf{n}}}\right),$$

where k is called thermal conductivity which is an important thermal property of fluid. "

Definition 2.5.7. (**Thermal Diffusivity**) [51]
"Thermal diffusivity is material,s property which identifies the unsteady heat conduction. Mathematically, it can be written as,

$$\alpha = \frac{k}{\rho C_p},$$

where k, ρ and C_p represents the thermal conductivity of material, the density and the specific heat capacity. In SI system unit and dimension of thermal diffusivity are m^2s^{-1} and $[LT^{-1}]$ respectively. "

2.6 Dimensionless Numbers

Definition 2.6.1. (**Reynolds Number** Re) [51]
"It is a dimensionless number which is used to clarify the different flow behaviours like turbulent or laminar flow. It helps to measure the ratio between inertial force and the viscous force. Mathematically,

$$Re = \frac{\frac{\rho U^2}{L}}{\frac{\mu U}{L^2}} \Longrightarrow Re = \frac{LU}{\nu},$$

where U denotes the free stream velocity, L the characteristics length. At low Reynolds number, laminar flow arises where the viscous forces are dominant. At high Reynolds number, turbulent flow arises where the inertial forces are dominant."

Definition 2.6.2. (**Prandtal Number** Pr) [51]
"It is the ratio between the momentum diffusivity (ν) and thermal diffusivity (α).

Mathematically, it can be defined as

$$Pr = \frac{\nu}{\alpha} = \frac{\mu/\rho}{k/c_p} = \frac{\mu c_p}{k},$$

where μ represents the dynamic viscosity, c_p denotes the specific heat and k stands for thermal conductivity. The relative thickness of thermal and momentum boundary layer is controlled by Prandtal number. For small Pr, heat distributed rapidly corresponds to the momentum."

Definition 2.6.3. (**Nusselt Number** Nu) [51]

"It is the ratio of the convective to the conductive heat transfer to the boundary. Mathematically,

$$Nu = \frac{hL}{k},$$

where h stands for convective heat transfer, L for the characteristics length and k stands for the thermal conductivity."

Definition 2.6.4. (**Sherwood Number** Sh_x) [51]

"It is the nondimensional quantity which show the ratio of the mass transport by convection to the transfer of mass by diffusion. Mathematically:

$$Sh_x = \frac{kL}{D},$$

here L is characteristics length, D is the mass diffusivity and k is the mass transfer coefficient."

Definition 2.6.5. (**Skin Friction Coefficient** C_{fx}) [51]

"Skin friction coefficient occurs between the fluid and the solid surface which leads to slow down the motion of the fluid. The skin friction coefficient can be defined as

$$C_{fx} = \frac{2\tau_w}{\rho U^2},$$

where τ_w denotes the wall shear stress, ρ the density and U the free-stream velocity."

Definition 2.6.6. (**Eckert Number** Ec) [51]

"It is the dimensionless number used in continuum mechanics. It describes the relation between flows and the boundary layer enthalpy difference and it is used for characterized heat dissipation. Mathematically,

$$Ec = \frac{u^2}{c_p \nabla T},"$$

2.7 Basic Governing Laws and Equations for Fluid Motion

We need to satisfy the basic fundamental laws of physics which include mass conservation, momentum conservation (Newton's second law of motion) and energy conservation (First law of thermodynamics) to describe the fluid dynamics [49, 57–59],

Definition 2.7.1. (**Law of Conservation of Mass**)

"The mass inside a system is conserved and does not change. or

The time rate of change of mass inside a system is equals to zero.

$$\text{i.e.,} \quad \frac{Dm}{Dt} = 0,$$

where m is the mass of fluid flowing in a system or control volume [49, 57]"

Definition 2.7.2. (**Continuity Equation**) [59]

"The conservation of mass of fluid entering and leaving the control volume, the resulting mass balance is called the equation of continuity. From this law it is concluded that mass is conserved. Mathematically form is

$$\frac{\partial \rho}{\partial t} + \nabla.(\rho \mathbf{V}) = 0.$$

where, $\mathbf{V}$ is velocity of fluid. For steady case rate of time will be constant, so continuity equation becomes

$$\nabla.(\rho \mathbf{V}) = 0.$$

For the case of incompressible flow, density does not changes so continuity equation can be re-written as,

$$\nabla.\mathbf{V} = 0. \tag{2.1}$$

For incompressible and irrotational flow, the Eq. (2.1) can be transformed in terms of velocity potential ψ, which is given by

$$\nabla^2\psi = 0. \tag{2.2}$$

Eq. (2.2) is known as Laplace equation."

Definition 2.7.3. (**Law of Conservation of Momentum**)
"To study the momentum equation, Newton's second law is of great importance. Newton's law of motion states that:
The rate of change of momentum of a body is equal to net forces acting on that body.
This statement leads to law of conservation of momentum, which states that:
The momentum of a system remains constant when the net force acting on it is zero."

Definition 2.7.4. (**Momentum Equation**)
"The principle of conservation of momentum can be expressed in the form of momentum equation, which is formulated as [49, 57]

$$\rho\left(\frac{\partial\mathbf{V}}{\partial t} + \mathbf{V}.(\nabla\mathbf{V})\right) = -\nabla p + \nabla.\tau^*_{ij} + \mathbf{F}_g, \tag{2.3}$$

where $p, \tau^*_{ij}, \mathbf{F}_g = \rho_g$ are termed as hydrostatic pressure, viscous stress tensor and body force. Viscous sress tensor τ^*_{ij}, is a tensor of rank 2 having nine stress components. It is written as

$$\tau^*_{ij} = \begin{pmatrix} \tau^*_{xx} & \tau^*_{xy} & \tau^*_{xz} \\ \tau^*_{yx} & \tau^*_{yy} & \tau^*_{yz} \\ \tau^*_{zx} & \tau^*_{zy} & \tau^*_{zz} \end{pmatrix}, \tag{2.4}$$

or

$$\tau^*_{ij} = \begin{pmatrix} \sigma^*_x & \tau^*_{xy} & \tau^*_{xz} \\ \tau^*_{yx} & \sigma^*_y & \tau^*_{yz} \\ \tau^*_{zx} & \tau^*_{zy} & \sigma^*_z \end{pmatrix}, \tag{2.5}$$

In Eq. (2.7), $\tau^*_{xy}, \tau^*_{xz}, \tau^*_{yx}, \tau^*_{yz}, \tau^*_{zx}$ and τ^*_{zy} are known as shear stresses while σ^*_x, σ^*_y and σ^*_z are called normal stresses.

In the case of incompressible and inviscid flows, the stress term in Eq. (2.3) is avoided to get the most simplified equation. Such momentum equation is known as the "Euler's momentum equation". It can be written as

$$\rho\left(\frac{\partial \mathbf{V}}{\partial t} + \mathbf{V}.(\nabla\mathbf{V})\right) = -\nabla p + \mathbf{F}_g." \tag{2.6}$$

Definition 2.7.5. (**Navier-Stokes Equation**)

"By redefining Eq. (2.3), given below is the most well known form of momentum equation, usually known as Navier-Stokes equation. It was first introduced by Claude-Louis Navier in 1821 and further improved by Sir George Gabriel Stokes [49, 58].

$$\rho\left(\frac{\partial \mathbf{V}}{\partial t} + \mathbf{V}.(\nabla\mathbf{V})\right) = -\nabla.\overline{\mathbf{T}}_{ij} + \mathbf{F}_g, \tag{2.7}$$

where $\overline{\mathbf{T}}_{ij}$ is called Cauchy stress tensor and $\mathbf{F}_g$ is known as body force term. Cauchy stress tensor is further defined as below

$$\overline{\mathbf{T}}_{ij} = \underbrace{-pI}_{\text{(pressure distribution term)}} + \underbrace{\tau^*_{ij}}_{\text{(deviatoric stress tensor term)}}. \tag{2.8}$$

In Eq. (2.8) the deviatoric stress tensor, i.e., τ^*_{ij} for Newtonian fluids is given below

$$\tau^*_{ij} = \mu\mathbf{A}_1, \tag{2.9}$$

where $\mathbf{A}_1$ is called first Rivlin Ericksen tensor [60] and its formulation is given by

$$\mathbf{A}_1 = \nabla\mathbf{V} + (\nabla\mathbf{V})^T. \tag{2.10}$$

The complete constitutive relation in Eq. (2.8) can be expressed as

$$\overline{\mathbf{T}}_{ij} = -p\mathbf{I} + \mu\left[\nabla\mathbf{V} + (\nabla\mathbf{V})^T\right]. \tag{2.11}$$

The gradient relation of three-dimensional velocity field $\mathbf{V}(u, v, w)$ is written as

$$\nabla\mathbf{V} = \begin{pmatrix} \frac{\partial u}{\partial x} & \frac{\partial v}{\partial x} & \frac{\partial w}{\partial x} \\ \frac{\partial u}{\partial y} & \frac{\partial v}{\partial y} & \frac{\partial w}{\partial y} \\ \frac{\partial u}{\partial z} & \frac{\partial v}{\partial z} & \frac{\partial w}{\partial z} \end{pmatrix},$$

and

$$(\nabla\mathbf{V})^T = \begin{pmatrix} \frac{\partial u}{\partial x} & \frac{\partial u}{\partial y} & \frac{\partial u}{\partial z} \\ \frac{\partial v}{\partial x} & \frac{\partial v}{\partial y} & \frac{\partial v}{\partial z} \\ \frac{\partial w}{\partial x} & \frac{\partial w}{\partial y} & \frac{\partial w}{\partial z} \end{pmatrix}.$$

By substituting these relations into Eq. 2.10,

$$A_1 = \begin{pmatrix} 2\frac{\partial u}{\partial x} & \frac{\partial v}{\partial x} + \frac{\partial u}{\partial y} & \frac{\partial w}{\partial x} + \frac{\partial u}{\partial z} \\ \frac{\partial u}{\partial y} + \frac{\partial v}{\partial x} & 2\frac{\partial v}{\partial y} & \frac{\partial w}{\partial y} + \frac{\partial v}{\partial z} \\ \frac{\partial u}{\partial z} + \frac{\partial w}{\partial x} & \frac{\partial v}{\partial z} + \frac{\partial w}{\partial y} & 2\frac{\partial w}{\partial z} \end{pmatrix}. \tag{2.12}$$

Substitution of Eq. (2.12) into Eq. (2.9) leads to the following

$$\tau^*_{ij} = \begin{pmatrix} 2\mu\frac{\partial u}{\partial x} & \mu\left(\frac{\partial v}{\partial x} + \frac{\partial u}{\partial y}\right) & \mu\left(\frac{\partial w}{\partial x} + \frac{\partial u}{\partial z}\right) \\ \mu\left(\frac{\partial u}{\partial y} + \frac{\partial v}{\partial x}\right) & 2\mu\frac{\partial v}{\partial y} & \mu\left(\frac{\partial w}{\partial y} + \frac{\partial v}{\partial z}\right) \\ \mu\left(\frac{\partial u}{\partial z} + \frac{\partial w}{\partial x}\right) & \mu\left(\frac{\partial v}{\partial z} + \frac{\partial w}{\partial y}\right) & 2\mu\frac{\partial w}{\partial z} \end{pmatrix}, \tag{2.13}$$

and from Eq. (2.9), pressure term is written in matrix form as

$$-pI = \begin{pmatrix} -p & 0 & 0 \\ 0 & -p & 0 \\ 0 & 0 & -p \end{pmatrix} \tag{2.14}$$

By using Eqs. (2.13) and (2.14) into Eq. (2.9) we get

$$\overline{\mathbf{T}}_{ij} = \begin{pmatrix} \overline{\mathbf{T}}_{xx} & \overline{\mathbf{T}}_{xy} & \overline{\mathbf{T}}_{xz} \\ \overline{\mathbf{T}}_{yx} & \overline{\mathbf{T}}_{yy} & \overline{\mathbf{T}}_{yz} \\ \overline{\mathbf{T}}_{zx} & \overline{\mathbf{T}}_{zy} & \overline{\mathbf{T}}_{zz} \end{pmatrix},$$

and following are the x, y and z components of $\nabla.\overline{\mathbf{T}}_{ij}$

$$(\nabla.\overline{\mathbf{T}}_{ij})_x = -\frac{\partial p}{\partial x} + \mu\left(\frac{\partial^2 u}{\partial x^2} + \frac{\partial^2 u}{\partial y^2} + \frac{\partial^2 u}{\partial z^2}\right), \tag{2.15}$$

$$(\nabla.\overline{\mathbf{T}}_{ij})_y = -\frac{\partial p}{\partial y} + \mu\left(\frac{\partial^2 v}{\partial x^2} + \frac{\partial^2 v}{\partial y^2} + \frac{\partial^2 v}{\partial z^2}\right), \tag{2.16}$$

$$(\nabla.\overline{\mathbf{T}}_{ij})_z = -\frac{\partial p}{\partial z} + \mu\left(\frac{\partial^2 w}{\partial x^2} + \frac{\partial^2 w}{\partial y^2} + \frac{\partial^2 w}{\partial z^2}\right). \tag{2.17}$$

After the substitution of Eqs. (2.15) to (2.17) into Eq. (2.7), we will get a set of equations known as "Navier-Stokes equations" for Newtonian and incompressible flow, i.e.,

$$\rho\left(\frac{\partial \mathbf{V}}{\partial t} + \mathbf{V}.(\nabla\mathbf{V})\right) = -\nabla p + \mu\Delta\mathbf{V} + \mathbf{F}_g." \tag{2.18}$$

Definition 2.7.6. (**First Law of Thermodynamics**)

"First law of thermodynamics is nothing more than the principle of conservation of energy. First law of thermodynamics states that:

The variation in internal energy $\widetilde{E}$ of a system during any transformation is equal to the amount of energy that system receives from the environment and the work done by the system. Mathematically, it is represented as

$$\Delta\widetilde{E} = \widetilde{Q} - \widetilde{W},$$

where $\Delta\widetilde{E}, \widetilde{Q}$ and $\widetilde{W}$ are termed as change in internal energy, heat added to the system and work done by the system respectively."

Definition 2.7.7. (**Energy Equation**)

"The energy conservation of a system can be expressed in rate form as:

Rate of change of energy in system or control volume = (Rate of in flow of energy Rate of out flow of energy) + (Rate of heat addition due to conduction) + (Rate of internal heat generation within control volume) + (Rate of work done by the forces acting on control volume).

The energy equation in terms of first law of thermodynamics is written below [61, 62]

$$\rho\frac{D\widetilde{E}}{Dt} + \nabla q^{**} - q^{***} + p(\nabla.\mathbf{V}) - \tau^{*}_{ij}.(\nabla.\mathbf{V}) = 0, \tag{2.19}$$

where

$$\begin{aligned}\tau^{*}_{ij}.(\nabla\mathbf{V}) = &\left(\sigma_x\frac{\partial u}{\partial x} + \tau^{*}_{xy}\frac{\partial u}{\partial y} + \tau^{*}_{xz}\frac{\partial u}{\partial z}\right) + \left(\tau^{*}_{yx}\frac{\partial v}{\partial x} + \sigma_y\frac{\partial v}{\partial y} + \tau^{*}_{yz}\frac{\partial v}{\partial z}\right)\\ &+ \left(\tau^{*}_{zx}\frac{\partial w}{\partial x} + \tau^{*}_{zy}\frac{\partial w}{\partial y} + \sigma_z\frac{\partial w}{\partial z}\right).\end{aligned} \tag{2.20}$$

Substituting the values from Eq. (2.13) into Eq. (2.20), we get

$$\begin{aligned}\tau^{*}_{ij}.(\nabla\mathbf{V}) =&\mu\Bigg[2\left(\left(\frac{\partial u}{\partial x}\right)^2 + \left(\frac{\partial v}{\partial y}\right)^2 + \left(\frac{\partial w}{\partial z}\right)^2\right) + \left(\frac{\partial u}{\partial y} + \frac{\partial v}{\partial x}\right)^2\\ &+ \left(\frac{\partial w}{\partial y} + \frac{\partial v}{\partial z}\right)^2 + \left(\frac{\partial u}{\partial z} + \frac{\partial w}{\partial x}\right)^2\Bigg],\\ &= \mu\Phi,\end{aligned} \tag{2.21}$$

where Φ is called "viscous dissipation".

After applying Eq. (2.21) into Eq. (2.19), we get

$$\rho\frac{D\widetilde{E}}{Dt} + \nabla q^{**} - q^{***} + p(\nabla.\mathbf{V}) - \mu\Phi = 0, \tag{2.22}$$

where the rate of work done by pressure forces on fluid, i.e., $p(\nabla.\mathbf{V})$ becomes zero due to the contribution of continuity equation, so

$$\rho\frac{D\widetilde{E}}{Dt} + \rho\mathbf{V}.(\nabla\widetilde{E}) + \nabla q^{**} - q^{***} - \mu\Phi = 0. \tag{2.23}$$

Adopting the definition 2.4.13 of enthalpy into Eq. (2.23), it can be written as

$$\widetilde{E} = \left(\hat{h} - \frac{p}{\rho}\right), \tag{2.24}$$

$$\rho\left(\frac{\partial\left(\hat{h}-\frac{p}{\rho}\right)}{\partial t}\right)+\rho\mathbf{V}\left(\nabla\left(\hat{h}-\frac{p}{\rho}\right)\right)+\nabla q^{**}-q^{***}-\mu\Phi=0, \tag{2.25}$$

$$\rho\frac{\partial\hat{h}}{\partial t}-\frac{\partial p}{\partial t}+\rho\vec{V}.\left(\nabla\hat{h}\right)-\mathbf{V}.\left(\nabla p\right)=-\nabla q^{**}+q^{***}+\mu\Phi. \tag{2.26}$$

After applying the definition of Fourier's law 2.5.6, we get

$$\rho\frac{\partial\hat{h}}{\partial t}-\frac{\partial p}{\partial t}+\rho\mathbf{V}.\left(\nabla\hat{h}\right)-\mathbf{V}.\left(\nabla p\right)=-\nabla.(-\kappa\nabla T)+q^{***}+\mu\Phi, \tag{2.27}$$

$$\rho\left(\frac{\partial\hat{h}}{\partial t}+\mathbf{V}.\left(\nabla\hat{h}\right)\right)=\left(\frac{\partial p}{\partial t}+\mathbf{V}.\left(\nabla p\right)\right)+\nabla.(\kappa\nabla T)+q^{***}+\mu\Phi. \tag{2.28}$$

Substituting another physical relationship of enthalpy $\hat{h}$, which is defined as [62]:

$$d\hat{h}=C_p dT,$$

then Eq. (2.28) will be transformed into

$$\rho C_p\left(\frac{\partial T}{\partial t}+\mathbf{V}.(\nabla T)\right)=\left(\frac{\partial p}{\partial t}+\mathbf{V}.\left(\nabla p\right)\right)+(\kappa\Delta T)+q^{***}+\mu\Phi, \tag{2.29}$$

$$\rho C_p\left(\frac{DT}{Dt}\right)=\frac{Dp}{Dt}+(\kappa\Delta T)+q^{***}+\mu\Phi. \tag{2.30}$$

If the fluid is viscous, incompressible and steady, also for simplicity by ignoring the internal heating and viscous dissipation effects we get the following most generalized form of energy equation:

$$\left(u\frac{\partial T}{\partial x}+v\frac{\partial T}{\partial y}+w\frac{\partial T}{\partial z}\right)=\frac{\kappa}{\rho C_p}\left(\frac{\partial^2 T}{\partial x^2}+\frac{\partial^2 T}{\partial y^2}+\frac{\partial^2 T}{\partial z^2}\right), \tag{2.31}$$

$$\left(u\frac{\partial T}{\partial x}+v\frac{\partial T}{\partial y}+w\frac{\partial T}{\partial z}\right)=\alpha\left(\frac{\partial^2 T}{\partial x^2}+\frac{\partial^2 T}{\partial y^2}+\frac{\partial^2 T}{\partial z^2}\right), \tag{2.32}$$

where α is called thermal diffusivity."

2.8 Solution Methodology

"Shooting Method is used to solve the higher order nonlinear ordinary differential equations. To implement this technique, we first convert the higher order ODEs to the system of first order ODEs. After that we assume the missing initial conditions and the differential equations are then integrated numerically using the Runge-Kutta method as an initial value problem. The accuracy of the assumed missing initial condition is then checked by comparing the calculated values of the dependent variables at the terminal point with their given value there. If the boundary conditions are not fulfilled up to the required accuracy, with the new set of initial conditions, then they are modified by Newtons method. The process is repeated again until the required accuracy is achieved. To explain the shooting method, we consider the following general second order boundary value problem,

$$y''(x) = f(x, y, y'(x)) \tag{2.33}$$

subject to the boundary conditions

$$y(0) = 0, y(L) = A \tag{2.34}$$

[63] By denoting y by y_1 and y_1' by y_2, Eq. (2.33) can be written in the form of following system of first order equations.

$$\left.\begin{aligned} y_1' &= y_2, & y_1(0) &= 0, \\ y_2' &= f(x, y_1, y_2), & y_1(L) &= A. \end{aligned}\right\} \tag{2.35}$$

Denote the missing initial condition by $y_2(0) = s$, to have

$$\left.\begin{aligned} y_1' &= y_2, & y_1(0) &= 0, \\ y_2' &= f(x, y_1, y_2), & y_1(0) &= s. \end{aligned}\right\} \tag{2.36}$$

Now the problem is to find s such that the solution of the IVP (2.36) satisfies the boundary condition $y(L) = A$. In other words, if the solutions of the initial value problem (2.36) are denoted by $y_1(x, s)$ and $y_2(x, s)$, one should search for that value of s which is an approximate root the equation.

$$y_1(L, s) - A = \phi(s) = 0. \tag{2.37}$$

To find an approximate root of the Eq. (2.37) by the Newtons method, the iteration formula is given by

$$s_{n+1} = s_n - \frac{\phi(s_n)}{d\phi(s_n)/ds}, \tag{2.38}$$

$$s_{n+1} = s_n - \frac{y_1(L, s_n) - A}{dy_1(L, s_n))/ds}. \tag{2.39}$$

To find the derivatives of y_1 with respect of s, differentiate (2.36) with respect to s. For simplification, use the following notations

$$\frac{dy_1}{ds} = y_3, \quad \frac{dy_2}{ds} = y_4 \tag{2.40}$$

$$\left.\begin{aligned} y_3' &= y_4, & y_3(0) &= 0, \\ y_4' &= \frac{\partial f}{\partial y_1} y_3 + \frac{\partial f}{\partial y_2} y_4, & y_4(0) &= 1. \end{aligned}\right\} \tag{2.41}$$

Now, solving the IVP Eq. (2.41), the value of y_3 at L can be computed. This value is actually the derivative of y_1 with respect to s computed at L. Setting the value of $y_3(L, s)$ in Eq. (2.39), the modified value of s can be achieved. This new value of s is used to solve the Eq. (2.36) and the process is repeated until the value of s is within a described degree of accuracy."

Chapter 3

Effect of Viscous Dissipation and Chemical Reaction on MHD Stagnation Point Flow of Nanofluids in Porous Medium

3.1 Introduction

Numerical study of MHD viscous, incompressible and two-dimensional nanofluid flow past a flat plate in a uniform permeable medium has been taken under consideration. Conversion of non-linear partial differential equations describing the flow problem into a set of ordinary differential equations has been carried out by employing appropriate similarity transformations. Shooting method has been employed for the numerical treatment of the proposed flow equations. Effect of pertinent flow parameters on the non-dimensional velocity, temperature and concentration profiles has been illustrated via tables and graphs. The limiting case of the present study affirms that the obtained numerical results reflect a very good agreement with those from published literature. In this chapter, a detailed review of [48] has been provided.

3.2 Problem Formulatiuon

The present model aims to investigate the incompressible water base nanofluids containing two types of nanoparticles, i.e. Copper (Cu) and Alumina (Al_2O_3) flow over a flat plate in a porous medium. Magnatic field of strength B is applied normal to the fluid flow. Under the effect of thermal radiation and heat absorption parameter the characteristics of flow; heat and mass transfer is examined. The coordinate system is chosen such a way that x-axis is along the flow where as y-axis is perpendicular to the plate. The surface of the flat plate is maintained at a constant temperature $T_w = T_\infty + T_0 e^{\frac{x}{2L}}$ higher than the constant temperature T_∞ of the ambient nanofluid T_0 is a constant measuring the rate of temperature increase along the surface. It has been assumed that the velocity of the flat plate is $u = ae^{\frac{x}{L}}$ and the free stream velocity U_∞. The concentration at the surface is $C_w = C_\infty + C_0 e^{\frac{x}{2L}}$, which is also higher then the ambient concentration C_∞. The initial reference concentration denoted by C_0. The geometry of the flow model is shown in Figure 3.1.

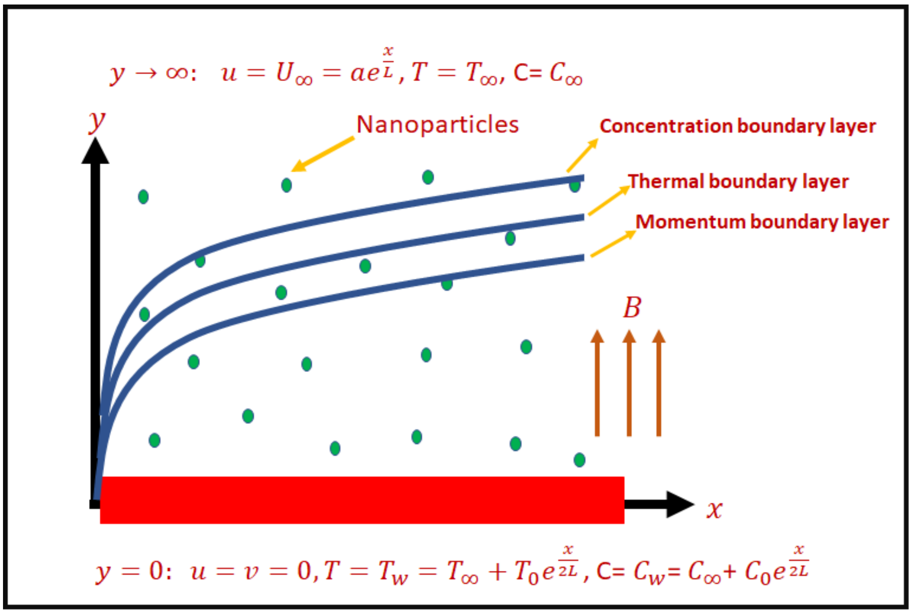

FIGURE 3.1: Geometry of physical model.

Under the constraints, the governing boundary layer equations for proposed problem are given as [48] :

$$\frac{\partial u}{\partial x}+\frac{\partial v}{\partial y}=0, \tag{3.1}$$

$$u\frac{\partial u}{\partial x}+v\frac{\partial u}{\partial y}=U_\infty\frac{dU_\infty}{dx}+\nu_{nf}\frac{\partial^2 u}{\partial y^2}+\frac{\nu_{nf}}{k}(U_\infty-u)+\frac{\sigma B^2}{\rho_{nf}}(U_\infty-u), \tag{3.2}$$

$$u\frac{\partial T}{\partial x}+v\frac{\partial T}{\partial y}=\alpha_{nf}\frac{\partial^2 T}{\partial y^2}-\frac{1}{(\rho c_p)_{nf}}\frac{\partial q_r}{\partial y}+\frac{\mu_{nf}}{(\rho c_p)_{nf}}\left(\frac{\partial u}{\partial y}\right)^2, \tag{3.3}$$

$$u\frac{\partial C}{\partial x}+v\frac{\partial C}{\partial y}=D\frac{\partial^2 C}{\partial y^2}-K(C-C_\infty). \tag{3.4}$$

The corresponding conditions at the boundary are

$$\left.\begin{array}{ll} \left.\begin{array}{l} u=v=0, T=T_w=T_\infty+T_0e^{\frac{x}{2L}},\\ C=C_w=C_\infty+C_0e^{\frac{x}{2L}}, \end{array}\right\} \quad \text{at} & y=0,\\ u=U_\infty=ae^{\frac{x}{L}}, T=T_\infty, C=C_\infty, \quad \text{as} & y\to\infty, \end{array}\right\} \tag{3.5}$$

here σ_s is the electrical conductivity of the base-fluid whereas $\sigma_{nf}, \nu_{nf}, \rho_{nf}, \alpha_{nf}, k_{nf}$, are the electric conductivity, the effective viscosity, the effective density, the effective thermal diffusivity and the thermal conductivity of the nanofluid, D is the species diffusivity, $k=k_0e^{\frac{-x}{L}}$ is the non-uniform permeability, $K(x)$ is the variable reaction rate given by $K(x)=K_0e^{\frac{x}{L}}$, respectively. These quantities are formulated as follows [48]:

$$\begin{aligned}
\rho_{nf} &= (1-\phi)\rho_f+\phi\rho_s,\\
\mu_{nf} &= \frac{\mu_f}{(1-\phi)^{2.5}},\\
\alpha_{nf} &= \frac{k_{nf}}{(\rho c_p)_{nf}},\\
(\rho c_p)_{nf} &= (1-\phi)(\rho c_p)_f+\phi(\rho c_p)_s,\\
\sigma_{nf} &= (1-\phi)\sigma_f+\phi\sigma_s,\\
k_{nf} &= k_f\frac{k_s+2k_f-2\phi(k_f-k_s)}{k_s+2k_f+2\phi(k_f-k_s)},\\
\nu_f &= \frac{\mu_f}{\rho_f}.
\end{aligned}$$

Item	$\rho(\mathrm{kg/m^3})$	$\mathrm{c_p(J/kg\ K)}$	k(W/mK)	$\beta \times 10^5(\mathrm{K^{-1}})$
Pure water	997.1	4179	0.613	21
Copper	8933	385	401	1.67
Alumina	3970	765	40	0.85

Table 3.1: Thermo-physical properties of water and nanoparticles.

The Rosseland radiative heat flux q_r, is given by

$$q_r = -\frac{4\sigma^*}{3k^*}\frac{\partial T^4}{\partial y}, \tag{3.6}$$

where σ^* is the Stefan-Boltzman constant and k^* is the absorption coefficient. If the temperature difference is very small, then the temperature T^4 can be expanded about T_∞ using Taylor series, as follows:

$$T_4 = T_\infty^4 + \frac{4T_\infty^3}{1!}(T-T_\infty)^1 + \frac{12T_\infty^2}{2!}(T-T_\infty)^2 + \frac{24T_\infty^1}{3!}(T-T_\infty)^3 + \frac{24T_\infty}{4!}(T-T_\infty)^4.$$

Ignoring the higher order terms, we have

$$T^4 = T_\infty^4 + 4T_\infty^3(T-T_\infty),$$
$$\Rightarrow T^4 = T_\infty^4 + 4T_\infty^3 T - 4T_\infty^4,$$
$$\Rightarrow T^4 = 4T_\infty^3 T - 3T_\infty^4,$$

$$\Rightarrow \frac{\partial T^4}{\partial y} = 4T_\infty^3\frac{\partial T}{\partial y}. \tag{3.7}$$

Using (3.7) into (3.6) and then differentiating w.r.t y, we get

$$\frac{\partial q_r}{\partial y} = \frac{-16\sigma^* T_\infty^3}{3k^*}\frac{\partial^2 T}{\partial y^2}. \tag{3.8}$$

Then (3.3) gets the following form:

$$u\frac{\partial T}{\partial x} + v\frac{\partial T}{\partial y} = \alpha_{nf}\frac{\partial^2 T}{\partial y^2} + \frac{16\sigma^* T_\infty^3}{3(\rho c_p)_{nf}k^*}\frac{\partial^2 T}{\partial y^2} + \frac{\nu_{nf}}{(\rho c_p)_{nf}}\left(\frac{\partial u}{\partial y}\right)^2. \tag{3.9}$$

3.3 Similarity Transformation

For the conversion of the mathematical model (3.1)-(3.4) into the dimensionless form, the following similarity transformation has been utilized from [48] as:

$$\eta = y\sqrt{\frac{a}{2L\nu_f}}e^{\frac{x}{2L}}, \quad \psi = \sqrt{2aL\nu_f}e^{\frac{x}{2L}}f(\eta), \; \theta(\eta) = \frac{T - T_\infty}{T_w - T_\infty}, \quad h(\eta) = \frac{C - C_\infty}{C_w - C_\infty}.$$

The detailed procedure for the conversion of the partial differential Eqs. (3.1)-(3.4) to the ordinary differential equations in the dimensionless form has been discussed below:

Let ψ be the stream function satisfying the continuity equation in the following sense:

$$u = \frac{\partial \psi}{\partial y}, \; v = -\frac{\partial \psi}{\partial x}. \tag{3.10}$$

Consider the velocity components and there partial derivative as follows:

$$\begin{aligned}
u &= \frac{\partial \psi}{\partial y} \\
&= \frac{\partial \psi}{\partial \eta}\frac{\partial \eta}{\partial y} \\
&= \sqrt{2aL\nu_f}e^{\frac{x}{2L}}f'(\eta)\sqrt{\frac{a}{2\nu_f L}}e^{\frac{x}{2L}} \\
&= \sqrt{\frac{2a^2L\nu_f}{2\nu_f L}}e^{\frac{2x}{2L}}f'(\eta) = ae^{\frac{x}{L}}f'(\eta).
\end{aligned}$$

$$\begin{aligned}
\frac{\partial u}{\partial x} &= \frac{\partial}{\partial x}\left(ae^{\frac{x}{L}}f'(\eta)\right) \\
&= a\left(\frac{\partial f'(\eta)}{\partial \eta}.\frac{\partial \eta}{\partial x}.e^{\frac{x}{L}} + f'(\eta).\frac{\partial}{\partial x}(e^{\frac{x}{L}})\right) \\
&= a\left(f''(\eta).\frac{\partial \eta}{\partial x}.e^{\frac{x}{L}} + f'(\eta).\frac{\partial}{\partial x}(e^{\frac{x}{L}})\right) \\
&= a\left(f''(\eta).y\sqrt{\frac{a}{2\nu_f L}}e^{\frac{x}{2L}}.\frac{1}{2L}e^{\frac{x}{L}} + \frac{1}{L}.f'(\eta)e^{\frac{x}{L}}\right) \\
&= a\left(\frac{\eta f''(\eta)}{2L} + \frac{1}{L}f'(\eta)\right)e^{\frac{x}{L}}
\end{aligned}$$

$$= \frac{ae^{\frac{x}{L}}}{2L}\Bigg(\eta f''(\eta) + 2f'(\eta)\Bigg). \tag{3.11}$$

$$\begin{aligned}
v = -\frac{\partial \psi}{\partial x} &= -\frac{\partial}{\partial x}\Bigg(\sqrt{2aL\nu_f}f(\eta)e^{\frac{x}{2L}}\Bigg)\\
&= -\sqrt{2aL\nu_f}\Bigg(\frac{\partial f(\eta)}{\partial x}e^{\frac{x}{2L}} + f(\eta)\frac{\partial}{\partial x}e^{\frac{x}{2L}}\Bigg)\\
&= -\sqrt{2aL\nu_f}\Bigg(\frac{\partial f(\eta)}{\partial \eta}.\frac{\partial \eta}{\partial x}.e^{\frac{x}{2L}} + f(\eta).e^{\frac{x}{2L}}\frac{1}{2L}\Bigg)\\
&= -\sqrt{2aL\nu_f}\Bigg(f'(\eta)y\sqrt{\frac{a}{2\nu_f L}}e^{\frac{x}{2L}}.e^{\frac{x}{2L}}\frac{1}{2L} + \frac{1}{2L}f(\eta)e^{\frac{x}{2L}}\Bigg)\\
&= -\sqrt{2aL\nu_f}\Bigg(\eta f'(\eta)e^{\frac{x}{2L}}\frac{1}{2L} + \frac{1}{2L}f(\eta)e^{\frac{x}{2L}}\Bigg)\\
&= -\sqrt{2aL\nu_f}\frac{e^{\frac{x}{2L}}}{2L}\Bigg(\eta f'(\eta) + f(\eta)\Bigg).
\end{aligned}$$

$$\begin{aligned}
\frac{\partial v}{\partial y} =& -\sqrt{2aL\nu_f}\Bigg(\frac{\partial}{\partial y}(\eta f(\eta)) + \frac{\partial f'(\eta)}{\partial y}\Bigg)\frac{1}{2L}e^{\frac{x}{2L}}\\
=& -\sqrt{2aL\nu_f}\Bigg(\frac{\partial \eta}{\partial y}f'(\eta) + \frac{\partial f'(\eta)}{\partial \eta}\frac{\partial \eta}{\partial y}\eta + \frac{\partial f(\eta)}{\partial \eta}\frac{\partial \eta}{\partial y}\Bigg)\frac{1}{2L}e^{\frac{x}{2L}}\\
=& -\frac{\sqrt{2aL\nu_f}}{2L}\Bigg(\sqrt{\frac{a}{2L\nu_f}}e^{\frac{x}{2L}}f'(\eta) + \eta f''(\eta)\sqrt{\frac{a}{2L\nu_f}}e^{\frac{x}{2L}}\\
&+ f'(\eta)\sqrt{\frac{a}{2L\nu_f}}e^{\frac{x}{2L}}\Bigg)e^{\frac{x}{2L}}\\
=& -\frac{\sqrt{2aL\nu_f}}{2L}\sqrt{\frac{a}{2L\nu_f}}\Bigg(f'(\eta) + \eta f''(\eta) + f'(\eta)\Bigg)e^{\frac{x}{2L}}e^{\frac{x}{2L}}\\
=& -\frac{ae^{\frac{x}{L}}}{2L}\Bigg(\eta f''(\eta) + 2f'(\eta)\Bigg)
\end{aligned} \tag{3.12}$$

Verification of the continuity equation has been carried out as:

$$\frac{\partial u}{\partial x} + \frac{\partial v}{\partial y} = \frac{a}{2L}\Bigg(\eta f''(\eta) + 2f'(\eta)\Bigg)e^{\frac{x}{L}} - \frac{a}{2L}\Bigg(\eta f''(\eta) + 2f'(\eta)\Bigg)e^{\frac{x}{L}} = 0.$$

Next eq. (3.2) will be converted into the dimensionless form. The procedure includes the following conversion of different terms from dimensional to the non dimensional form:

$$\begin{aligned}\frac{\partial u}{\partial y} &= ae^{\frac{x}{L}}\frac{\partial f'}{\partial \eta}.\frac{\partial \eta}{\partial y}\\ &= ae^{\frac{x}{L}}\frac{x}{L}f''(\eta).\sqrt{\frac{a}{2L\nu_f}}e^{\frac{x}{2L}}\\ &= a\sqrt{\frac{a}{2L\nu_f}}e^{\frac{3x}{2L}}f''(\eta)\end{aligned}$$

$$\begin{aligned}u\frac{\partial u}{\partial x} &= \left(ae^{\frac{x}{L}}f'(\eta)\right)\frac{a}{2L}\left(\eta f''(\eta)+2f'(\eta)\right)e^{\frac{x}{L}}\\ &= \frac{a^2}{2L}e^{\frac{2x}{L}}\left(\eta f'(\eta)f''(\eta)+2f'^2(\eta)\right). \qquad (3.13)\end{aligned}$$

$$\begin{aligned}v\frac{\partial u}{\partial y} &= \left(-\frac{\sqrt{2aL\nu_f}}{2L}e^{\frac{x}{2L}}\eta f'(\eta)+f(\eta)\right).\left(a\sqrt{\frac{a}{2L\nu_f}}e^{\frac{3x}{2L}}f''(\eta)\right)\\ &= -a\frac{\sqrt{2aL\nu_f}}{2L}\sqrt{\frac{a}{2L\nu_f}}e^{\frac{x}{2L}}e^{\frac{3x}{2L}}\left(\eta f'(\eta)f''(\eta)+f''(\eta)f(\eta)\right)\\ &= -\frac{a^2}{2L}e^{\frac{2x}{L}}\left(\eta f''(\eta)f'(\eta)+f''(\eta)f(\eta)\right) \qquad (3.14)\end{aligned}$$

Using (3.13) and (3.14), the left side of (3.2) becomes:

$$\begin{aligned}u\frac{\partial u}{\partial x}+v\frac{\partial u}{\partial y} =&\frac{a^2}{2L}\left(\eta f''(\eta)f'(\eta)+2f'^2(\eta)\right)\\ &-\frac{a^2}{2L}e^{\frac{2x}{L}}\left(\eta f''(\eta)f'(\eta)+f''(\eta)f(\eta)\right)\\ =&\frac{a^2}{2L}e^{\frac{2x}{L}}\left(2f'^2(\eta)-f''(\eta)f(\eta)\right).\end{aligned}$$

To convert the right side of Eq. (3.2) into the dimensionless form, the following procedure has been followed:

$$\begin{aligned}U_\infty\frac{dU_\infty}{dx} &= ae^{\frac{x}{L}}\frac{d}{dx}\left(ae^{\frac{x}{L}}\right)\\ &= ae^{\frac{x}{L}}\frac{1}{L}ae^{\frac{x}{L}}\\ &= \frac{a^2}{L}e^{\frac{2x}{L}} \qquad (3.15)\end{aligned}$$

$$\begin{aligned}
\frac{\partial^2 u}{\partial y^2} &= \frac{\partial}{\partial y}\left(\frac{\partial u}{\partial y}\right) = \frac{\partial}{\partial y}\left(a\sqrt{\frac{a}{2L\nu_f}}e^{\frac{3x}{2L}}f''(\eta)\right)\\
&= a\sqrt{\frac{a}{2L\nu_f}}e^{\frac{3x}{2L}}\frac{\partial f''}{\partial \eta}.\frac{\partial \eta}{\partial y} = a\sqrt{\frac{a}{2L\nu_f}}e^{\frac{3x}{2L}}f'''(\eta)\sqrt{\frac{a}{2L\nu_f}}e^{\frac{x}{2L}}\\
&= \frac{a^2}{2L\nu_f}e^{\frac{2x}{L}}f'''(\eta).
\end{aligned}$$

$$\begin{aligned}
\nu_{nf}\frac{\partial^2 u}{\partial y^2} &= \frac{\mu_{nf}}{\rho_{nf}}\left(\frac{\partial^2 u}{\partial y^2}\right)\\
&= \frac{\mu_f}{(1-\phi)^{2.5}((1-\phi)\rho_f+\phi\rho_s)}\left(\frac{a^2}{2L\nu_f}e^{\frac{2x}{L}}f'''(\eta)\right)\\
&= \frac{\mu_f a^2 e^{\frac{2x}{L}}}{\frac{\mu_f}{\rho_f}2L(1-\phi)^{2.5}\rho_f(1-\phi+\frac{\phi\rho_s}{\rho_f})}f'''(\eta) \qquad \left(\because \nu_f = \frac{\mu_f}{\rho_f}\right)\\
&= \frac{a^2 e^{\frac{2x}{L}}}{2L(1-\phi)^{2.5}(1-\phi+\frac{\phi\rho_s}{\rho_f})}f'''(\eta) \qquad (3.16)
\end{aligned}$$

$$\begin{aligned}
\frac{\nu_{nf}}{k}(U_\infty - u) &= \frac{\mu_f}{k_0 e^{-\frac{x}{L}}(1-\phi)^{2.5}\left((1-\phi)\rho_f+\phi\rho_s\right)}.\left(ae^{\frac{x}{L}} - ae^{\frac{x}{L}}f'(\eta)\right)\\
&= \frac{\nu_f\rho_f}{\rho_f k_0(1-\phi)^{2.5}\left(1-\phi+\frac{\phi\rho_s}{\rho_f}\right)}ae^{\frac{x}{L}}e^{\frac{x}{L}}\left(1-f'(\eta)\right)\\
&= \frac{a\nu_f e^{\frac{2x}{L}}}{k_0(1-\phi)^{2.5}\left(1-\phi+\phi\frac{\rho_s}{\rho_f}\right)}\left(1-f'(\eta)\right) \qquad (3.17)
\end{aligned}$$

$$\begin{aligned}
\frac{\sigma B^2}{\rho_{nf}}(U_\infty - u) &= \frac{\sigma(B_0 e^{\frac{x}{2L}})^2}{(1-\phi)\rho_f+\phi\rho_s}\left(ae^{\frac{x}{L}} - ae^{\frac{x}{L}}f'(\eta)\right)\\
&= \frac{\sigma(B_0 e^{\frac{x}{2L}})^2}{(1-\phi)\rho_f+\phi\rho_s}ae^{\frac{x}{L}}\left(1-f'(\eta)\right)\\
&= \frac{\sigma B_0^2 a e^{\frac{2x}{L}}}{\rho_f\left(1-\phi+\frac{\phi\rho_s}{\rho_f}\right)}\left(1-f'(\eta)\right). \qquad (3.18)
\end{aligned}$$

Using (3.15) - (3.18) in the right side of (3.2), we get

$$\begin{aligned}
&U_\infty\frac{dU_\infty}{dx} + \nu_{nf}\frac{\partial^2 u}{\partial y^2} + \frac{\nu_{nf}}{k}(U_\infty - u) + \frac{\sigma B^2}{\rho_{nf}}(U_\infty - u)\\
&= \frac{a^2 e^{\frac{2x}{L}}}{L} + \frac{a^2 e^{\frac{2x}{L}}f'''(\eta)}{2L(1-\phi)^{2.5}\left(1-\phi+\frac{\phi\rho_s}{\rho_f}\right)}
\end{aligned}$$

$$+\frac{a\nu_f e^{\frac{2x}{L}}}{k_0(1-\phi)^{2.5}\left(1-\phi+\phi\frac{\rho_s}{\rho_f}\right)}\left(1-f'(\eta)\right)$$
$$+\frac{\sigma B_0^2 a e^{\frac{2x}{L}}}{\rho_f\left(1-\phi+\frac{\phi\rho_s}{\rho_f}\right)}\left(1-f'(\eta)\right)$$

Hence the dimensionless form of (3.2) becomes

$$\frac{a^2e^{\frac{2x}{L}}}{2L}\left(2f'^2(\eta)-f''(\eta)f(\eta)\right)=\frac{a^2e^{\frac{2x}{L}}}{2L}\left[2+\frac{1}{(1-\phi)^{2.5}(1-\phi+\frac{\phi\rho_s}{\rho_f})}f'''(\eta)\right.$$
$$\left.+\frac{2L\nu_f}{ak_0(1-\phi)^{2.5}(1-\phi+\phi\frac{\rho_s}{\rho_f})}\left(1-f'(\eta)\right)+\frac{2L\sigma B_0^2}{a\rho_f(1-\phi+\frac{\phi\rho_s}{\rho_f})}\left(1-f'(\eta)\right)\right]$$
$$\Rightarrow 2f'^2(\eta)-f''(\eta)f(\eta)=2+\frac{f'''(\eta)}{(1-\phi)^{2.5}(1-\phi+\frac{\phi\rho_s}{\rho_f})}$$
$$+\left(\frac{2L\nu_f}{ak_0(1-\phi)^{2.5}(1-\phi+\phi\frac{\rho_s}{\rho_f})}+\frac{2L\sigma B_0^2}{a\rho_f(1-\phi+\frac{\phi\rho_s}{\rho_f})}\right)\left(1-f'(\eta)\right)$$
$$\Rightarrow -2+2f'^2(\eta)-f''(\eta)f(\eta)=\frac{f'''(\eta)}{(1-\phi)^{2.5}(1-\phi+\frac{\phi\rho_s}{\rho_f})}$$
$$+\left(\frac{2L\nu_f}{ak_0(1-\phi)^{2.5}(1-\phi+\phi\frac{\rho_s}{\rho_f})}+\frac{2L\sigma B_0^2}{a\rho_f(1-\phi+\frac{\phi\rho_s}{\rho_f})}\right)\left(1-f'(\eta)\right)$$
$$\Rightarrow \frac{f'''(\eta)}{(1-\phi)^{2.5}(1-\phi+\frac{\phi\rho_s}{\rho_f})}+2\left(1-f'^2(\eta)\right)+f(\eta)f''(\eta)$$
$$\left[\frac{1}{(1-\phi)^{2.5}\left(1-\phi+\frac{\phi\rho_s}{\rho_f}\right)}\left(\frac{2L\nu_f}{ak_0}+\frac{2L\sigma B_0^2}{a\rho_f}(1-\phi)^{2.5}\right)\left(1-f'(\eta)\right)\right]=0. \tag{3.19}$$

Next, we include the procedure for the conversion of (3.3) into the dimensionless form:

$$\theta(\eta)=\frac{T-T_\infty}{T_w-T_\infty}$$
$$\Rightarrow\quad T=(T_w-T_\infty)\theta(\eta)+T_\infty$$
$$=(T_w-T_\infty)\theta(\eta)+T_\infty$$

$$=(T_\infty+T_0e^{\frac{x}{2L}}-T_\infty)\theta(\eta)+T_\infty$$
$$=T_0e^{\frac{x}{2L}}\theta(\eta)+T_\infty.$$

$$\begin{aligned}\frac{\partial T}{\partial x} &= T_0\Bigg(\theta(\eta)\frac{\partial}{\partial x}(e^{\frac{x}{2L}}) + e^{\frac{x}{2L}}\frac{\partial \theta(\eta)}{\partial \eta}\frac{\partial \eta}{\partial x}\Bigg) + \frac{\partial}{\partial x}T_\infty \\ &= \frac{T_0}{2L}\Bigg(\theta(\eta)e^{\frac{x}{2L}} + e^{\frac{x}{2L}}\theta'(\eta)y\sqrt{\frac{a}{2L\nu_f}}e^{\frac{x}{2L}}\Bigg) \\ &= \frac{T_0}{2L}e^{\frac{x}{2L}}(\theta(\eta) + \eta\theta'(\eta)). \end{aligned} \tag{3.20}$$

$$\begin{aligned} u\frac{\partial T}{\partial x} &= ae^{\frac{x}{L}}f'(\eta)\frac{T_0e^{\frac{x}{2L}}}{2L}\Bigg(\theta(\eta) + \eta\theta'(\eta)\Bigg) \\ &= a\frac{T_0}{2L}e^{\frac{3x}{2L}}f'(\eta)\Bigg(\theta(\eta) + \eta\theta'(\eta)\Bigg) \end{aligned} \tag{3.21}$$

$$\begin{aligned}\frac{\partial T}{\partial y} &= \frac{\partial}{\partial y}\Bigg(T_0e^{\frac{x}{2L}}\theta(\eta)\Bigg) \\ &= T_0e^{\frac{x}{2L}}\frac{\partial \theta(\eta)}{\partial \eta}\frac{\partial \eta}{\partial y} \\ &= T_0e^{\frac{x}{2L}}\theta'(\eta)\sqrt{\frac{a}{2L\nu_f}}e^{\frac{x}{2L}} \\ &= T_0e^{\frac{x}{L}}\sqrt{\frac{a}{2L\nu_f}}\theta'(\eta). \end{aligned}$$

$$\begin{aligned} v\frac{\partial T}{\partial y} &= \Bigg(-\frac{1}{2L}\sqrt{2aL\nu_f}e^{\frac{x}{2L}}(\eta f'(\eta) + f(\eta))\Bigg)\Bigg(T_0e^{\frac{x}{L}}\sqrt{\frac{a}{2L\nu_f}}\theta'(\eta)\Bigg) \\ &= -\frac{T_0}{2L}\sqrt{2aL\nu_f}\sqrt{\frac{a}{2aL\nu_f}}e^{\frac{x}{2L}}e^{\frac{x}{2L}}\Bigg(\eta f'(\eta) + f(\eta)\Bigg)\theta'(\eta) \\ &= -\frac{T_0}{2L}\sqrt{\frac{2a^2L\nu_f}{2aL\nu_f}}e^{\frac{3x}{2L}}\Bigg(\eta f'(\eta)\theta'(\eta) + f(\eta)\theta'(\eta)\Bigg) \\ &= -\frac{aT_0e^{\frac{3x}{2L}}}{2L}\Bigg(\eta f'(\eta)\theta'(\eta) + f(\eta)\theta'(\eta)\Bigg) \end{aligned} \tag{3.22}$$

Using (3.21) and (3.22), the left side of (3.3) gets the following form:

$$\begin{aligned} u\frac{\partial T}{\partial x} + v\frac{\partial T}{\partial y} =& \frac{aT_0e^{\frac{3x}{2L}}}{2L}\Bigg(f'(\eta)\theta(\eta) + \eta f'(\eta)\theta'(\eta)\Bigg) \\ &- \frac{aT_0e^{\frac{3x}{2L}}}{2L}\Bigg(\eta f'(\eta)\theta'(\eta) + f(\eta)\theta'(\eta)\Bigg) \\ =& \frac{aT_0e^{\frac{3x}{2L}}}{2L}\Bigg(f'(\eta)\theta(\eta) - f(\eta)\theta'(\eta)\Bigg). \end{aligned}$$

To convert the right side of (3.3) into dimensionless form, we proceed as follows:

$$\begin{aligned}\frac{\partial^2 T}{\partial y^2} &= \frac{\partial}{\partial y}\left(\frac{\partial T}{\partial y}\right)\left(T_0\sqrt{\frac{a}{2\nu_f L}}e^{\frac{x}{L}}\theta'(\eta)\right)\\ &= T_0\sqrt{\frac{a}{2\nu_f L}}e^{\frac{x}{L}}\frac{\partial\theta'}{\partial\eta}\frac{\partial\eta}{\partial y} = T_0\sqrt{\frac{a}{2\nu_f L}}e^{\frac{x}{L}}\theta''(\eta)\sqrt{\frac{a}{2\nu_f L}}e^{\frac{x}{2L}}\\ &= T_0\left(\sqrt{\frac{a}{2\nu_f L}}\right)^2 e^{\frac{x}{L}}e^{\frac{x}{2L}}\theta''(\eta)\\ &= \frac{aT_0}{2\nu_f L}e^{\frac{3x}{2L}}\theta''(\eta)\end{aligned}$$

$$\alpha_{nf}\frac{\partial^2 T}{\partial y^2} = \frac{k_{nf}}{(\rho c_p)_{nf}}\frac{aT_0}{2\nu_f L}e^{\frac{3x}{2L}}\theta''(\eta). \tag{3.23}$$

$$\begin{aligned}\frac{1}{(\rho c_p)_{nf}}\frac{\partial q_r}{\partial y} &= \frac{1}{(\rho c_p)_{nf}}\frac{-16\sigma^* T_\infty^3}{3k^*}\frac{aT_0 e^{\frac{3x}{2L}}}{2\nu_f L}\theta''(\eta)\\ &= \frac{-16\sigma^* T_\infty^3}{3k^*(\rho c_p)_{nf}}\frac{aT_0 e^{\frac{3x}{2L}}}{2L\nu_f}\theta''(\eta).\end{aligned} \tag{3.24}$$

$$\begin{aligned}\frac{\mu_{nf}}{(\rho c_p)_{nf}}\left(\frac{\partial u}{\partial y}\right)^2 &= \frac{\mu_{nf}}{(\rho c_p)_{nf}}\left(a\sqrt{\frac{a}{2L\nu_f}}e^{\frac{3x}{2L}}f''(\eta)\right)^2\\ &= \frac{\mu_{nf}}{(\rho c_p)_{nf}}\frac{a^3}{2L\nu_f}\left(e^{\frac{3x}{2L}}\right)^2 f''^2(\eta)\end{aligned} \tag{3.25}$$

Using (3.23) - (3.25), the dimensionless form of right side of (3.3) is as follows.

$$\begin{aligned}&\alpha_{nf}\frac{\partial^2 T}{\partial y^2} - \frac{1}{(\rho c_p)}\frac{\partial q_r}{\partial y} + \frac{\mu_{nf}}{(\rho c_p)_{nf}}\left(\frac{\partial u}{\partial y}\right)^2\\ &= \frac{K_{nf}T_0 a e^{\frac{3x}{2L}}}{2\nu_f L(\rho c_p)_{nf}}\theta''(\eta) + \frac{16\sigma^* T_\infty^3 a T_0 e^{\frac{3x}{2L}}}{6k^*\nu_f L(\rho c_p)_{nf}}\theta''(\eta) + \frac{a^3\left(e^{\frac{3x}{2L}}\right)^2\mu_{nf}}{2L\nu_f(\rho c_p)_{nf}}f''^2(\eta)\\ &= \frac{aT_0 e^{\frac{3x}{2L}}}{2L}\left[\frac{k_{nf}}{\nu_f(\rho c_p)_{nf}}\theta''(\eta)\frac{16\sigma^* T_\infty^3}{3k^*\nu_f(\rho c_p)_{nf}}\theta''(\eta)\right.\\ &\quad\left. + \frac{\mu_{nf}\left(a^2 e^{\frac{3x}{2L}}\right)}{\nu_f T_0(\rho c_p)_{nf}}f''^2(\eta)\right]\\ &= \frac{aT_0 e^{\frac{3x}{2L}}}{2L}\left[\left(\frac{k_{nf}}{k_f}\frac{(\rho c_p)_f}{\rho c_p)_{nf}}\frac{k_f}{\rho c_p)_f}\frac{1}{\nu_f}\right)\theta''(\eta) + \left(\frac{(\rho c_p)_f}{\rho c_p)_{nf}}\frac{k_f}{(\rho c_p)_f\nu_f}\frac{16\sigma^* T_\infty^3}{3k^* k_f}\right)\theta''(\eta)\right.\\ &\quad\left. + \left(\frac{\mu_{nf}}{\mu_f}\frac{(\rho c_p)_f}{\rho c_p)_{nf}}\frac{\mu_f}{(\rho c_p)_f}\frac{\left(a^2 e^{\frac{3x}{2L}}\right)}{T_0\nu_f}\right)f''^2(\eta)\right]\end{aligned}$$

$$
\begin{aligned}
&= \frac{aT_0 e^{\frac{3x}{2L}}}{2L}\Bigg[\left(\frac{k_f}{k_{nf}}\frac{1}{\left(1-\phi+\frac{\phi(\rho c_p)_s}{(\rho c_p)_f}\right)}\frac{\alpha_f}{\nu_f}\right)\theta''(\eta) \qquad \left(\because \alpha_f = \frac{k_f}{(\rho c_p)_f}\right)\\
&+\left(\frac{1}{\left(1-\phi+\frac{\phi(\rho c_p)_s}{(\rho c_p)_f}\right)}\frac{\alpha_f}{\nu_f}\frac{16\sigma^* T_\infty^3}{3k^* k_f}\right)\theta''(\eta)\\
&+\frac{1}{(1-\phi)^{2.5}\left(1-\phi+\frac{\phi(\rho c_p)_s}{(\rho c_p)_f}\right)}\frac{\mu_f}{\rho_f}\frac{1}{\nu_f}\frac{\left(a^2 e^{\frac{3x}{2L}}\right)}{T_0 (c_p)_f} f''^2(\eta)\Bigg]\\
&= \frac{aT_0 e^{\frac{3x}{2L}}}{2L}\Bigg[\left(\frac{k_{nf}}{k_f}\frac{1}{\left(1-\phi+\frac{\phi(\rho c_p)_s}{(\rho c_p)_f}\right)}\frac{1}{P_r}\right)\theta''(\eta) \qquad \left(\because P_r = \frac{\nu_f}{\alpha_f}\right)\\
&+\left(\frac{1}{\left(1-\phi+\frac{\phi(\rho c_p)_s}{(\rho c_p)_f}\right)}\frac{1}{P_r}\frac{16\sigma^* T_\infty^3}{3k^* k_f}\right)\theta''(\eta)\\
&+\left(\frac{1}{(1-\phi)^{2.5}\left(1-\phi+\frac{\phi(\rho c_p)_s}{(\rho c_p)_f}\right)}\frac{(a e^{\frac{x}{L}})^2}{(T_w - T_\infty)(c_p)_f}\right) f''^2(\eta)\Bigg] \qquad (3.26)\\
&\qquad\qquad \left(\because \mu_f = \rho_f \nu_f, T_0 = \frac{T_w - T_\infty}{e^{\frac{x}{L}}}\right)
\end{aligned}
$$

Therefore the dimensionless form of (3.3) becomes:

$$
\begin{aligned}
\frac{aT_0 e^{\frac{3x}{2L}}}{2L}\Big(f'(\eta)\theta(\eta) - f(\eta)\theta'(\eta)\Big) &= \frac{aT_0 e^{\frac{3x}{2L}}}{2L}\Bigg[\left(\frac{k_{nf}}{k_f}\frac{1}{\left(1-\phi+\frac{\phi(\rho c_p)_s}{(\rho c_p)_f}\right)}\frac{1}{P_r}\right)\theta''(\eta)\\
&+\left(\frac{1}{\left(1-\phi+\frac{\phi(\rho c_p)_s}{(\rho c_p)_f}\right)}\frac{1}{P_r}\frac{16\sigma^* T_\infty^3}{3k^* k_f}\right)\theta''(\eta)\\
&+\frac{(U_\infty)^2 f''^2(\eta)}{(1-\phi)^{2.5}\left(1-\phi+\frac{\phi(\rho c_p)_s}{(\rho c_p)_f}\right)(T_w - T_\infty)(c_p)_f}\Bigg]\\
\Rightarrow \Big(f'(\eta)\theta(\eta) - f(\eta)\theta'(\eta)\Big)P_r &= \Bigg[\left(\frac{k_{nf}}{k_f}\frac{1}{\left(1-\phi+\frac{\phi(\rho c_p)_s}{(\rho c_p)_f}\right)}\right)\theta''(\eta)\\
&+\left(\frac{1}{\left(1-\phi+\frac{\phi(\rho c_p)_s}{(\rho c_p)_f}\right)}\frac{16\sigma^* T_\infty^3}{3k^* k_f}\right)\theta''(\eta)\\
&+\frac{P_r}{(1-\phi)^{2.5}\left(1-\phi+\frac{\phi(\rho c_p)_s}{(\rho c_p)_f}\right)}\frac{(U_\infty)^2 f''^2(\eta)}{(T_w - T_\infty)(c_p)_f}\Bigg]
\end{aligned}
$$

$$\begin{aligned}
&\Rightarrow \Big(f'(\eta)\theta(\eta) - f(\eta)\theta'(\eta)\Big)P_r = \frac{1}{\left(1-\phi+\frac{\phi(\rho c_p)_s}{(\rho c_p)_f}\right)}\Bigg[\left(\frac{k_{nf}}{k_f}\right)\theta''(\eta) \\
&\qquad + \left(\frac{16\sigma^* T_\infty^3}{3k^* k_f}\right)\theta''(\eta) \\
&\qquad + \frac{1}{(1-\phi)^{2.5}}P_r\frac{(U_\infty)^2}{(T_w-T_\infty)(c_p)_f}f''^2(\eta)\Bigg] \\
&\Rightarrow \Big(f'(\eta)\theta(\eta) - f(\eta)\theta'(\eta)\Big)P_r = \frac{1}{\left(1-\phi+\frac{\phi(\rho c_p)_s}{(\rho c_p)_f}\right)}\Bigg[\left(\frac{k_{nf}}{k_f}+\frac{16\sigma^* T_\infty^3}{3k^* k_f}\right)\theta''(\eta) \\
&\qquad + \frac{1}{(1-\phi)^{2.5}}P_r\frac{(U_\infty)^2}{(T_w-T_\infty)(c_p)_f}f''^2(\eta)\Bigg].
\end{aligned}$$

$$\begin{aligned}
&\Rightarrow \left(1-\phi+\frac{\phi(\rho c_p)_s}{(\rho c_p)_f}\right)\Big(f'(\eta)\theta(\eta) - f(\eta)\theta'(\eta)\Big)P_r = \Bigg[\left(\frac{k_{nf}}{k_f}+\frac{16\sigma^* T_\infty^3}{3k^* k_f}\right)\theta''(\eta) \\
&\quad + \frac{1}{(1-\phi)^{2.5}}P_r\frac{(U_\infty)^2}{(T_w-T_\infty)(c_p)_f}f''^2(\eta)\Bigg]. \\
&\Rightarrow \left(\frac{k_{nf}}{k_f}+\frac{16\sigma^* T_\infty^3}{3k^* k_f}\right)\theta''(\eta) + P_r\left(1-\phi+\frac{\phi(\rho c_p)_s}{(\rho c_p)_f}\right)\Big(-f'(\eta)\theta(\eta) + f(\eta)\theta'(\eta)\Big) \\
&\quad + \frac{1}{(1-\phi)^{2.5}}P_r\frac{(U_\infty)^2}{(T_w-T_\infty)(c_p)_f}f''^2(\eta)\Bigg].
\end{aligned}$$

Next, we include the procedure for the conversion of (3.4) into the dimensionless form:

$$\begin{aligned}
h(\eta) &= \frac{C-C_\infty}{C_w-C_\infty} \\
\Rightarrow C &= h(\eta)(C_w-C_\infty)+C_\infty \\
&= h(\eta)(C_0 e^{\frac{x}{2L}})+C_\infty
\end{aligned}$$

$$\begin{aligned}
\frac{\partial C}{\partial x} &= h(\eta)\frac{\partial}{\partial x}(C_0 e^{\frac{x}{2L}}) \\
&= C_0\frac{e^{\frac{x}{2L}}}{2L}h(\eta) + C_0 e^{\frac{x}{2L}}\frac{\partial h(\eta)}{\partial \eta}\frac{\partial \eta}{\partial x} \\
&= C_0\frac{e^{\frac{x}{2L}}}{2L}h(\eta) + C_0 e^{\frac{x}{2L}}h'(\eta)y\sqrt{\frac{a}{2\nu_f L}}\frac{e^{\frac{x}{2L}}}{2L} \\
&= C_0\frac{e^{\frac{x}{2L}}}{2L}\left(h(\eta)+\eta h'(\eta)\right)
\end{aligned}$$

$$\begin{aligned}u\frac{\partial C}{\partial x} &= af'(\eta)e^{\frac{x}{L}}C_0\frac{e^{\frac{x}{2L}}}{2L}\left(h(\eta)+\eta h'(\eta)\right)\\ &= \frac{ae^{\frac{3x}{2L}}}{2L}C_0(h(\eta)f'(\eta)+\eta h'(\eta)f'(\eta))\end{aligned} \tag{3.27}$$

$$\begin{aligned}\frac{\partial C}{\partial y} &= C_0e^{\frac{x}{2L}}\frac{\partial h(\eta)}{\partial \eta}\frac{\partial \eta}{\partial y}\\ &= C_0e^{\frac{x}{2L}}h'(\eta)\sqrt{\frac{a}{2\nu_f L}}e^{\frac{x}{2L}}\\ &= C_0e^{\frac{x}{L}}h'(\eta)\sqrt{\frac{a}{2\nu_f L}}\end{aligned}$$

$$\begin{aligned}v\frac{\partial C}{\partial y} &= -\sqrt{2aL\nu_f}\frac{e^{\frac{x}{2L}}}{2L}\left(\eta f'(\eta)+f(\eta)\right)C_0\sqrt{\frac{a}{2\nu_f L}}e^{\frac{x}{L}}h'(\eta)\\ &= -C_0\frac{ae^{\frac{3x}{2L}}}{2L}(\eta f'(\eta)h'(\eta)+f(\eta)h'(\eta)).\end{aligned} \tag{3.28}$$

Using (3.27) and (3.28) in the left side of (3.4), we get

$$\begin{aligned}u\frac{\partial C}{\partial x}+v\frac{\partial C}{\partial y} &= C_0\frac{ae^{\frac{3x}{2L}}}{2L}(h(\eta)f'(\eta)+\eta h'(\eta)f'(\eta)-\eta f'(\eta)h'(\eta)-f(\eta)h'(\eta))\\ &= \frac{ae^{\frac{3x}{2L}}}{2L}C_0(f'(\eta)h(\eta)-h'(\eta)f(\eta)).\end{aligned} \tag{3.29}$$

To convert the right side of (3.4) into the dimensionless form, we proceed as follows:

$$\begin{aligned}\frac{\partial^2 C}{\partial y^2} &= \frac{\partial}{\partial y}\left(\sqrt{\frac{a}{2L\nu_f}}C_0e^{\frac{x}{L}}h'(\eta)\right)\\ &= \left(C_0e^{\frac{x}{L}}\sqrt{\frac{a}{2L\nu_f}}\frac{\partial h'(\eta)}{\partial \eta}\frac{\partial \eta}{\partial y}\right)\\ &= C_0e^{\frac{x}{L}}\sqrt{\frac{a}{2L\nu_f}}h''(\eta)\sqrt{\frac{a}{2L\nu_f}}e^{\frac{x}{2L}}\\ &= C_0e^{\frac{x}{L}}e^{\frac{x}{2L}}\frac{a}{2L\nu_f}h''(\eta)\\ &= C_0e^{\frac{3x}{2L}}\frac{a}{2L\nu_f}h''(\eta)\end{aligned} \tag{3.30}$$

$$\begin{aligned} h(\eta) &= \frac{C - C_\infty}{C_w - C_\infty} \\ \Rightarrow (C - C_\infty) &= h(\eta)(C_w - C_\infty) \\ \Rightarrow K(C - C_\infty) &= K_0 e^{\frac{x}{L}} h(\eta)(C_\infty + C_0 e^{\frac{x}{2L}} - C_\infty) \\ &= C_0 K_0 e^{\frac{3x}{2L}} h(\eta) \end{aligned} \tag{3.31}$$

Using (3.30) and (3.31) in the right side of (3.4), we get

$$\begin{aligned} D\frac{\partial^2 C}{\partial y^2} - K(C - C_\infty) &= DC_0 e^{\frac{3x}{2L}} \frac{a}{2L\nu_f} h''(\eta) - C_0 K_0 e^{\frac{3x}{2L}} h(\eta) \\ &= C_0 e^{\frac{3x}{2L}} \left(D\frac{a}{2L\nu_f} h''(\eta) - K_0 h(\eta) \right). \end{aligned} \tag{3.32}$$

Hence the dimensionless form of (3.4) becomes:

$$\begin{aligned} &C_0 \frac{a e^{\frac{3x}{2L}}}{2L} (f'(\eta)h(\eta) - h'(\eta)f(\eta)) = C_0 e^{\frac{3x}{2L}} \left(\frac{Dah''(\eta)}{2L\nu_f} - K_0 h(\eta) \right) \\ &\Rightarrow \frac{a}{2L} (f'(\eta)h(\eta) - h'(\eta)f(\eta)) = \frac{Da}{2L\nu_f} h''(\eta) - K_0 h(\eta) \\ &\Rightarrow (f'(\eta)h(\eta) - h'(\eta)f(\eta)) = \frac{D}{\nu_f} h''(\eta) - \frac{2L}{a} K_0 h(\eta) \\ &\Rightarrow \frac{\nu_f}{D} (f'(\eta)h(\eta) - h'(\eta)f(\eta)) = h''(\eta) - \frac{2LK_0\nu_f}{a} h(\eta) \\ &\Rightarrow \left(\frac{\nu_f}{D} (f'(\eta)h(\eta) - h'(\eta)f(\eta)) + \frac{2LK_0\nu_f}{a} h(\eta) \right) = h''(\eta) \\ &\Rightarrow h''(\eta) + \frac{\nu_f}{D} (f'(\eta)h(\eta) - h'(\eta)f(\eta)) - \frac{2LK_0\nu_f}{a} h(\eta) = 0. \end{aligned}$$

The final dimensionless form of the governing model is:

$$\begin{aligned} &\frac{1}{(1-\phi)^{2.5}\left(1 - \phi + \phi\frac{\rho_s}{\rho_f}\right)} f''' + ff'' + 2(1 - f'^2) \\ &\quad + \frac{1}{(1-\phi)^{2.5}\left(1 - \phi + \phi\frac{\rho_s}{\rho_f}\right)} (P + (1-\phi)^{2.5} M)(1 - f') = 0, \end{aligned} \tag{3.33}$$

$$\left(\frac{k_{nf}}{k_f} + R \right) \theta'' + P_r \left(1 - \phi + \frac{\phi(\rho c_p)_s}{(\rho c_P)_f} \right) (f\theta' - f'\theta) + \frac{1}{(1-\phi)^{2.5}} Ecf''^2 = 0, \tag{3.34}$$

$$h'' + Sc(fh' - f'h - \gamma h) = 0. \tag{3.35}$$

The associated boundary conditions (3.5) get the form:

$$\left.\begin{aligned} &f=0, f'=0, \theta=1, h=1, \quad && \text{at} \quad \eta=0, \\ &f'\to 1, \theta\to 0, h\to 0, && \text{as} \quad \eta\to\infty. \end{aligned}\right\} \tag{3.36}$$

Different parameters used in the above equations have the following formulations:

$$\begin{aligned} &M=\frac{2\sigma B_0^2 L}{a\rho_f}, P_r=\frac{\nu_f}{\alpha_f}, Sc=\frac{\nu_f}{D}, P=\frac{2L\nu_f}{ak_0} \\ &R=\frac{16\sigma^* T_\infty^3}{3k^* k_f}, \gamma=\frac{K_0}{a}, Ec=\frac{U_\infty^2 e^{\frac{-3x}{L}}}{(c_p)_f(T_w-T_\infty)}. \end{aligned} \tag{3.37}$$

3.4 Physical Quantities of Interest

The skin friction coefficient is defined as:

$$C_{fx}=\frac{2\tau_w}{\rho_f U_\infty^2}, \tag{3.38}$$

where τ_w is the wall shear stress.

$$\begin{aligned} \frac{\partial u}{\partial y} &= \frac{\partial}{\partial y}(ae^{\frac{x}{L}} f'(\eta)) \\ &= ae^{\frac{x}{L}} \frac{\partial f'(\eta)}{\partial(\eta)} \frac{\partial(\eta)}{\partial y} \\ &= ae^{\frac{x}{L}} f''(\eta)\sqrt{\frac{a}{2L\nu_f}} e^{\frac{x}{2L}} \\ \Rightarrow \left.\frac{\partial u}{\partial y}\right|_{y=0} &= a\sqrt{\frac{a}{2L\nu_f}} e^{\frac{x}{L}} e^{\frac{x}{2L}} f''(0) \\ \tau_w &= \mu_{nf}\left.\left(\frac{\partial u}{\partial y}\right)\right|_{y=0} \\ &= \frac{\mu_f}{(1-\phi)^{2.5}} a\sqrt{\frac{a}{2L\nu_f}} e^{\frac{x}{L}} e^{\frac{x}{2L}} f''(0) \end{aligned} \tag{3.39}$$

Using (3.38) in (3.39), we get the following form:

$$
\begin{aligned}
C_{fx} &= \frac{2}{\rho_f U_\infty^2}\frac{\mu_f}{(1-\phi)^{2.5}} a\sqrt{\frac{a}{2L\nu_f}} e^{\frac{x}{L}} e^{\frac{x}{2L}} f''(0) \\
&= \frac{2}{U_\infty^2}\frac{\nu_f}{(1-\phi)^{2.5}} a\sqrt{\frac{a}{2L\nu_f}} e^{\frac{x}{L}} e^{\frac{x}{2L}} f''(0) \qquad \therefore \nu_f = \frac{\mu_f}{\rho_f} \\
&= \sqrt{\frac{2\nu_f a}{L}}\frac{1}{U_\infty^2} a e^{\frac{x}{L}} \frac{x}{2L}\frac{f''(0)}{(1-\phi)^{2.5}} \\
&= \sqrt{\frac{2\nu_f a}{L}}\frac{1}{U_\infty^2} U_\infty \frac{x}{2L}\frac{f''(0)}{(1-\phi)^{2.5}} \qquad \therefore U_\infty = a e^{\frac{x}{L}} \\
&= \sqrt{\frac{2\nu_f a}{L}}\frac{1}{U_\infty} \left(e^{\frac{x}{L}}\right)^{\frac{1}{2}} \frac{f''(0)}{(1-\phi)^{2.5}} \\
&= \frac{\sqrt{\frac{x}{L}}}{\sqrt{\frac{xU_\infty}{2v_f}}}\frac{f''(0)}{(1-\phi)^{2.5}} \\
&= \frac{\sqrt{\frac{x}{L}}}{\sqrt{\frac{Re_x}{2}}}\frac{f''(0)}{(1-\phi)^{2.5}} \\
\Rightarrow \frac{C_{fx}\sqrt{\frac{Re_x}{2}}}{\sqrt{\frac{x}{L}}} &= \frac{f''(0)}{(1-\phi)^{2.5}}.
\end{aligned}
$$

The local Nusselt number is defined as:

$$
Nu_x = -\frac{xq_w}{k_f(T_w - T_\infty)}, \tag{3.40}
$$

the wall heat flux q_w is given by

$$
\begin{aligned}
q_w &= -k_{nf}\left(\frac{\partial T}{\partial y}\right)\Big|_{y=0} \\
\frac{\partial T}{\partial y} &= \frac{\partial}{\partial y}(T_0 e^{\frac{x}{2L}}\theta(\eta)) \\
&= T_0 e^{\frac{x}{2L}}\frac{\partial\theta(\eta)}{\partial\eta}\frac{\partial\eta}{\partial y} \\
&= T_0 e^{\frac{x}{2L}}\theta'(\eta)\sqrt{\frac{a}{2L\nu_f}} e^{\frac{x}{2L}} \\
&= T_0 e^{\frac{x}{L}}\sqrt{\frac{a}{2L\nu_f}}\theta'(\eta) \\
q_w &= -k_{nf} T_0 e^{\frac{x}{L}}\sqrt{\frac{a}{2L\nu_f}}\theta'(0)
\end{aligned} \tag{3.41}
$$

Using (3.40) in (3.41), we get the following form:

$$
\begin{aligned}
Nu_x &= -\frac{x(k_{nf}T_0e^{\frac{x}{L}})\sqrt{\frac{a}{2L\nu_f}}\theta'(0)}{k_f(T_w-T_\infty)} \\
&= -\frac{-xk_{nf}(T_w-T_\infty)e^{\frac{x}{L}}\sqrt{\frac{a}{2L\nu_f}}\theta'(0)}{k_fe^{\frac{x}{2L}}(T_w-T_\infty)} && \because T_0=\frac{(T_w-T_\infty)}{e^{\frac{x}{2L}}} \\
&= \frac{xk_{nf}\sqrt{\frac{a}{2L\nu_f}}(e^{\frac{x}{L}})^{\frac{1}{2}}\theta'(0)}{k_f} \\
&= \frac{xk_{nf}\sqrt{\frac{1}{2L\nu_f}}(ae^{\frac{x}{L}})^{\frac{1}{2}}\theta'(0)}{k_f} \\
&= \frac{xk_{nf}\sqrt{\frac{1}{2L\nu_f}}(U_\infty)^{\frac{1}{2}}\theta'(0)}{k_f} && \because U_\infty=ae^{\frac{x}{L}} \\
&= \frac{xk_{nf}\sqrt{\frac{xU_\infty}{2xL\nu_f}}\theta'(0)}{k_f} \\
&= \sqrt{\frac{x}{2L}}\frac{k_{nf}}{k_f}\sqrt{Re_x}\theta'(0) && \because Re_x=\frac{xU_\infty}{\nu_f} \\
\Rightarrow \sqrt{\frac{2L}{x}}\sqrt{\frac{1}{Re_x}}Nu_x &= -\frac{k_{nf}}{k_f}\theta'(0)
\end{aligned}
$$

The local Sherwood number is defined as:

$$
Sh_x = \frac{xq_m}{D(C_w-C_\infty)} \tag{3.42}
$$

$$
q_m = -D\left(\frac{\partial C}{\partial y}\right)\bigg|_{y=0} \tag{3.43}
$$

$$
= C_0e^{\frac{x}{L}}h'(\eta)\sqrt{\frac{a}{2L\nu_f}} \tag{3.44}
$$

Using (3.42) in (3.44) we get:

$$\begin{aligned}
Sh_x &= \frac{-xDC_0\sqrt{\frac{a}{2L\nu_f}}e^{\frac{x}{L}}h'(0)}{D(C_w - C_\infty)} \\
Sh_x &= \frac{-xC_0\sqrt{\frac{a}{2L\nu_f}}e^{\frac{x}{L}}h'(0)}{(C_w - C_\infty)} \\
&= \frac{-xC_0\sqrt{\frac{a}{2L\nu_f}}e^{\frac{x}{L}}h'(0)}{(C_w - C_w - C_0e^{\frac{x}{2L}})} \qquad \therefore C_\infty = C_w - C_0e^{\frac{x}{2L}} \\
&= \frac{-x\sqrt{\frac{a}{2L\nu_f}}e^{\frac{x}{L}}h'(0)}{(-e^{\frac{x}{2L}})} \\
&= -x\sqrt{\frac{a}{2L\nu_f}}e^{\frac{x}{L}}h'(0)e^{\frac{-x}{2L}} \\
&= -x\sqrt{\frac{a}{2L\nu_f}}h'(0)e^{\frac{x}{2L}} \\
&= -x\sqrt{\frac{a}{2L\nu_f}}h'(0)(e^{\frac{x}{L}})^{\frac{1}{2}} \\
&= -x\sqrt{\frac{ae^{\frac{x}{L}}}{2L\nu_f}}h'(0) \\
&= -x\sqrt{\frac{xU_\infty}{2L\nu_f}}h'(0) \\
&= -\left(\sqrt{\frac{xU_\infty}{\nu_f}}\right)\left(x\sqrt{\frac{1}{x2L}}h'(0)\right) \\
&= -\sqrt{Re_x}\sqrt{\frac{x}{2L}}h'(0) \\
\Rightarrow Sh_x\sqrt{\frac{1}{Re_x}}\sqrt{\frac{2L}{x}} &= -h'(0)
\end{aligned}$$

3.5 Solution Methodology

In order to solve the system of ordinary differential Eqs. (3.33)-(3.35), the shooting method together with the Runge-Katta method of order four has been used. First, Eq. (3.33) is numerically solved and then the calculated results of f, f' and f'' are used in Eq. (3.34) and (3.35). Since the Eq. (3.33) is independent of θ and h. Then in order to solve the Eq. (3.33) independently by using shooting method, the following notations have been introduced:

$$f = y_1, f' = y_1' = y_2, f'' = y_2' = y_3, f''' = y_3',$$

By using the above notations in Eq. (3.33), we get the system of equations

$$\begin{aligned}
&y_1' = y_2, && y_1(0) = 0\\
&y_2' = y_3, && y_2(0) = 0\\
&y_3' = -b_1(y_1y_3 + 2(1 - y_2^2)) - (P + (1-\phi)^{2.5}M)(1 - y_2), && y_3(0) = s
\end{aligned}$$

$$\text{where } \; b_1 = (1-\phi)^{2.5}(1 - \phi + \phi\frac{\rho_s}{\rho_f}),$$

The above initial value problem will be solved numerically by the RK4 method. To get the approximate solution, the domain of the problem has been taken as $[0, \eta_\infty]$ instead of $[0, \infty]$, where η_∞ is an appropriate finite positive real number with chosen initial guess s such that:

$$y_1(\eta_\infty, s) - 1 = 0. \tag{3.45}$$

To solve the above algebraic Eq. (3.45), we use the Newton's method which has the following iterative procedure:

$$s^{(k+1)} = s^{(k)} - \left(\frac{\partial y_1}{\partial s}\right)^{-1}\left(y_1(\eta_\infty, s) - 1\right). \tag{3.46}$$

In order to obtain $\left(\frac{\partial y_1}{\partial s}\right)^{-1}$, we further introduce the following notations:

$$\frac{\partial y_1}{\partial s} = y_4, \frac{\partial y_2}{\partial s} = y_5, \frac{\partial y_3}{\partial s} = y_6.$$

As a result of these new notations, the Newton's iterative scheme gets the form:

$$s^{(k+1)} = s^{(k)} - (y_4)^{-1}\left(y_1(\eta_\infty, s) - 1\right).$$

Now differentiate the above system of three first order ODEs with respect to s, we get another system of six ODEs. Writing all these six ODEs together, we have the following initial value problem (IVP), which needs to be solved:

$$
\begin{aligned}
&y_1' = y_2, && y_1(0) = 0,\\
&y_2' = y_3, && y_2(0) = 0,\\
&y_3' = -b_1(y_1y_3 + 2(1-y_2^2)) - (P + (1-\phi)^{2.5}M)(1-y_2), && y_3(0) = s,\\
&y_4' = y_5, && y_4(0) = 0,\\
&y_5' = y_6, && y_5(0) = 0,\\
&y_6' = -b_1(y_4y_3 + y_1y_6 - 4y_2y_5) + (P + (1-\phi)^{2.5}M)y_5, && y_6(0) = 1.
\end{aligned}
$$

Next, we have to solve Eq. (3.34) for the known value of f. For this we use the same procedure as considered for Eq. (3.33). For that let us denote:

$$
\begin{aligned}
\theta &= z_1,\\
\theta' &= z_1' = z_2,\\
\theta'' &= z_1'' = z_2',\\
f \quad &= d_1, f' = d_2, f'' = d_3.
\end{aligned}
$$

By using the above notations in Eq. (3.34), we get the following system of equations:

$$
\begin{aligned}
z_1' &= z_2, && z_1(0) = 0,\\
z_2' &= -\frac{1}{\left(\frac{k_{nf}}{k_f} + R\right)}\left[P_r\left(1-\phi+\frac{\phi(\rho c_p)_s}{(\rho c_p)_f}\right)(d_1z_2 - d_2z_1)\right.\\
&\quad \left. + \frac{1}{(1-\phi)^{2.5}}Ecd_3^2\right], && z_2(0) = r.
\end{aligned}
$$

The above initial value problem will be solved again using RK4 method. The computational domain is truncated in the similar way as before. In the above system of equations, the missing condition is r which needs to be refined such that:

$$z_1(\eta_\infty, r) - 1 = 0. \tag{3.47}$$

To solve the above algebraic Eq. (3.47), we use the Newton's method which has the following iterative procedure:

$$r^{(k+1)} = r^{(k)} - \left(\frac{\partial z_1}{\partial r}\right)^{-1} \Big(z_1(\eta_\infty, r) - 1\Big) \tag{3.48}$$

In order to obtain $\left(\frac{\partial z_1}{\partial r}\right)^{-1}$, we further introduce the following notations:

$$\frac{\partial z_1}{\partial r} = z_3, \frac{\partial z_2}{\partial r} = z_4.$$

As a result of these new notations, the Newton's iterative scheme gets the form:

$$r^{(k+1)} = r^{(k)} - (z_3)^{-1} \Big(z_1(\eta_\infty, r) - 1\Big).$$

Now differentiate the above system of two first order ODEs with respect to r, we get another system of four ODEs. Writing all these four ODEs together, we have the following initial value problem (IVP), which needs to be solved.

$$\begin{aligned}
z_1' &= z_2, & z_1(0) &= 0,\\
z_2' &= -\frac{1}{\left(\frac{k_{nf}}{k_f} + R\right)} \left[P_r \left(1 - \phi + \frac{\phi(\rho c_p)_s}{(\rho c_p)_f}\right)(d_1 z_2 - d_2 z_1) \right.\\
&\quad \left. + \frac{1}{(1-\phi)^{2.5}} Ecd_3^2\right], & z_2(0) &= r,\\
z_3' &= z_4, & z_3(0) &= 0,\\
z_4' &= -\frac{1}{\left(\frac{k_{nf}}{k_f} + R\right)} \left[P_r \left(1 - \phi + \frac{\phi(\rho c_p)_s}{(\rho c_p)_f}\right)(d_1 z_4 - d_2 z_3) \right.\\
&\quad \left. + \frac{1}{(1-\phi)^{2.5}} Ecd_3^2\right], & z_4(0) &= 1.
\end{aligned}$$

By using shooting techniques we have the solution of Eq. (3.34). Next, we have to solve Eq. (3.35) for the know value of f. For this we use the same procedure as considered for Eq. (3.33) and (3.34). For that let us denoted:

$$\begin{aligned} h &= g_1, \\ h' &= g_1' = g_2, \\ h'' &= g_1'' = g_2', \\ f &= d_1, f' = d_2, f'' = d_3. \end{aligned}$$

By using the above notations in Eq. (3.35), we get the following system of equation:

$$\begin{aligned} g_1' &= g_2, & g_1(0) &= 0, \\ g_2' &= -Sc(d_1 g_2 - d_2 g_1 - \gamma g_1), & g_2(0) &= w. \end{aligned}$$

The above initial value problem will be solved again using RK4 method. The computational domain is truncated in the similar way as before. In the above system of equations, the missing condition is w which needs to be refined such that:

$$g_1(\eta_\infty, w) - 1 = 0 \tag{3.49}$$

To solve the above algebraic Eq. (3.49), we use the Newton's method which has the following iterative procedure:

$$w^{(k+1)} = w^{(k)} - \left(\frac{\partial g_1}{\partial w}\right)^{-1} \bigg(g_1(\eta_\infty, w) - 1\bigg).$$

In order to obtain $\left(\frac{\partial g_1}{\partial w}\right)^{-1}$, we further introduce the following notations:

$$\frac{\partial g_1}{\partial w} = g_3, \frac{\partial g_2}{\partial w} = g_4.$$

As a result of these new notations, the Newton's iterative scheme gets the form:

$$w^{(k+1)} = w^{(k)} - (g_3)^{-1} \bigg(g_1(\eta_\infty, w) - 1\bigg).$$

Now differentiate the above system of two first order ODEs with respect to w, we get another system of four ODEs. Writing all these four ODEs together, we have the following initial value problem (IVP),which needs to be solved:

$$\begin{aligned}
g_1' &= g_2, & g_1(0) &= 0,\\
g_2' &= -Sc(d_1 g_2 - d_2 g_1 - \gamma g_1), & g_2(0) &= w,\\
g_3' &= g_4, & g_3(0) &= 0,\\
g_4' &= -Sc(d_1 g_4 - d_2 g_3 - \gamma g_3), & g_4(0) &= 1.
\end{aligned}$$

By using shooting techniques we have the solution of Eq. (3.35).

3.5.1 Validation of Code

For validation of the numerical code Tables 3.2 and 3.3 have been presented and the result are compared with the results of Mabood *et al.* [48]. In Tables 3.2 and 3.3 shows, an excellent agreement between the compared results and those of already published in the literature:

$\frac{1}{(1-\phi)^{2.5}} f''(0)$				
	Cu-water		Al_2O_3-water	
ϕ	Ref. [48]	Present result	Ref. [48]	Present result
0	1.6872	1.6871	1.6872	1.6871
0.1	2.5794	2.5793	2.1929	2.1928
0.2	3.5901	3.5902	2.8174	2.8172

TABLE 3.2: Comparison of skin friction $f''(0)$ with Ref. [48] when $P=M=R=Ec=0, P_r=6.2$ and $Sc=0.68$.

	$-\frac{k_{nf}}{k_f}\theta'(0)$			
	Cu-water		Al_2O_3-water	
ϕ	Ref. [48]	Present result	Ref. [48]	Present result
0	1.7148	1.7199	1.7148	1.7199
0.1	2.1358	2.1418	2.0230	2.0284
0.2	2.5400	2.5464	2.3345	2.3401

TABLE 3.3: Comparison results of Nusselt $\theta'(0)$ with Ref. [48] when $P = M = R = Ec = 0, P_r = 6.2$ and $Sc = 0.68$.

3.6 Result and Discussion

In this section, numerical results for velocity, temperature and concentration profiles are illustrated with graphs under the influence of different parameters.

Figure 3.2 (a) studies the effects of volume fraction of nanoparticles in the presence ($M = 5$) and absence ($M = 0$) of magnetic field. It is noted that velocity of the fluid increases gradually for both cases. This is due to the fact that nanoparticle are reducing the viscous effects which correspondingly increase the velocity profile. Similarly, Figure 3.2 (b) for Al_2O_3–water, it is observed that in case of hydrodynamic and hydromagnetic the velocity profile increases. From these figures, it is clear that an increment in the volume fraction of nanoparticles, the Al_2O_3–water nanofluid formed a thicker momentum boundary layer as compared to Cu–water nanofluid in these plots.

Figures 3.3 (a) exhibits the influence of solid volume fraction of nanoparticles ϕ on temperature profile for Cu–water nanofluids. Growing values of volume fraction of nanoparticles enhance the thermal conductivity of the nanofluids which then increases the temperature profile. From Figure 3.3 (b), it can be seen that the fluid temperature increases for alumina water within the boundary layer region as the value of the solid volume fraction increases from $\phi = 0$ to $\phi = 0.2\,(20\%)$. From these figures, it is observed that the thermal boundary layer for nanoparticles, namely Cu-water, is greater than that of Al_2O_3-water. This is because nanoparticles volume fraction parameter (of Cu) has high thermal conductivity, so the thickness of the thermal boundary layer increases.

Figure 3.4 (a) is presented to potary properties of volume fraction of nanoparticles together with the magnetic parameter M on concentration profile h. The concentration profile decays as the nanoparticle volume fraction rises. Figure 3.4 (b) is sketched to visualize the variation in the dimensionless concentration profile due to changes in the volume fraction of nanoparticles together with the magnetic parameter M. The dimensionless concentration h for Al_2O_3-water also demonstrates a declining behaviour. These figures, delineated to show that the concentration distribution undergoes a decrement if there is an enhancement in the volume fraction ϕ.

Figures 3.5 (a) is delineated to shows the impact of permeability parameter on fluid velocity for Cu-water nanofluid. Fluid velocity is enhanced marginally with an increment in the values of both the permeability parameter P and ϕ for Cu-water. Figures 3.5 (b) depicts that an increases in the permeability parameter P fluid velocity increases effectively for Al_2O_3–water nanofluid. Physically, an increase in permeability parameter causes as increase in the flow rate, so as flow rate increases the velocity of the fluid also increases.

Figures 3.6 (a) displays the influence of the volume fraction ϕ and permeability parameters P on the dimensionless temperature θ for Cu-water. When the porosity enhances significantly the thermal boundary layer is reduced. It is clearly observed that the temperature profile enhances marginally by enhancement in the volume fraction for magnified porosity. If we enhance the values of the permeability parameter, the temperature distribution is also enhanced. Figure 3.6 (b) depicts that the temperature profile is increased for the larger values of the permeability parameter P and the volume fraction ϕ for Al_2O_3–water nanofluid. An increase in the permeability material correspond to large void section thus increases in the temperature profile. Physically, in these figures the temperature profile enhances effective if with an increase in the ϕ.

Figures 3.7 (a) illustrates the influence of the higher estimation of nanoparticles on fluid temperature θ for Cu-water nanofluid with or without radiation. The dimensionless temperature field θ is increased as the thermal radiation parameter R is increased. It strengthens the fact that more heat is produced due in the radiation process. Figures 3.7 (b) depicts the variation in the dimensionless temperature θ due to the volume fraction ϕ for Al_2O_3-water nanofluid with or without radiation. The dimensionless temperature is enhanced as volume fraction ϕ is increased gradually. Physically, the thermal radiation effect temperature distribution of the nanofluid. As the thermal radiation boosts the thermal diffusion. Hence, the temperature increases as the thermal radiation rises for any form of nanoparticles.

Figures 3.8 (a) is framed to spectacles the effect of Eckert number on temperature profile θ for Cu-water nanofluid when fluctuating the volume fraction of the nanoparticles. When the value of the Eckert number is enhanced, the fluid realm is permited to store the energy. As a consequence of dissipation due to fractional heating, heat is produced. The effect of the viscous dissipation parameter i.e. the Eckert number Ec on the dimensionless temperature profile θ for Al_2O_3-water nanofluid is visualized in Figures 3.8 (b). It is analyzed that an increase in Ec causes an increase in θ and the boundary layer thickness. From this figure, we examine that for the higher estimation value of the thermal boundary thickness is enhanced with increasing values of ϕ and it will eventually magnify the temperature. In addition to that, an increment can be seen in the thermal boundary layer thickness.

Figures 3.9 (a) elucidates the effect of the chemical reaction parameter on concentration profile for Cu-water nanofluid. It is clear that as the chemical reaction parameter increases, the concentration profile drops significantly. Figures 3.9 (b) illustrates the effect of the chemical reaction parameter on the concentration profile for Al_2O_3-water nanofluid. Graphs of this figure indicate that concentration profile is reduced as chemical reaction parameter is hiked. However, increasing the volume fraction of nanoparticles has little effect on dimensionless concentration. Also, the concentration boundary layer thickness is depressed.

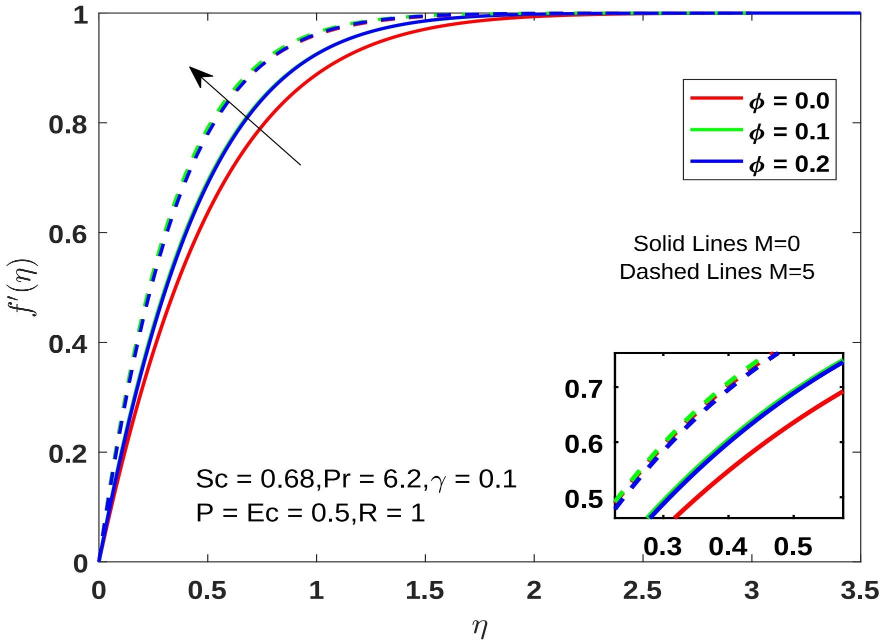

(a)Cu-**Water**

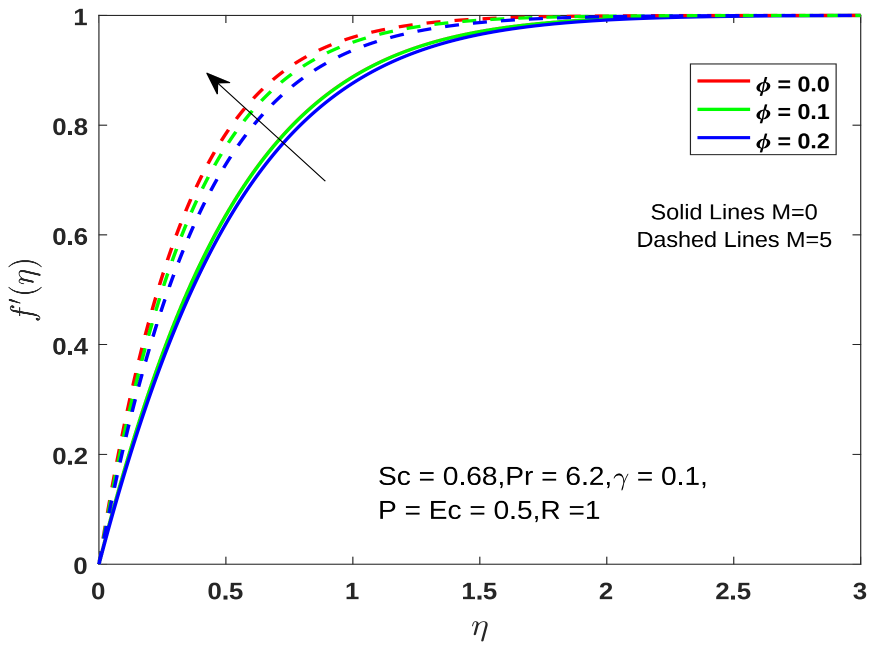

(b)Al_2O_3-**Water**

FIGURE 3.2: Impact of ϕ and M on the dimensionless velocity f'.

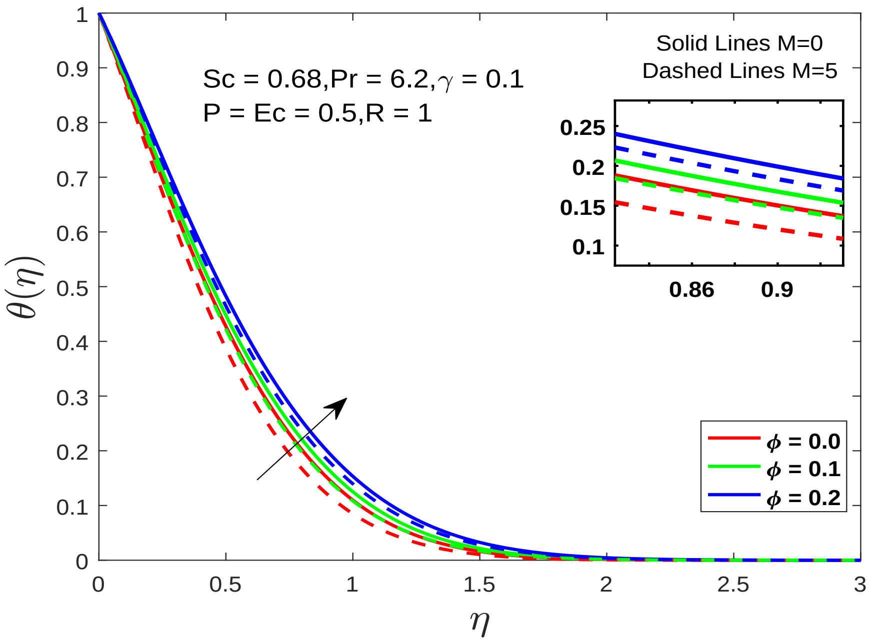

(a)Cu-**Water**

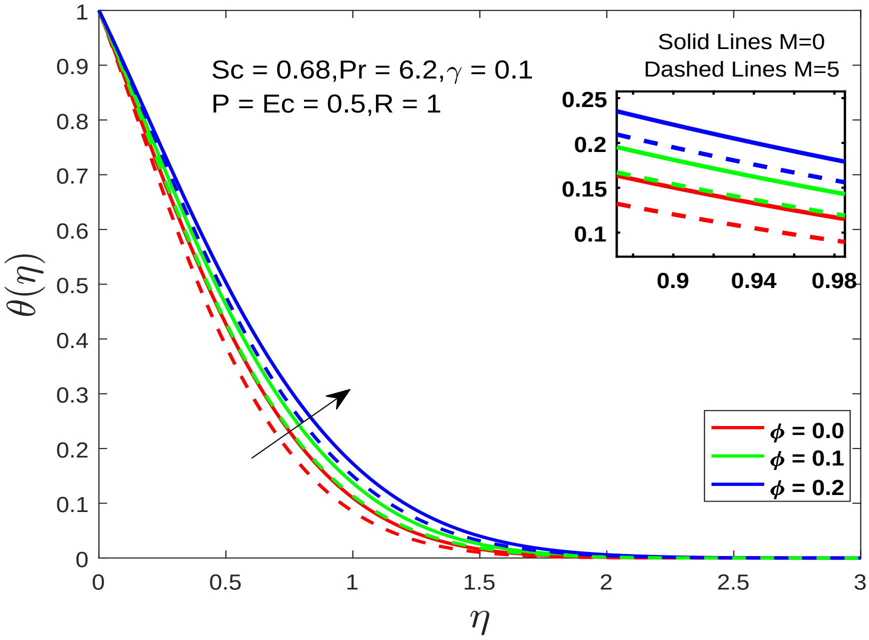

(b)Al_2O_3-**Water**

FIGURE 3.3: Impact of ϕ and M on the dimensionless temperature θ.

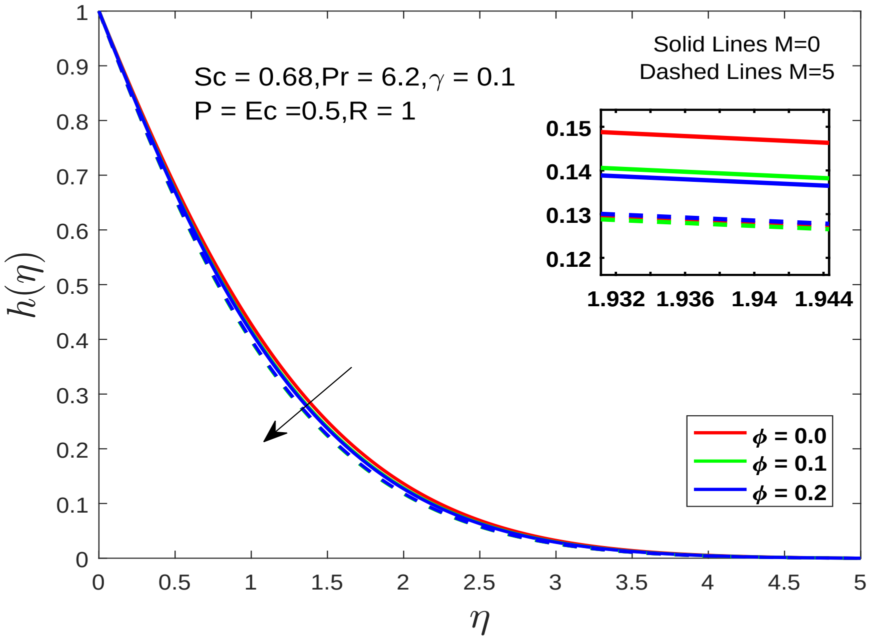

(a)Cu-**Water**

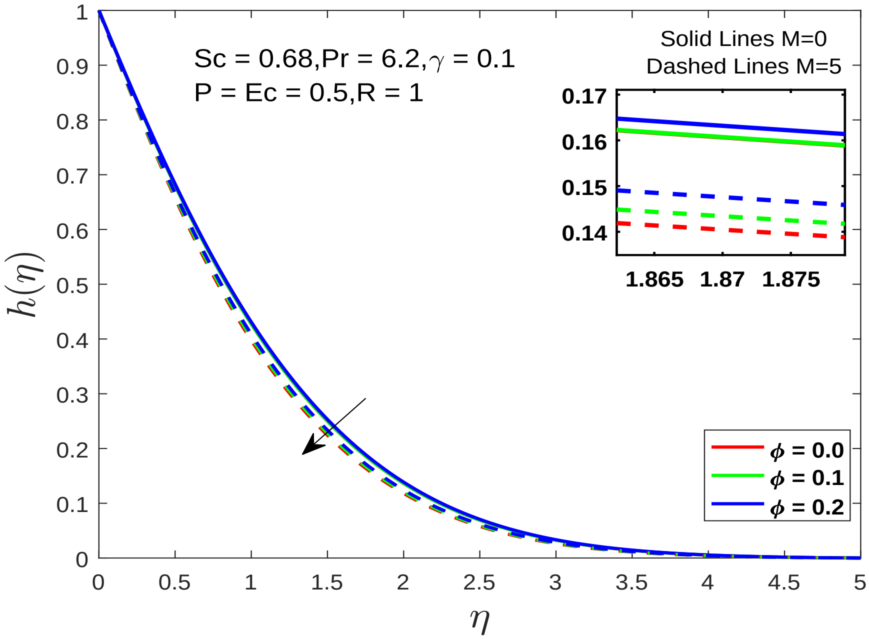

(b)Al_2O_3-**Water**

FIGURE 3.4: Impact of ϕ and M on the dimensionless concentration h.

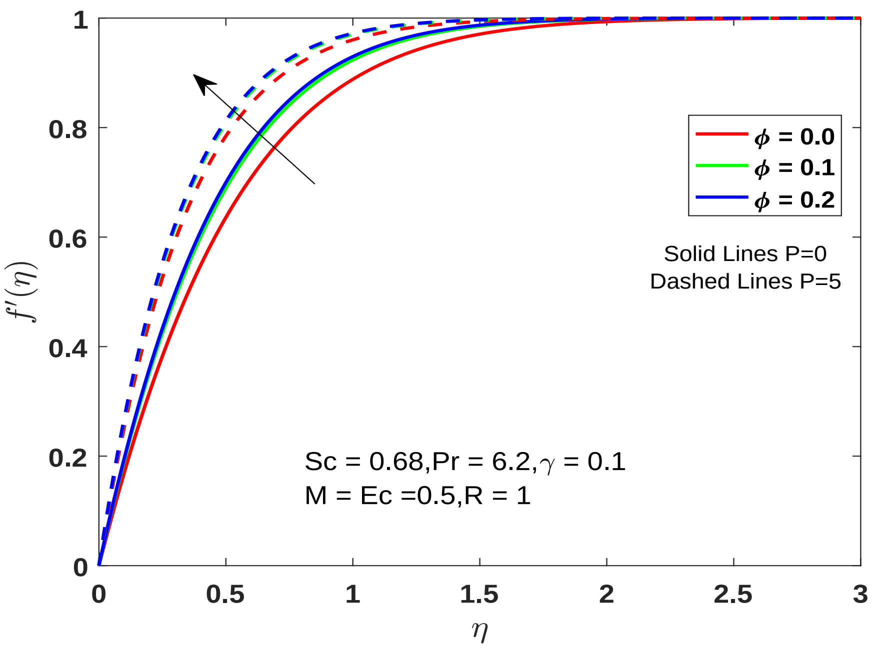

(a)Cu-**Water**

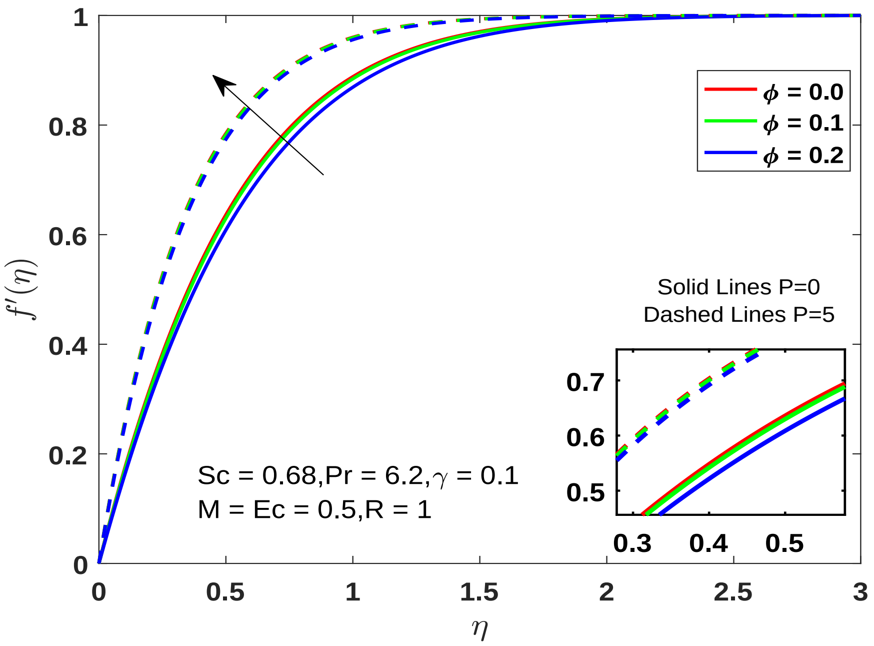

(b)Al_2O_3-**Water**

FIGURE 3.5: Impact of ϕ and P on the dimensionless velocity f'.

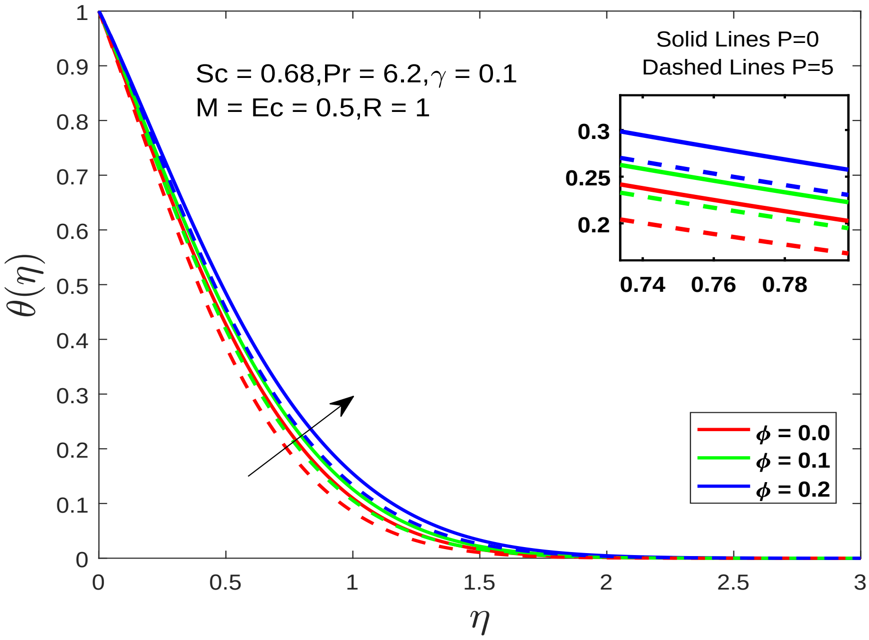

(a)Cu-**Water**

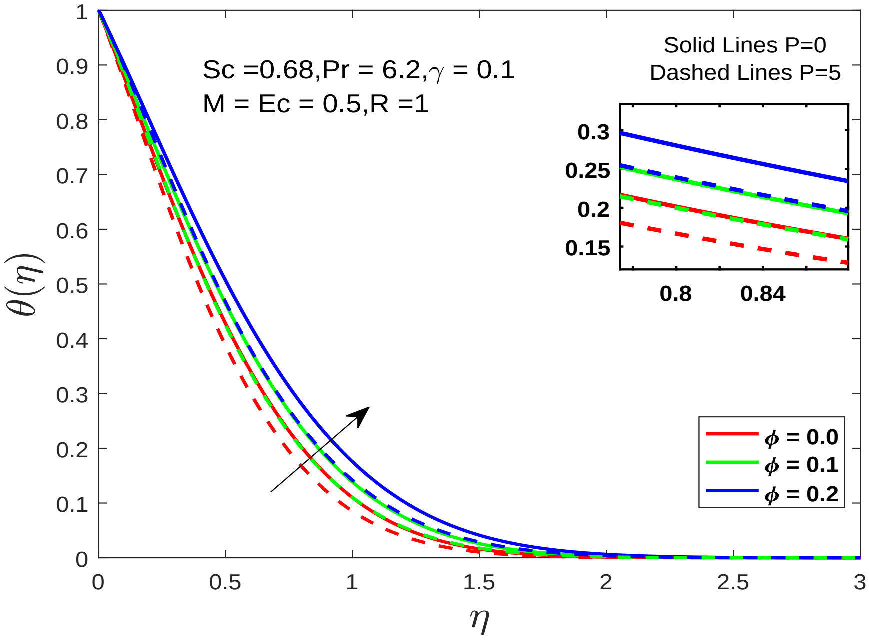

(b)Al_2O_3-**Water**

FIGURE 3.6: Impact of ϕ and P on the dimensionless temperature θ.

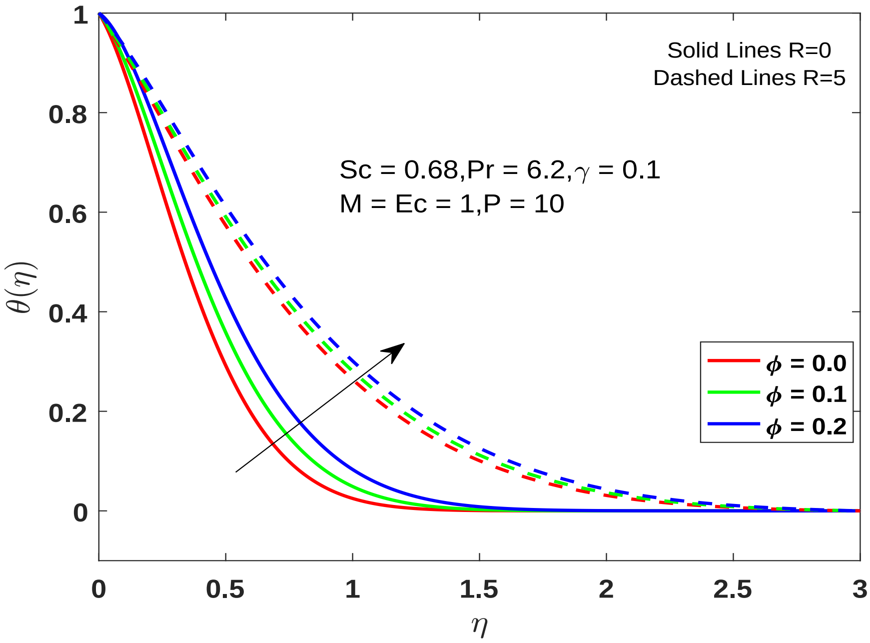

(a)Cu-**Water**

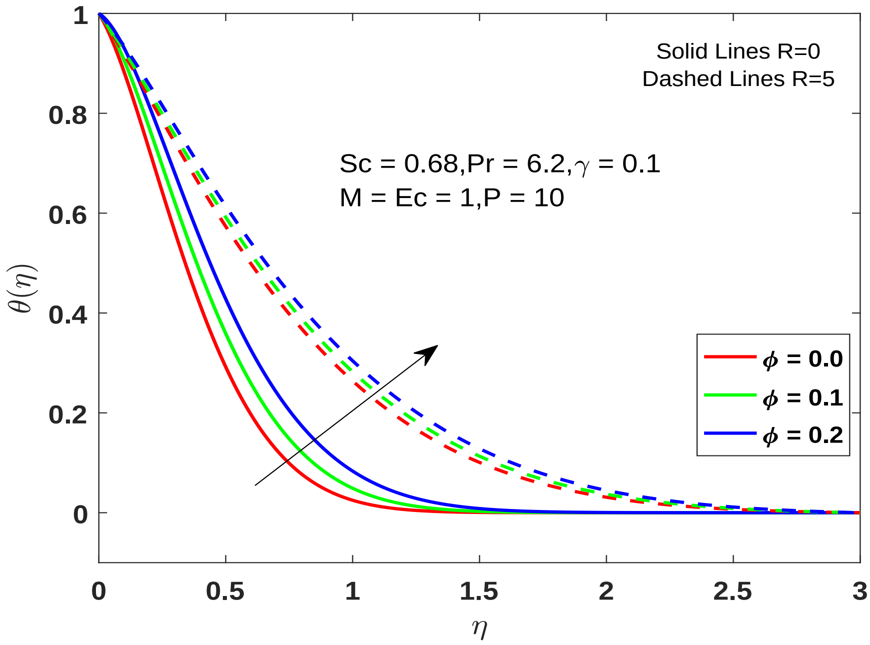

(b)Al_2O_3-**Water**

FIGURE 3.7: Impact of ϕ and R on the dimensionless temperature θ.

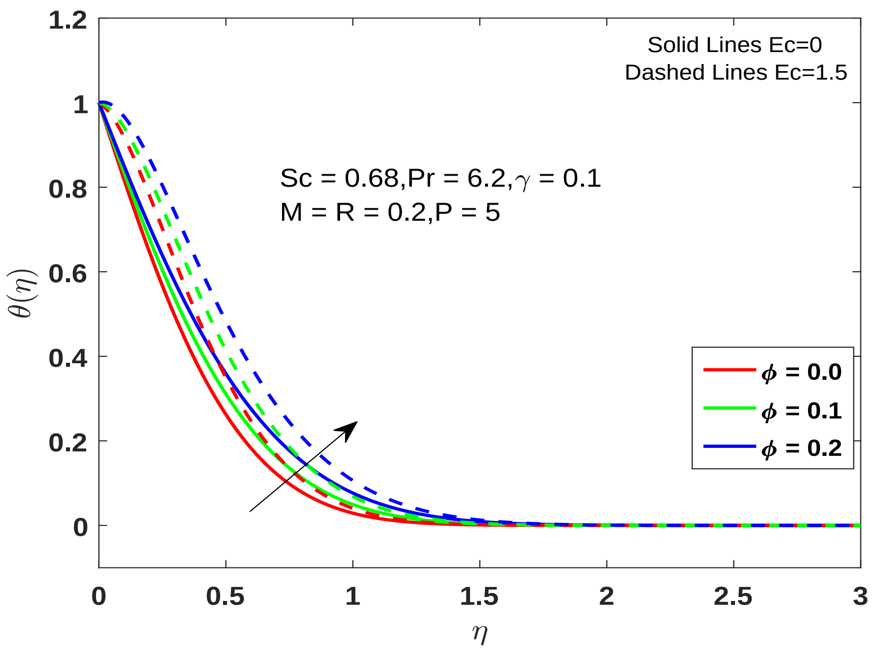

(a)Cu-**Water**

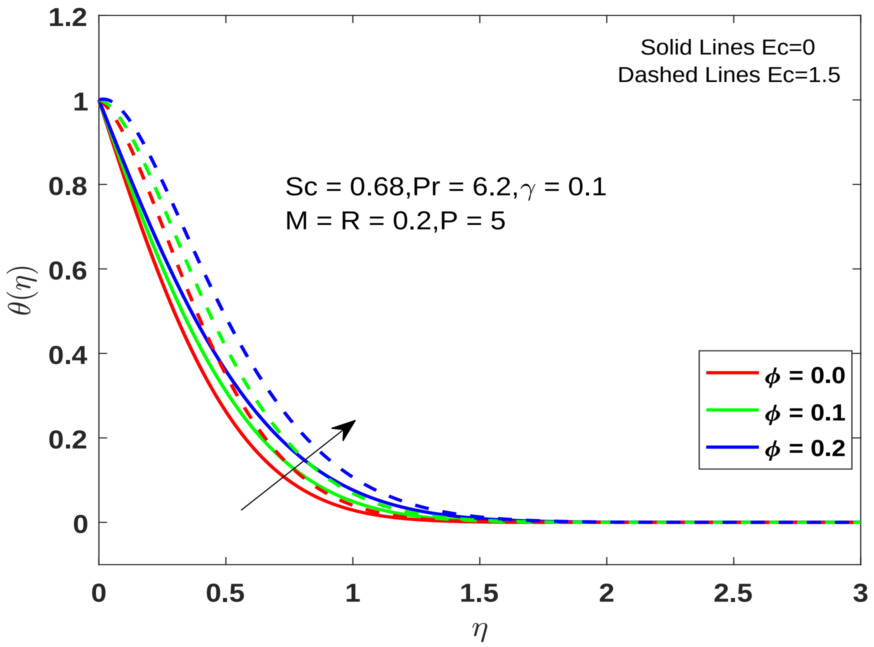

(b)Al_2O_3-**Water**

FIGURE 3.8: Impact of ϕ and Ec on the dimensionless temperature θ.

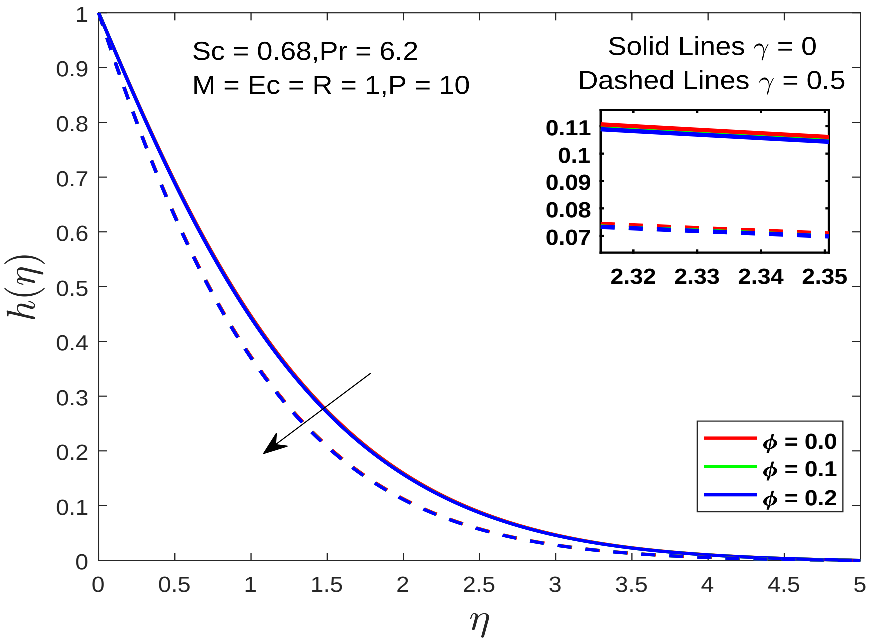

(a)Cu-**Water**

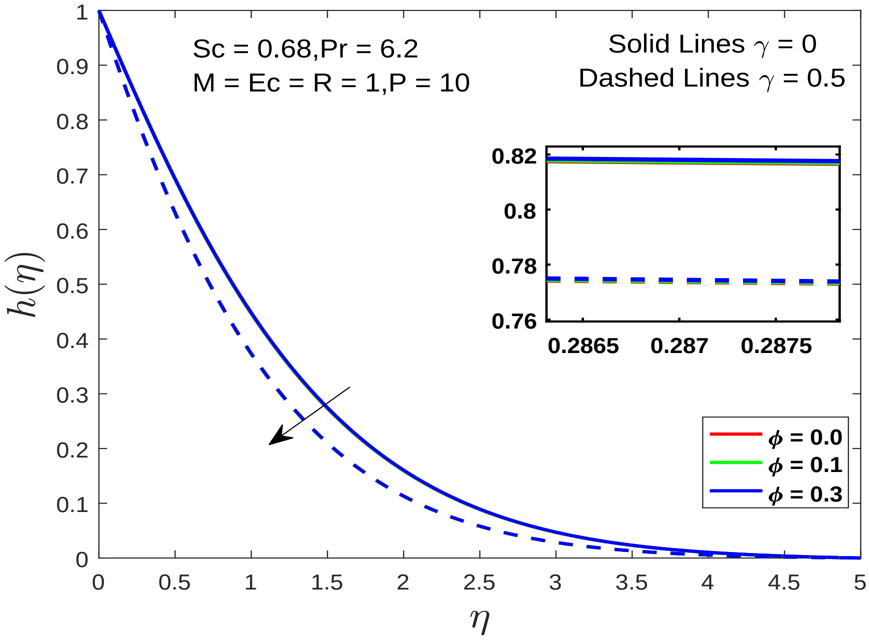

(b)Al_2O_3-**Water**

FIGURE 3.9: Impact of ϕ and γ on the dimensionless temperature θ.

Chapter 4

MHD Stagnation Point Flow of Radiative Nanofluid with Higher Order Chemical Reaction and Joule Heating

In this chapter we extend the model of Mabood *et al.* [48] by considering the effect of Joule heating, inclined magnetic field and nth order chemical reaction. Heat and mass transfer are analyzed for the steady and incompressible flow by taking into account the effect of viscous dissipations, nth order chemical reaction and Joule heating in a porous medium. Nonlinear PDEs are converted into a system of ODEs by using an appropriate similarity transformation. We have achieved the numerical solution of the system of ODEs by using the technique namely the shooting technique along with Runge-Kutta method of order four. The results for different governing parameters for velocity, energy and concentration profiles are deliberated through graphical and tabular form.

4.1 Problem Formulatiuon

This chapter aims to analyse the 2D, incompressible nanofluid flow in porous medium. The flow occupied the space $y > 0$. Magnetic field of strength B is applied with an inclination angle α with the horizontal axis. Furthermore x-axis is in the direction of flow and y-axis is normal to it. Energy transport analysis is also carried out in the presence of thermal radiation, viscous dissipation and Joule heating. Moreover, the concentration of flow is discussed with the help of concentration equation under the effect of nth order chemical reaction. To enhance the heat transfer characteristics of base fluid water, we have used a well known nanofluid model that's "Tiwari Das" model [64]. In this regime 2-different nanoparticales are choosen namely Cu and Al_2O_3. The thermo-physical properties of the fluid with nanoparticles are given in Table 3.1.

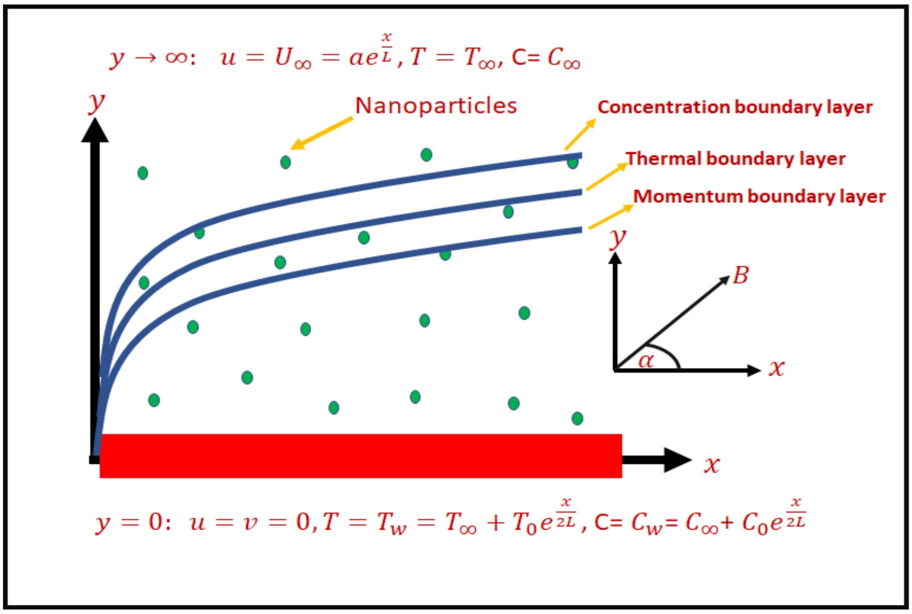

FIGURE 4.1: Geometry of physical model.

Under the above constraint the related equations are given as:

$$\frac{\partial u}{\partial x} + \frac{\partial v}{\partial y} = 0, \tag{4.1}$$

$$u\frac{\partial u}{\partial x}+v\frac{\partial u}{\partial y}=U_\infty\frac{dU_\infty}{dx}+\nu_{nf}\frac{\partial^2 u}{\partial y^2}+\frac{\nu_{nf}}{k}(U_\infty-u)+\frac{\sigma B^2}{\rho_{nf}}\sin^2\alpha(U_\infty-u), \tag{4.2}$$

$$u\frac{\partial T}{\partial x}+v\frac{\partial T}{\partial y}=\alpha_{nf}\frac{\partial^2 T}{\partial y^2}-\frac{1}{(\rho c_p)_{nf}}\frac{\partial q_r}{\partial y}+\frac{\mu_{nf}}{(\rho c_p)_{nf}}\left(\frac{\partial u}{\partial y}\right)^2+\frac{\sigma B^2}{(\rho c_p)_{nf}}\sin^2\alpha(u-U_\infty)^2, \tag{4.3}$$

$$u\frac{\partial C}{\partial x}+v\frac{\partial C}{\partial y}=D\frac{\partial^2 C}{\partial y^2}-K(C-C_\infty)^n. \tag{4.4}$$

The corresponding conditions at the boundary are

$$\left.\begin{array}{ll}\left.\begin{array}{l}u=v=0, T=T_w=T_\infty+T_0e^{\frac{x}{2L}},\\ C=C_w=C_\infty+C_0e^{\frac{x}{2L}},\end{array}\right\} & \text{at} \quad y=0,\\ u=U_\infty=ae^{\frac{x}{L}}, T=T_\infty, C=C_\infty, & \text{as} \quad y\to\infty.\end{array}\right\} \tag{4.5}$$

The Rosseland approximation has been considered for the radiation. For smaller value of temperature difference, the temperature T^4 might be expanded about T_∞ using Taylor series and ignoring the higher order terms, the formulae for the radiative heat flux q_r is stated below.

$$\frac{\partial q_r}{\partial y}=\frac{-16\sigma^* T_\infty^3}{3k^*}\frac{\partial^2 T}{\partial y^2}. \tag{4.6}$$

4.2 Similarity Transformation

In this section similar to Chapter 3, we transform the governing system of PDEs along with boundary condition into a dimensionless form by using appropriate similarity transformations. The similarity transformation used are as follows [48]:

$$\eta=y\sqrt{\frac{a}{2L\nu_f}}e^{\frac{x}{2L}},\quad \psi=\sqrt{2aL\nu_f}e^{\frac{x}{2L}}f(\eta),\ \theta(\eta)=\frac{T-T_\infty}{T_w-T_\infty},\quad h(\eta)=\frac{C-C_\infty}{C_w-C_\infty}.$$

The detailed procedure for the verification of the continuity Eq. (4.1) has been discussed in Chapter 3.

Now Eq. (4.2) will be converted into the dimensionless form. The left hand side of Eq. (4.2) can be written as:

$$\begin{aligned}
u\frac{\partial u}{\partial x}+v\frac{\partial u}{\partial y}=&\frac{a^2}{2L}\Big(\eta f''(\eta)f'(\eta)+2f'^2(\eta)\Big)\\
&-\frac{a^2}{2L}e^{\frac{2x}{L}}\Big(\eta f''(\eta)f'(\eta)+f''(\eta)f(\eta)\Big)\\
=&\frac{a^2}{2L}e^{\frac{2x}{L}}\Big(2f'^2(\eta)-f''(\eta)f(\eta)\Big).
\end{aligned}$$

Furthermore, the first, second and third expressions on the right hand side of Eq. (4.2) have been transformed into the dimensionless form as stated below:

$$U_\infty\frac{dU_\infty}{dx}=\frac{a^2}{L}e^{\frac{2x}{L}} \tag{4.7}$$

$$\begin{aligned}
\nu_{nf}\frac{\partial^2 u}{\partial y^2}&=\frac{\mu_{nf}}{\rho_{nf}}\left(\frac{\partial^2 u}{\partial y^2}\right)\\
&=\frac{a^2e^{\frac{2x}{L}}}{2L(1-\phi)^{2.5}(1-\phi+\frac{\phi\rho_s}{\rho_f})}f'''(\eta)
\end{aligned}$$

$$\begin{aligned}
\frac{\nu_{nf}}{k}(U_\infty-u)&=\frac{\mu_f}{k_0e^{-\frac{x}{L}}(1-\phi)^{2.5}\Big((1-\phi)\rho_f+\phi\rho_s\Big)}\Big(ae^{\frac{x}{L}}-ae^{\frac{x}{L}}f'(\eta)\Big)\\
&=\frac{\nu_f\rho_f}{\rho_fk_0(1-\phi)^{2.5}\Big(1-\phi+\frac{\phi\rho_s}{\rho_f}\Big)}ae^{\frac{x}{L}}e^{\frac{x}{L}}\Big(1-f'(\eta)\Big)\\
&=\frac{a\nu_fe^{\frac{2x}{L}}}{k_0(1-\phi)^{2.5}\Big(1-\phi+\phi\frac{\rho_s}{\rho_f}\Big)}\Big(1-f'(\eta)\Big).
\end{aligned}$$

On the similar note, conversion of the remaining terms of the right hand side of Eq. (4.2) into the dimensionless form is stated below:

$$\begin{aligned}
\frac{\sigma B^2\sin^2\alpha}{\rho_{nf}}(U_\infty-u)&=\frac{\sigma(B_0e^{\frac{x}{2L}})^2\sin^2\alpha}{(1-\phi)\rho_f+\phi\rho_s}\Big(ae^{\frac{x}{L}}-ae^{\frac{x}{L}}f'(\eta)\Big)\\
&=\frac{\sigma(B_0e^{\frac{x}{2L}})^2\sin^2\alpha}{(1-\phi)\rho_f+\phi\rho_s}ae^{\frac{x}{L}}\Big(1-f'(\eta)\Big)\\
&=\frac{\sigma B_0^2ae^{\frac{2x}{L}}\sin^2\alpha}{\rho_f\Big(1-\phi+\frac{\phi\rho_s}{\rho_f}\Big)}\Big(1-f'(\eta)\Big).
\end{aligned} \tag{4.8}$$

Using (4.7) - (4.8) in the right side of (4.2), we get

$$
\begin{aligned}
&U_\infty \frac{dU_\infty}{dx} + \nu_{nf}\frac{\partial^2 u}{\partial y^2} + \frac{\nu_{nf}}{k}(U_\infty - u) + \frac{\sigma B^2 \sin^2\alpha}{\rho_{nf}}(U_\infty - u) \\
&= \frac{a^2 e^{\frac{2x}{L}}}{L} + \frac{a^2 e^{\frac{2x}{L}} f'''(\eta)}{2L(1-\phi)^{2.5}\left(1-\phi+\frac{\phi\rho_s}{\rho_f}\right)} \\
&+ \frac{a\nu_f e^{\frac{2x}{L}}}{k_0(1-\phi)^{2.5}\left(1-\phi+\phi\frac{\rho_s}{\rho_f}\right)} \\
&+ \frac{\sigma B_0^2 a e^{\frac{2x}{L}}\sin^2\alpha}{\rho_f\left(1-\phi+\frac{\phi\rho_s}{\rho_f}\right)}\Big(1-f'(\eta)\Big).
\end{aligned}
\tag{4.9}
$$

Hence the dimensionless form of (4.2) becomes

$$
\begin{aligned}
&\frac{a^2 e^{\frac{2x}{L}}}{2L}\Big(2f'^2(\eta) - f''(\eta)f(\eta)\Big) = \frac{a^2 e^{\frac{2x}{L}}}{2L}\Bigg[2 + \frac{1}{(1-\phi)^{2.5}(1-\phi+\frac{\phi\rho_s}{\rho_f})}f'''(\eta) \\
&+ \frac{2L\nu_f}{ak_0(1-\phi)^{2.5}(1-\phi+\phi\frac{\rho_s}{\rho_f})}\Big(1-f'(\eta)\Big) + \frac{2L\sigma B_0^2\sin^2\alpha}{a\rho_f(1-\phi+\frac{\phi\rho_s}{\rho_f})}\Big(1-f'(\eta)\Big)\Bigg] \\
&\Rightarrow 2f'^2(\eta) - f''(\eta)f(\eta) = 2 + \frac{f'''(\eta)}{(1-\phi)^{2.5}(1-\phi+\frac{\phi\rho_s}{\rho_f})} \\
&+ \left(\frac{2L\nu_f}{ak_0(1-\phi)^{2.5}(1-\phi+\phi\frac{\rho_s}{\rho_f})} + \frac{2L\sigma B_0^2\sin^2\alpha}{a\rho_f(1-\phi+\frac{\phi\rho_s}{\rho_f})}\right)\Big(1-f'(\eta)\Big) \\
&\Rightarrow -2 + 2f'^2(\eta) - f''(\eta)f(\eta) = \frac{f'''(\eta)}{(1-\phi)^{2.5}(1-\phi+\frac{\phi\rho_s}{\rho_f})} \\
&+ \left(\frac{2L\nu_f}{ak_0(1-\phi)^{2.5}(1-\phi+\phi\frac{\rho_s}{\rho_f})} + \frac{2L\sigma B_0^2\sin^2\alpha}{a\rho_f(1-\phi+\frac{\phi\rho_s}{\rho_f})}\right)\Big(1-f'(\eta)\Big) \\
&\Rightarrow \frac{f'''(\eta)}{(1-\phi)^{2.5}(1-\phi+\frac{\phi\rho_s}{\rho_f})} + 2\left(1-f'^2(\eta)\right) + f(\eta)f''(\eta) \\
&\qquad \left[\frac{1}{(1-\phi)^{2.5}\left(1-\phi+\frac{\phi\rho_s}{\rho_f}\right)}\left(\frac{2L\nu_f}{ak_0} + \frac{2L\sigma B_0^2\sin^2\alpha}{a\rho_f}(1-\phi)^{2.5}\right)\Big(1-f'(\eta)\Big)\right] = 0.
\end{aligned}
\tag{4.10}
$$

Next, we include the procedure for the conversion of (4.3) into the dimensionless form. The left hand side of Eq. (4.3) into the dimensionless form is similar to that discussed in Chapter 3.

$$
\begin{aligned}
u\frac{\partial T}{\partial x}+v\frac{\partial T}{\partial y}=&\frac{aT_0e^{\frac{3x}{2L}}}{2L}\Big(f'(\eta)\theta(\eta)+\eta f'(\eta)\theta'(\eta)\Big)\\
&-\frac{aT_0e^{\frac{3x}{2L}}}{2L}\Big(\eta f'(\eta)\theta'(\eta)+f(\eta)\theta'(\eta)\Big)\\
=&\frac{aT_0e^{\frac{3x}{2L}}}{2L}f'(\eta)\Big(\theta(\eta)-\eta\theta'(\eta)\Big).
\end{aligned}
$$

Furthermore, the first, second and third expressions on the right hand side of Eq. (4.3) have been transformed into the dimensionless form as stated below:

$$
\alpha_{nf}\frac{\partial^2 T}{\partial y^2}=\frac{k_{nf}}{(\rho c_p)_{nf}}\frac{aT_0}{2\nu_f L}e^{\frac{3x}{2L}}\theta''(\eta). \tag{4.11}
$$

$$
\begin{aligned}
\frac{1}{(\rho c_p)_{nf}}\frac{\partial q_r}{\partial y}&=\frac{1}{(\rho c_p)_{nf}}\frac{-16\sigma^*T_\infty^3}{3k^*}\frac{aT_0e^{\frac{3x}{2L}}}{2\nu_f L}\theta''(\eta)\\
&=\frac{-16\sigma^*T_\infty^3}{3k^*(\rho c_p)_{nf}}\frac{aT_0e^{\frac{3x}{2L}}}{2L\nu_f}\theta''(\eta).\\
\frac{\mu_{nf}}{(\rho c_p)_{nf}}\left(\frac{\partial u}{\partial y}\right)^2&=\frac{\mu_{nf}}{(\rho c_p)_{nf}}\left(a\sqrt{\frac{a}{2L\nu_f}}e^{\frac{3x}{2L}}f''(\eta)\right)^2\\
&=\frac{\mu_{nf}}{(\rho c_p)_{nf}}\frac{a^3}{2L\nu_f}\left(e^{\frac{3x}{2L}}\right)^2 f''^2(\eta).
\end{aligned}
$$

On the similar note, conversion of the remaining terms of the right hand side of Eq. (4.3) into the dimensionless form has been stated below:

$$
\begin{aligned}
\frac{\sigma B^2\sin^2\alpha}{(\rho c_p)_{nf}}(u-U_\infty)^2&=\frac{\sigma(B_0e^{\frac{x}{2L}})^2\sin^2\alpha}{(\rho c_p)_{nf}}(ae^{\frac{x}{L}}f'(\eta)-ae^{\frac{x}{L}})^2\\
&=\frac{\sigma(B_0e^{\frac{x}{2L}})^2\sin^2\alpha}{(\rho c_p)_{nf}}(ae^{\frac{x}{L}}(f'(\eta)-1))^2.
\end{aligned} \tag{4.12}
$$

Using (4.11) - (4.12), the dimensionless form of right side of (4.3) is as follows:

$$
\begin{aligned}
&\alpha_{nf}\frac{\partial^2 T}{\partial y^2}-\frac{1}{(\rho c_p)}\frac{\partial q_r}{\partial y}+\frac{\mu_{nf}}{(\rho c_p)_{nf}}\left(\frac{\partial u}{\partial y}\right)^2+\frac{\sigma B^2\sin^2\alpha}{(\rho c_p)_{nf}}(u-U_\infty)^2\\
&=\frac{K_{nf}T_0ae^{\frac{3x}{2L}}}{2\nu_f L(\rho c_p)_{nf}}\theta''(\eta)+\frac{16\sigma^*T_\infty^3aT_0e^{\frac{3x}{2L}}}{6k^*\nu_f L(\rho c_p)_{nf}}\theta''(\eta)+\frac{a^3\left(e^{\frac{3x}{2L}}\right)^2\mu_{nf}}{2L\nu_f(\rho c_p)_{nf}}f''^2(\eta)\\
&+\frac{\sigma(B_0e^{\frac{x}{2L}})^2\sin^2\alpha}{(\rho c_p)_{nf}}(ae^{\frac{x}{L}}(f'(\eta)-1))^2
\end{aligned}
$$

$$
\begin{aligned}
&= \frac{K_{nf} T_0 a e^{\frac{3x}{2L}}}{2\nu_f L(\rho c_p)_{nf}} \theta''(\eta) + \frac{16\sigma^* T_\infty^3 a T_0 e^{\frac{3x}{2L}}}{6k^* \nu_f L(\rho c_p)_{nf}} \theta''(\eta) + \frac{a^3 \left(e^{\frac{3x}{2L}}\right)^2 \mu_{nf}}{2L\nu_f (\rho c_p)_{nf}} f''^2(\eta) \\
&\quad + \frac{\sigma (B_0 e^{\frac{x}{2L}})^2 \sin^2\alpha}{(\rho c_p)_{nf}} (a e^{\frac{x}{L}} (f'(\eta) - 1))^2 \\
&= \frac{a T_0 e^{\frac{3x}{2L}}}{2L} \Bigg[\frac{k_{nf}}{\nu_f (\rho c_p)_{nf}} \theta''(\eta) \frac{16\sigma^* T_\infty^3}{3k^* \nu_f (\rho c_p)_{nf}} \theta''(\eta) \\
&\quad + \frac{\mu_{nf} \left(a^2 e^{\frac{3x}{2L}}\right)}{\nu_f T_0 (\rho c_p)_{nf}} f''^2(\eta) + \frac{\sigma (B_0 e^{\frac{x}{2L}})^2 a e^{\frac{2x}{L}} 2L}{T_0 e^{\frac{3x}{2L}} (\rho c_p)_{nf}} (f'(\eta) - 1)^2 \Bigg] \\
&= \frac{a T_0 e^{\frac{3x}{2L}}}{2L} \Bigg[\left(\frac{k_{nf}}{k_f} \frac{(\rho c_p)_f}{\rho c_p)_{nf}} \frac{k_f}{\rho c_p)_f} \frac{1}{\nu_f} \right) \theta''(\eta) + \left(\frac{(\rho c_p)_f}{\rho c_p)_{nf}} \frac{k_f}{(\rho c_p)_f \nu_f} \frac{16\sigma^* T_\infty^3}{3k^* k_f} \right) \theta''(\eta) \\
&\quad + \left(\frac{\mu_{nf}}{\mu_f} \frac{(\rho c_p)_f}{\rho c_p)_{nf}} \frac{\mu_f}{(\rho c_p)_f} \frac{\left(a^2 e^{\frac{3x}{2L}}\right)}{T_0 \nu_f} \right) f''^2(\eta) \\
&\quad + \left(\frac{(\rho c_p)_f}{(\rho c_p)_{nf}} \frac{1}{(\rho c_p)_f} \frac{2L\sigma (B_0 e^{\frac{x}{2L}})^2 U_\infty^2 \sin^2\alpha}{T_0 e^{\frac{3x}{2L}}} \right) (f'(\eta) - 1)^2 \Bigg] \\
&= \frac{a T_0 e^{\frac{3x}{2L}}}{2L} \Bigg[\left(\frac{k_f}{k_{nf}} \frac{1}{\left(1 - \phi + \frac{\phi(\rho c_p)_s}{(\rho c_p)_f}\right)} \frac{\alpha_f}{\nu_f} \right) \theta''(\eta) \qquad \left(\because \alpha_f = \frac{k_f}{(\rho c_p)_f} \right) \\
&\quad + \left(\frac{1}{\left(1 - \phi + \frac{\phi(\rho c_p)_s}{(\rho c_p)_f}\right)} \frac{\alpha_f}{\nu_f} \frac{16\sigma^* T_\infty^3}{3k^* k_f} \right) \theta''(\eta) \\
&\quad + \left(\frac{1}{(1-\phi)^{2.5} \left(1 - \phi + \frac{\phi(\rho c_p)_s}{(\rho c_p)_f}\right)} \frac{\mu_f}{\rho_f} \frac{1}{\nu_f} \frac{\left(a^2 e^{\frac{3x}{2L}}\right)}{T_0 (c_p)_f} \right) f''^2(\eta) \\
&\quad + \left(\frac{1}{\left(1 - \phi + \frac{\phi(\rho c_p)_s}{(\rho c_p)_f}\right)} \frac{1}{(\rho c_p)_f} \frac{2L\sigma (B_0 e^{\frac{x}{2L}})^2 (U_\infty)^2 \sin^2\alpha}{a T_0 e^{\frac{3x}{2L}}} \right) (f'(\eta) - 1)^2 \Bigg] \\
&= \frac{a T_0 e^{\frac{3x}{2L}}}{2L} \Bigg[\left(\frac{k_{nf}}{k_f} \frac{1}{\left(1 - \phi + \frac{\phi(\rho c_p)_s}{(\rho c_p)_f}\right)} \frac{1}{P_r} \right) \theta''(\eta) \qquad \left(\because P_r = \frac{\nu_f}{\alpha_f} \right) \\
&\quad + \left(\frac{1}{\left(1 - \phi + \frac{\phi(\rho c_p)_s}{(\rho c_p)_f}\right)} \frac{1}{P_r} \frac{16\sigma^* T_\infty^3}{3k^* k_f} \right) \theta''(\eta) \\
&\quad + \left(\frac{1}{(1-\phi)^{2.5} \left(1 - \phi + \frac{\phi(\rho c_p)_s}{(\rho c_p)_f}\right)} \frac{(a e^{\frac{x}{L}})^2}{(T_w - T_\infty)(c_p)_f} \right) f''^2(\eta) \\
&\quad + \left(\frac{1}{\left(1 - \phi + \frac{\phi(\rho c_p)_s}{(\rho c_p)_f}\right)} \frac{1}{(\rho c_p)_f} \frac{2L\sigma e^{\frac{x}{2L}} (B_0 e^{\frac{x}{2L}})^2 (U_\infty)^2 \sin^2\alpha}{a(T_w - T_\infty) e^{\frac{3x}{2L}}} \right) (f'(\eta) - 1)^2 \Bigg]
\end{aligned}
$$

Therefore the dimensionless form of (4.3) becomes:

$$
\begin{aligned}
\frac{aT_0e^{\frac{3x}{2L}}}{2L}\Big(f'(\eta)\theta(\eta)-f(\eta)\theta'(\eta)\Big) = {} & \frac{aT_0e^{\frac{3x}{2L}}}{2L}\Bigg[\Bigg(\frac{k_{nf}}{k_f}\frac{1}{\Big(1-\phi+\frac{\phi(\rho c_p)_s}{(\rho c_p)_f}\Big)}\frac{1}{P_r}\Bigg)\theta''(\eta) \\
& +\Bigg(\frac{1}{\Big(1-\phi+\frac{\phi(\rho c_p)_s}{(\rho c_p)_f}\Big)}\frac{1}{P_r}\frac{16\sigma^*T_\infty^3}{3k^*k_f}\Bigg)\theta''(\eta) \\
& +\frac{(U_\infty)^2f''^2(\eta)}{(1-\phi)^{2.5}\Big(1-\phi+\frac{\phi(\rho c_p)_s}{(\rho c_p)_f}\Big)(T_w-T_\infty)(c_p)_f} \\
& +\Bigg(\frac{1}{\Big(1-\phi+\frac{\phi(\rho c_p)_s}{(\rho c_p)_f}\Big)}\frac{1}{\rho_f(c_p)_f} \\
& \frac{2L\sigma e^{\frac{x}{2L}}(B_0e^{\frac{x}{2L}})^2(U_\infty)^2\sin^2\alpha}{a(T_w-T_\infty)e^{\frac{3x}{2L}}}\Bigg)(f'(\eta)-1)^2\Bigg]
\end{aligned}
$$

$$
\begin{aligned}
\Rightarrow \Big(f'(\eta)\theta(\eta)-f(\eta)\theta'(\eta)\Big)P_r = {} & \Bigg[\Bigg(\frac{k_{nf}}{k_f}\frac{1}{\Big(1-\phi+\frac{\phi(\rho c_p)_s}{(\rho c_p)_f}\Big)}\Bigg)\theta''(\eta) \\
& +\Bigg(\frac{1}{\Big(1-\phi+\frac{\phi(\rho c_p)_s}{(\rho c_p)_f}\Big)}\frac{16\sigma^*T_\infty^3}{3k^*k_f}\Bigg)\theta''(\eta) \\
& +\frac{P_r}{(1-\phi)^{2.5}\Big(1-\phi+\frac{\phi(\rho c_p)_s}{(\rho c_p)_f}\Big)}\frac{(U_\infty)^2f''^2(\eta)}{(T_w-T_\infty)(c_p)_f} \\
& +\Bigg(\frac{2L\sigma(B_0)^2\sin^2\alpha}{a(T_w-T_\infty)}\frac{1}{(1-\phi+\frac{\phi(\rho c_p)_s}{(\rho c_p)_f})} \\
& \frac{Pr(U_\infty)^2}{(\rho c_p)_f}\Bigg)(f'(\eta)-1)^2\Bigg]
\end{aligned}
$$

$$
\begin{aligned}
\Rightarrow \Big(f'(\eta)\theta(\eta)-f(\eta)\theta'(\eta)\Big)P_r = {} & \frac{1}{\Big(1-\phi+\frac{\phi(\rho c_p)_s}{(\rho c_p)_f}\Big)}\Bigg[\Bigg(\frac{k_{nf}}{k_f}\Bigg)\theta''(\eta) \\
& +\Bigg(\frac{16\sigma^*T_\infty^3}{3k^*k_f}\Bigg)\theta''(\eta) \\
& +\frac{1}{(1-\phi)^{2.5}}P_r\frac{(U_\infty)^2}{(T_w-T_\infty)(c_p)_f}f''^2(\eta) \\
& +\frac{2L\sigma(B_0)^2\sin^2\alpha}{a\rho_f}P_r\frac{(U_\infty)^2}{(T_w-T_\infty)(c_p)_f}(f'(\eta)-1)^2\Bigg]
\end{aligned}
$$

$$
\Rightarrow \Big(f'(\eta)\theta(\eta)-f(\eta)\theta'(\eta)\Big)P_r = \frac{1}{\Big(1-\phi+\frac{\phi(\rho c_p)_s}{(\rho c_p)_f}\Big)}\Bigg[\Bigg(\frac{k_{nf}}{k_f}+\frac{16\sigma^*T_\infty^3}{3k^*k_f}\Bigg)\theta''(\eta)
$$

$$+\frac{1}{(1-\phi)^{2.5}}P_r\frac{(U_\infty)^2}{(T_w-T_\infty)(c_p)_f}f''^2(\eta)$$
$$+\frac{2L\sigma(B_0)^2\sin^2\alpha}{a\rho_f}P_r\frac{(U_\infty)^2}{(T_w-T_\infty)(c_p)_f}(f'(\eta)-1)^2\Bigg].$$

$$\Rightarrow\left(1-\phi+\frac{\phi(\rho c_p)_s}{(\rho c_p)_f}\right)\Big(f'(\eta)\theta(\eta)-f(\eta)\theta'(\eta)\Big)P_r=\left[\left(\frac{k_{nf}}{k_f}+\frac{16\sigma^*T_\infty^3}{3k^*k_f}\right)\theta''(\eta)\right.$$
$$+\frac{1}{(1-\phi)^{2.5}}P_r\frac{(U_\infty)^2}{(T_w-T_\infty)(c_p)_f}f''^2(\eta)$$
$$\left.+\frac{2L\sigma(B_0)^2\sin^2\alpha}{a\rho_f}P_r\frac{(U_\infty)^2}{(T_w-T_\infty)(c_p)_f}(f'(\eta)-1)^2\right].$$
$$\Rightarrow\left(\frac{k_{nf}}{k_f}+\frac{16\sigma^*T_\infty^3}{3k^*k_f}\right)\theta''(\eta)+P_r\left(1-\phi+\frac{\phi(\rho c_p)_s}{(\rho c_p)_f}\right)\Big(-f'(\eta)\theta(\eta)+f(\eta)\theta'(\eta)\Big)$$
$$+\frac{1}{(1-\phi)^{2.5}}P_r\frac{(U_\infty)^2}{(T_w-T_\infty)(c_p)_f}f''^2(\eta)$$
$$+\frac{2L\sigma(B_0)^2\sin^2\alpha}{a\rho_f}P_r\frac{(U_\infty)^2}{(T_w-T_\infty)(c_p)_f}(f'(\eta)-1)^2\Bigg].$$

Next, we include the procedure for the conversion of (4.4) into the dimensionless form. The left hand side of Eq. (4.4) into the dimensionless form is similar to that discussed in Chapter 3.

$$\begin{aligned}u\frac{\partial C}{\partial x}+v\frac{\partial C}{\partial y}&=C_0\frac{ae^{\frac{3x}{2L}}}{2L}(h(\eta)f'(\eta)+\eta h'(\eta)f'(\eta)-\eta f'(\eta)h'(\eta)-f(\eta)h'(\eta))\\&=\frac{ae^{\frac{3x}{2L}}}{2L}C_0(f'(\eta)h(\eta)-h'(\eta)f(\eta)).\end{aligned}\tag{4.13}$$

To convert the right side of (4.4) into the dimensionless form, we proceed as follows:

$$\begin{aligned}\frac{\partial^2 C}{\partial y^2}&=\frac{\partial}{\partial y}\left(\sqrt{\frac{a}{2L\nu_f}}C_0e^{\frac{x}{L}}h'(\eta)\right)\\&=\left(C_0e^{\frac{x}{L}}\sqrt{\frac{a}{2L\nu_f}}\frac{\partial h'(\eta)}{\partial\eta}\frac{\partial\eta}{\partial y}\right)\\&=C_0e^{\frac{x}{L}}\sqrt{\frac{a}{2L\nu_f}}h''(\eta)\sqrt{\frac{a}{2L\nu_f}}e^{\frac{x}{2L}}\\&=C_0e^{\frac{x}{L}}e^{\frac{x}{2L}}\frac{a}{2L\nu_f}h''(\eta)\\&=C_0e^{\frac{3x}{2L}}\frac{a}{2L\nu_f}h''(\eta)\end{aligned}$$

$$h^n(\eta) = \left(\frac{C - C_\infty}{C_w - C_\infty}\right)^n$$

$$\Rightarrow (C - C_\infty)^n = h^n(\eta)(C_w - C_\infty)^n$$

$$\Rightarrow K(C - C_\infty)^n = Kh^n(\eta)(C_w - C_\infty)^n$$

$$\Rightarrow K(C - C_\infty)^n = K_0 e^{\frac{x}{L}} h^n(\eta)(C_w - C_\infty)^n$$

Using (4.14) and (4.14) in the right side of (4.4), we get

$$D\frac{\partial^2 C}{\partial y^2} - K(C - C_\infty) = DC_0 e^{\frac{3x}{2L}} \frac{a}{2L\nu_f} h''(\eta) - K_0 e^{\frac{x}{L}} (C_w - C_\infty)^n h^n(\eta). \quad (4.14)$$

Hence the dimensionless form of (4.4) becomes:

$$C_0 \frac{ae^{\frac{3x}{2L}}}{2L}(f'(\eta)h(\eta) - h'(\eta)f(\eta)) = DC_0 e^{\frac{3x}{2L}} \frac{a}{2Lv_f} h''(\eta) - K_0 e^{\frac{x}{L}} (C_w - C_\infty)^n h^n(\eta)$$

$$\Rightarrow C_0 \frac{ae^{\frac{3x}{2L}}}{2L}(f'(\eta)h(\eta) - h'(\eta)f(\eta)) = C_0 e^{\frac{3x}{2L}} \left(\frac{Dah''(\eta)}{2L\nu_f} - \frac{K_0 e^{\frac{x}{L}} (C_w - C_\infty)^n}{e^{\frac{3x}{2L}} C_0} h^n(\eta)\right)$$

$$\Rightarrow \frac{a}{2L}(f'(\eta)h(\eta) - h'(\eta)f(\eta)) = \frac{a}{2L}\left(\frac{D}{\nu_f} h''(\eta) - \frac{2LK_0 e^{\frac{x}{L}} (C_w - C_\infty)^n}{ae^{\frac{3x}{2L}} C_0} h^n(\eta)\right)$$

$$\Rightarrow (f'(\eta)h(\eta) - h'(\eta)f(\eta)) = \frac{D}{\nu_f} h''(\eta) - \frac{2LK_0 (C_w - C_\infty)^n}{C_0 a e^{\frac{3x}{2L}} e^{\frac{-x}{L}}} h^n(\eta)$$

$$\Rightarrow \frac{\nu_f}{D}(f'(\eta)h(\eta) - h'(\eta)f(\eta)) = h''(\eta) - \frac{\nu_f}{D} \frac{2LK_0 (C_w - C_\infty)^n}{a(C_w - C_\infty)} h^n(\eta)$$

$$\Rightarrow \frac{\nu_f}{D}(f'(\eta)h(\eta) - h'(\eta)f(\eta)) = h''(\eta) - \frac{\nu_f}{D} \frac{2LK_0 (C_w - C_\infty)^{n-1}}{a} h^n(\eta)$$

$$\Rightarrow \left(\frac{\nu_f}{D}(f'(\eta)h(\eta) - h'(\eta)f(\eta)) + \frac{\nu_f}{D} \frac{2LK_0 (C_w - C_\infty)^{n-1}}{a} h^n(\eta)\right) = h''(\eta)$$

$$\Rightarrow h''(\eta) + \frac{\nu_f}{D}(f'(\eta)h(\eta) - h'(\eta)f(\eta)) - \frac{\nu_f}{D} \frac{2LK_0 (C_w - C_\infty)^{n-1}}{a} h^n(\eta) = 0.$$

Finally, the ODEs describing the governing flow problem can be re-collected in the following system:

$$\frac{1}{(1-\phi)^{2.5}\left(1-\phi+\phi\frac{\rho_s}{\rho_f}\right)} f''' + ff'' + 2(1 - f'^2)$$

$$+ \frac{1}{(1-\phi)^{2.5}\left(1-\phi+\phi\frac{\rho_s}{\rho_f}\right)} (P + (1-\phi)^{2.5} M \sin^2\alpha)(1 - f') = 0, \quad (4.15)$$

$$\left(\frac{k_{nf}}{k_f}+R\right)\theta''+P_r\left(1-\phi+\frac{\phi(\rho c_p)_s}{(\rho c_P)_f}\right)(f\theta'-f'\theta)+\frac{1}{(1-\phi)^{2.5}}Ec\,f''^2$$
$$+\sin^2\alpha\;P_r\;M\;Ec\,(f'-1)^2=0, \tag{4.16}$$

$$h''+Sc(fh'-f'h-\gamma_n h^n)=0. \tag{4.17}$$

The associated boundary conditions (4.5) get the form:

$$\left.\begin{array}{lll} f=0, f'=0, \theta=1, h=1, & \text{at} & \eta=0, \\ f'\to 1, \theta\to 0, h\to 0, & \text{as} & \eta\to\infty. \end{array}\right\} \tag{4.18}$$

Different parameters used in the above equations have the following formulations:

$$\begin{aligned} &M=\frac{2\sigma B_0^2 L}{a\rho_f}, P_r=\frac{\nu_f}{\alpha_f}, Sc=\frac{\nu_f}{D}, P=\frac{2L\nu_f}{ak_0},\\ &R=\frac{16\sigma^* T_\infty^3}{3k^* k_f}, \gamma_n=\frac{2LK_0(C_w-C_\infty)^{n-1}}{a}, Ec=\frac{U_\infty^2}{(c_p)_f(T_w-T_\infty)}. \end{aligned} \tag{4.19}$$

4.3 Physical Quantities of Interest

The detailed procedure of the dimensionless form of skin-friction coefficient, Nusselt number and Sherwood number have been discussed in Chapter 3.

The skin-friction coefficient, Nusselt number and Sherwood number in dimensionless form are given by:

$$\left.\begin{array}{l} \dfrac{\sqrt{Re_x/2}}{\sqrt{x/L}}C_{fx}=\dfrac{1}{(1-\phi)^{2.5}}f''(0), \\ \sqrt{\dfrac{2L}{x}}\dfrac{1}{\sqrt{Re_x}}Nu_x=-\dfrac{k_{nf}}{k_f}\theta'(0), \\ Sh_x\sqrt{\dfrac{1}{Re_x}}\sqrt{\dfrac{2L}{x}}=-h'(0). \end{array}\right\} \tag{4.20}$$

4.4 Solution Methodology

In order to solve the system of ordinary differential Eqs. (4.15)-(4.17), the shooting method together with the Runge-Katta method of order four has been used. First, Eq. (4.15) is numerically solved and then the calculated results of f, f' and f'' are used in Eq. (4.16) and (4.17). Since the Eq. (4.15) is independent of θ and h, the Eq. (4.15) can be solved independently by using shooting method, the following notations have been introduced:

$$f = y_1, f' = y_1' = y_2, f'' = y_2' = y_3, f''' = y_3'.$$

By using the above notations in Eq. (4.15), we get the system of equations

$$\begin{aligned}
&y_1' = y_2, && y_1(0) = 0,\\
&y_2' = y_3, && y_2(0) = 0,\\
&y_3' = -b_1(y_1y_3 + 2(1-y_2^2)) - (P + (1-\phi)^{2.5}M\sin^2\alpha)(1-y_2), && y_3(0) = L.
\end{aligned}$$

$$\text{where } \; b_1 = (1-\phi)^{2.5}(1-\phi+\phi\frac{\rho_s}{\rho_f}).$$

The above initial value problem will be solved numerically by the RK4 method. To get the approximate solution, the domain of the problem has been taken as $[0, \eta_\infty]$ instead of $[0, \infty]$, where η_∞ is an appropriate finite positive real number in such a way that the variation in the solution for $\eta > \eta_\infty$ is ignorable. Chosen initial guess L such that:

$$y_1(\eta_\infty, L) - 1 = 0. \tag{4.21}$$

To solve the above algebraic Eq. (4.21), we use the Newton's method which has the following iterative procedure:

$$L^{(k+1)} = L^{(k)} - \left(\frac{\partial y_1}{\partial L}\right)^{-1}\left(y_1(\eta_\infty, L) - 1\right). \tag{4.22}$$

In order to obtain $\left(\frac{\partial y_1}{\partial L}\right)^{-1}$, we further introduce the following notations:

$$\frac{\partial y_1}{\partial L} = y_4, \frac{\partial y_2}{\partial L} = y_5, \frac{\partial y_3}{\partial L} = y_6.$$

As a result of these new notations, the Newton's iterative scheme gets the form:

$$L^{(k+1)} = L^{(k)} - (y_4)^{-1}\Big(y_1(\eta_\infty, L) - 1\Big).$$

In order to get the value of y_4, differentiate the above system of three first order ODEs with respect to L, we get another system of six ODEs. Writing all these six ODEs together, we have the following initial value problem (IVP), which needs to be solved:

$$\begin{aligned}
y_1' &= y_2, & y_1(0) &= 0,\\
y_2' &= y_3, & y_2(0) &= 0,\\
y_3' &= -b_1(y_1y_3 + 2(1-y_2^2)) - (P + (1-\phi)^{2.5}M\sin^2\alpha)(1-y_2), & y_3(0) &= L,\\
y_4' &= y_5, & y_4(0) &= 0,\\
y_5' &= y_6, & y_5(0) &= 0,\\
y_6' &= -b_1(y_4y_3 + y_1y_6 - 4y_2y_5) + (P + (1-\phi)^{2.5}M\sin^2\alpha)y_5, & y_6(0) &= 1.
\end{aligned}$$

Next, we have to solve Eq. (4.16) for the known value of f. For this we use the same procedure as considered for Eq (4.15). For that let us denote:

$$\begin{aligned}
\theta &= z_1,\\
\theta' &= z_1' = z_2,\\
\theta'' &= z_1'' = z_2',\\
f \;\; &= d_1, f' = d_2, f'' = d_3.
\end{aligned}$$

By using the above notations in Eq. (4.16), we get the following system of equations:

$$\begin{aligned}
z_1' &= z_2, & z_1(0) &= 0,\\
z_2' &= -\frac{1}{\left(\frac{k_{nf}}{k_f} + R\right)}\Bigg[P_r\left(1 - \phi + \frac{\phi(\rho c_p)_s}{(\rho c_p)_f}\right)(d_1z_2 - d_2z_1)\\
&\quad + \frac{1}{(1-\phi)^{2.5}}Ecd_3^2 + \sin^2\alpha P_rMEc(d_2-1)^2\Bigg], & z_2(0) &= m.
\end{aligned}$$

The above initial value problem will be solved again using RK4 method. The computational domain is truncated in the similar way as before. In the above system of equations, the missing condition is m which needs to be refined such that:

$$z_1(\eta_\infty, m) - 1 = 0. \tag{4.23}$$

To solve the above algebraic Eq. (4.23), we use the Newton's method which has the following iterative procedure:

$$m^{(k+1)} = m^{(k)} - \left(\frac{\partial z_1}{\partial m}\right)^{-1} \Big(z_1(\eta_\infty, m) - 1\Big) \tag{4.24}$$

In order to obtain $\left(\frac{\partial z_1}{\partial m}\right)^{-1}$, we further introduce the following notations:

$$\frac{\partial z_1}{\partial m} = z_3, \frac{\partial z_2}{\partial m} = z_4.$$

As a result of these new notations, the Newton's iterative scheme gets the form:

$$m^{(k+1)} = m^{(k)} - (z_3)^{-1} \Big(z_1(\eta_\infty, m) - 1\Big).$$

Now differentiate the above system of two first order ODEs with respect to m, we get another system of four ODEs. Writing all these four ODEs together, we have the following initial value problem (IVP), which needs to be solved.

$$\begin{aligned}
z_1' &= z_2, && z_1(0) = 0,\\
z_2' &= -\frac{1}{\left(\frac{k_{nf}}{k_f} + R\right)}\left[P_r\left(1 - \phi + \frac{\phi(\rho c_p)_s}{(\rho c_p)_f}\right)(d_1 z_2 - d_2 z_1)\right.\\
&\quad \left. + \frac{1}{(1-\phi)^{2.5}} Ecd_3^2 + \sin^2\alpha\, P_r M Ec(d_2 - 1)^2\right], && z_2(0) = m,\\
z_3' &= z_4, && z_3(0) = 0,\\
z_4' &= -\frac{1}{\left(\frac{k_{nf}}{k_f} + R\right)}\left[P_r\left(1 - \phi + \frac{\phi(\rho c_p)_s}{(\rho c_p)_f}\right)(d_1 z_4 - d_2 z_3)\right], && z_4(0) = 1.
\end{aligned}$$

By using shooting techniques we have the solution of Eq. (4.16). Next, we have to solve Eq. (4.17) for the know value of f. For this we use the same procedure as considered for Eq (3.33) and (4.16). For that let us denoted:

$$
\begin{aligned}
h &= g_1, \\
h' &= g_1' = g_2, \\
h'' &= g_1'' = g_2', \\
f &= d_1, f' = d_2, f'' = d_3.
\end{aligned}
$$

By using the above notations in Eq. (4.17), we get the following system of equation:

$$
\begin{aligned}
g_1' &= g_2, & g_1(0) &= 0, \\
g_2' &= -Sc(d_1 g_2 - d_2 g_1 - \gamma_n g_1^n), & g_2(0) &= q.
\end{aligned}
$$

The above initial value problem will be solved again using RK4 method. The computational domain is truncated in the similar way as before. In the above system of equations, the missing condition is q which needs to be refined such that:

$$g_1(\eta_\infty, q) - 1 = 0 \tag{4.25}$$

To solve the above algebraic Eq. (4.25), we use the Newton's method which has the following iterative procedure:

$$q^{(k+1)} = q^{(k)} - \left(\frac{\partial g_1}{\partial q}\right)^{-1} \Big(g_1(\eta_\infty, q) - 1\Big).$$

In order to obtain $\left(\frac{\partial g_1}{\partial q}\right)^{-1}$, we further introduce the following notations:

$$\frac{\partial g_1}{\partial q} = g_3, \frac{\partial g_2}{\partial q} = g_4.$$

As a result of these new notations, the Newton's iterative scheme gets the form:

$$q^{(k+1)} = q^{(k)} - (g_3)^{-1}\Big(g_1(\eta_\infty, q) - 1\Big).$$

Now differentiate the above system of two first order ODEs with respect to q, we get another system of four ODEs. Writing all these four ODEs together, we have the following initial value problem (IVP),which needs to be solved:

$$\begin{aligned}
g_1' &= g_2, & g_1(0) &= 0,\\
g_2' &= -Sc(d_1 g_2 - d_2 g_1 - \gamma_n g_1^n), & g_2(0) &= q,\\
g_3' &= g_4, & g_3(0) &= 0,\\
g_4' &= -Sc(d_1 g_4 - d_2 g_3 - \gamma_n n g_1^{n-1} g_3), & g_4(0) &= 1.
\end{aligned}$$

By using shooting techniques we have the solution of Eq. (4.17).

4.5 Result and Discussion

In this section, the numerical results of skin-friction coefficient, Nusselt and Sherwood numbers are illustrated by tables and graphs to show the behaviour of the velocity, temperature and concentration by assuming various values of different physical parameters of interest.

In Tables 4.1-4.3 the numerical analysis of various physical parameters on C_{fx}, Nu_x and Sh_x under discussion is displayed. Tables 4.1-4.3 show that by increasing the values of ϕ skin friction, Nusselt number and Sherwood number is also increasing. For the larger permeability parameter P, the skin friction and Sherwood number are enhanced whereas the Nusselt number experiences an opposite behaviour. An enhancement in the skin friction, Nusselt and Sherwood numbers has been seen as M, R and γ assume the larger values. The higher estimation of Eckert number Ec de-escalate the Sherwood number.

$\frac{1}{(1-\phi)^{2.5}} f''(0)$									
ϕ	P	M	R	Ec	γ	α	n	Cu-water	Al_2O_3-water
0.0	0.5	2	1	0.5	0.1	$\pi/8$	1	1.9071	1.9071
0.1								2.8066	2.4563
0.2								3.8626	3.1575
0.1	0	0.5	1	0.5	0.1	$\pi/4$	2	2.6414	2.2657
	2							3.2181	2.9177
	5							3.9281	3.6863
0.1	0.5	1	1	0.5	0.1	$\pi/4$	1	2.8541	2.5104
			2					2.9656	2.6365
			3					3.0731	2.7570
0.2	5	0.2	0.2	0.5	0.1	$\pi/4$	1	5.3197	4.8336
				1.5				5.3197	4.8336
				2.5				5.3197	4.8336
0.2	0.5	1	1	0.5	0.0	$\pi/4$	2	3.9091	3.2141
					0.1			3.9091	3.2141
					0.2			3.9091	3.2141
0.1	0.5	1	1	0.5	0.1	$\pi/2$	2	2.9658	2.6371
						$\pi/4$		2.8543	2.5112
						$\pi/6$		2.7969	2.4458
0.2	0.5	1	1	0.5	0.1	$\pi/4$	1	3.9093	3.2157
							2	3.9093	3.2157
							3	3.9093	3.2157

TABLE 4.1: Numerical results of skin-friction coefficient $f''(0)$ when $P_r = 6.2$ and $Sc = 0.68$.

						$-\frac{k_{nf}}{k_f}\theta'(0)$			
ϕ	P	M	R	Ec	γ	α	n	Cu-water	Al_2O_3-water
0.0	0.5	2	1	0.5	0.1	$\pi/8$	1	2.6968	2.6968
0.1								3.2774	3.2611
0.2								3.8412	3.8445
0.1	0	0.5	1	0.5	0.1	$\pi/4$	2	3.2294	3.2044
	2							3.1901	3.1720
	5							3.1205	3.1053
0.1	0.5	1	1	0.5	0.1	$\pi/4$	1	3.5475	3.5594
		2						4.1741	4.2441
		3						4.7683	4.8848
0.2	10	1	1	0.5	0.1	$\pi/4$	1	2.5430	2.5292
			2					4.0249	4.1612
			3					5.6281	5.8017
0.2	5	0.2	0.2	0.5	0.1	$\pi/4$	1	2.0934	2.0997
				1.5				-0.1039	0.1945
				2.5				-2.3014	-1.7088
0.2	0.5	1	1	0.5	0.0	$\pi/4$	2	4.1929	4.2517
					0.1			4.1929	4.2517
					0.2			4.1929	4.2517
0.2	0.5	1	1	0.5	0.1	$\pi/2$	2	4.1752	4.2454
						$\pi/4$		3.5473	3.5598
						$\pi/6$		3.2198	3.1981
0.2	0.5	1	1	0.5	0.1	$\pi/4$	1	4.1958	4.2558
							2	4.1958	4.2558
							3	4.1958	4.2558

TABLE 4.2: Numerical results of Nusselt number $-\theta'(0)$ when $P_r = 6.2$ and $Sc = 0.68$.

					$-h'(0)$				
ϕ	P	M	R	Ec	γ	α	n	Cu-water	Al_2O_3-water
0.0	0.5	2	1	0.5	0.1	$\pi/8$	1	0.7923	0.7923
0.1								0.8113	0.8113
0.2								0.7844	0.7844
0.1	0	0.5	1	0.5	0.1	$\pi/4$	2	0.9398	0.9170
	2							0.9625	0.9477
	5							0.9850	0.9755
0.1	0.5	1	1	0.5	0.1	$\pi/4$	1	0.8242	0.8047
		2						0.8288	0.8108
		3						0.8331	0.8164
0.2	5	0.2	0.2	0.5	0.1	$\pi/4$	1	0.7155	0.7014
				1.5				0.7155	0.7014
				2.5				0.7155	0.7014
0.2	0.2	1	1	0.5	0.0	$\pi/4$	2	0.6958	0.6663
					0.1			0.7227	0.6943
					0.2			0.7490	0.7215
0.1	0.5	1	1	0.5	0.1	$\pi/2$	2	0.8479	0.8312
						$\pi/4$		0.8436	0.8255
						$\pi/6$		0.8413	0.8225
0.2	0.5	1	1	0.5	0.1	$\pi/4$	1	0.8561	0.8288
							2	0.8466	0.8192
							3	0.8416	0.8140

TABLE 4.3: Numerical results of Sherwood number$-h'(0)$ when $P_r=6.2$ and $Sc=0.68$.

For the higher estimation of inclination angle α, the skin-friction coefficient and the Sherwood number de-escalate whereas the Nusselt number increases marginally. Due to increasing higher order chemical reaction parameter n, the values of skin friction, Sherwood number are same and Nusselt number values decrease.

This section presents the graphical view of different parameters obtained while non-dimensionalizing the above physical model.

Figures 4.2-4.4 are sketched to present the influence of the volume fraction ϕ on velocity, temperature and concentration profiles. The nanoparticle volume fraction parameter ϕ is varied from 0.0 (0%) to 0.2 (20%). The nanoparticles used in the study are copper (Cu) and alumina (Al_2O_3). Figure 4.2 shows the impact of the volume fraction on the fluid velocity. In this figure, we observe that the velocity increases with an increase in the volume fraction of nanoparticles for Cu-water while the effect of "nanoparticle volume fraction" ϕ parameter for Al_2O_3–water on the velocity profile in the boundary layer. It is observed that the velocity profile is zero at the surface, increases and tends to unity as the distance increases from the boundary. Increasing values of the nanoparticle volume fraction parameter is to decrease the velocity profile for Al_2O_3–water.

Figure 4.3 elucidates the effect of the volume fraction on temperature profile. Analysis of the graph shows that the increasing values of the nanoparticles volume fraction parameter ϕ is to enhance the temperature profile and tends asymptotically to zero as the distance increases from the boundary for both Cu-water and Al_2O_3–water. Also the thermal boundary layer for nanoparticles, namely Cu-water, is greater than that of pure water. This is because nanoparticles volume fraction parameter has high thermal conductivity, so the thickness of the thermal boundary layer increases.

Figure 4.4 delineates the impact of the volume fraction ϕ on the concentration profile h. A decreasing behaviour is found in the dimensionless concentration h for Cu-water and increase marginally for Al_2O_3–water for the dimensionless concentration h.

Figures 4.5-4.7 present the impact of the magnetic parameter on the velocity, temperature and concentration profiles. Figure 4.5 shows the effect of magnetic parameter M, that employs viscous drag force on the flow which results in the deceleration of momentum, therefore with the increase of M the velocity boundary layer thickness increases. Velocity profile shows that with increasing values of M the velocity increases. Figure 4.6 is prepared to visualize the impact of the magnetic parameter M on the temperature $\theta(\eta)$. It is observed that increasing the value of M results in the decrease of thermal boundary layer thickness.

Figure 4.7 displays the effect of the magnetic parameter M on concentration profile. The higher values of M decrease the concentration profile. From these figures the fact that an opposing force is generated by the magnetic field, generally referred as the Lorentz force, which increase the motion of the fluid resulting in a decrement in the momentum boundary layer thickness and increment in the thermal and concentration boundary layer thickness.

Figure 4.8 elucidates the effect of the radiation parameter R on the temperature profile. The dimensionless temperature profile and the thermal boundary layer thickness increase gradually with an increase in the values of the radiation parameter R. Physically, it strengthens the fact that more heat is produced due to the radiation process for which the temperature profile is increased.

The outcome of Ec on the temperature profile has been characterized through Figure 4.9 for both Cu-water and Al_2O_3-water. Physically, the Eckert number depicts the relation between the kinetic energy of the fluid particles and the boundary layer enthalpy. The kinetic energy of the fluid particles rises as Ec assumes the larger values. Hence, the temperature of the fluid increased and therefore, the associated thermal boundary layer thickness is enhanced.

Figure 4.10 portrays the influence of chemical reaction parameter γ on the concentration profile, while other parameters are fixed for both Cu-water and Al_2O_3-water. Concentration falls when chemical reaction parameter γ increases. Furthermore, the larger values of γ result in a decrement in the chemical molecular diffusion and hence the concentration profile de-escalates and the associated concentration boundary layer thickness is reduced. This result is true in the cases of destructive chemical reaction $\gamma > 0$ and generative chemical reaction$\gamma < 0$.

Figures 4.11-4.13 are framed to delineate the impact of higher order of chemical reaction n on the velocity, temperature and concentration profiles. Figure 4.11 clearly reveals that the velocity of Cu-water nanofluid is high than the Al_2O_3-water nanofluid. It is evident from the Figure 4.12 that the temperature of Cu-water nanofluid is less than the Al_2O_3-water nanofluid. In Figure 4.13 the concentration profile increases with higher order chemical reaction parameter. For higher order reactions, the rate of increase in the concentration is less as compared with lower order reactions. Here numerical solutions are equipped in the range of $1 \leq n \leq 3$. To expose the effect of the permeability parameter P on the dimensionless velocity, temperature and concentration profiles, Figures 4.14-4.16 are sketched. Figure 4.14 depicts that an increases in the permeability parameter P velocity profile increase effectively. Physically, an increase in the permeability material correspond to large void section thus increases in the velocity profile. From Figure 4.15, it is noticed that higher values of the permeability parameter P than decreases the temperature profile. Actually by the increasing permeability of medium we are decreasing the viscous effects then low heat is produced which reduces the temperature profile. Figure 4.16 depicts the impact of permeability parameter P on the concentration profile. By increase in the permeability parameter P, the concentration profile decreases marginally. Moreover, the concentration boundary layer thickness also shows a declining behaviour.

Figures 4.17-4.19 are sketched to show the impact of inclined magnetic field α on the velocity, temperature and concentration distributions. Figure 4.17 depicts the impact of inclination angle α on the velocity. Physically an increase in the inclination angle we are actually increase the Lorentz force which are friction forces thus correspondingly the decreases velocity profile. Figure 4.18 divulges the temperature distributions for the boosting values of α. Physically by increasing the inclination angle we are increase the Lorentz force which generate more heat and thus increase the temperature profile. Figure 4.19 is displayed to analyze the impact of the inclination angle α on concentration profile. From the graph of this figure it is clear that the concentration profile is intensified for the growing values of the α.

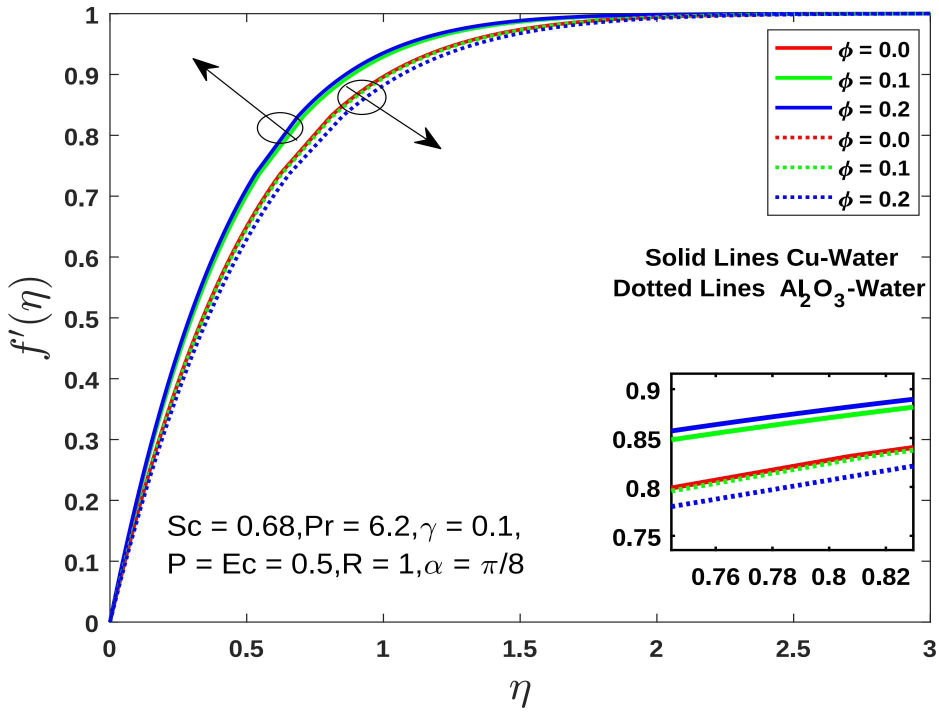

FIGURE 4.2: Impact of ϕ on the dimensionless velocity f'

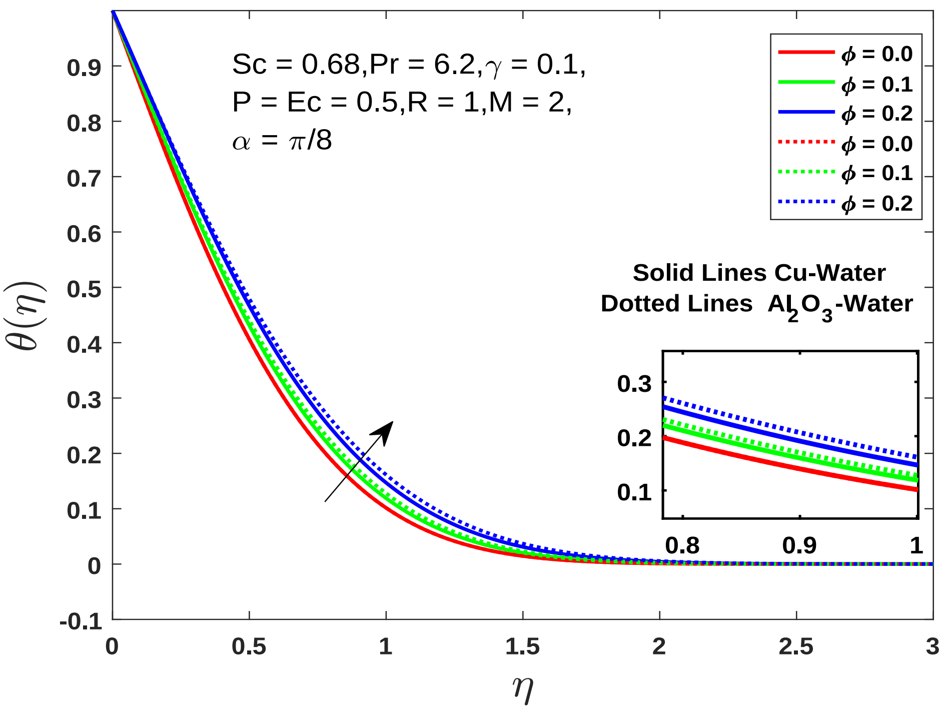

FIGURE 4.3: Impact of ϕ on the dimensionless temperature θ

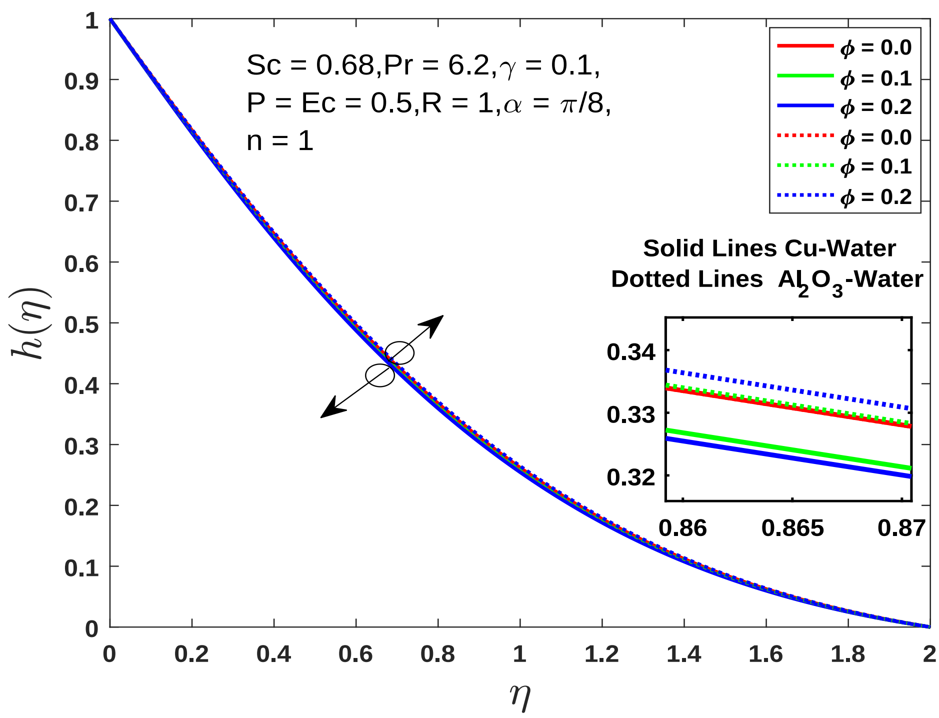

FIGURE 4.4: Impact of ϕ on the dimensionless concentration h

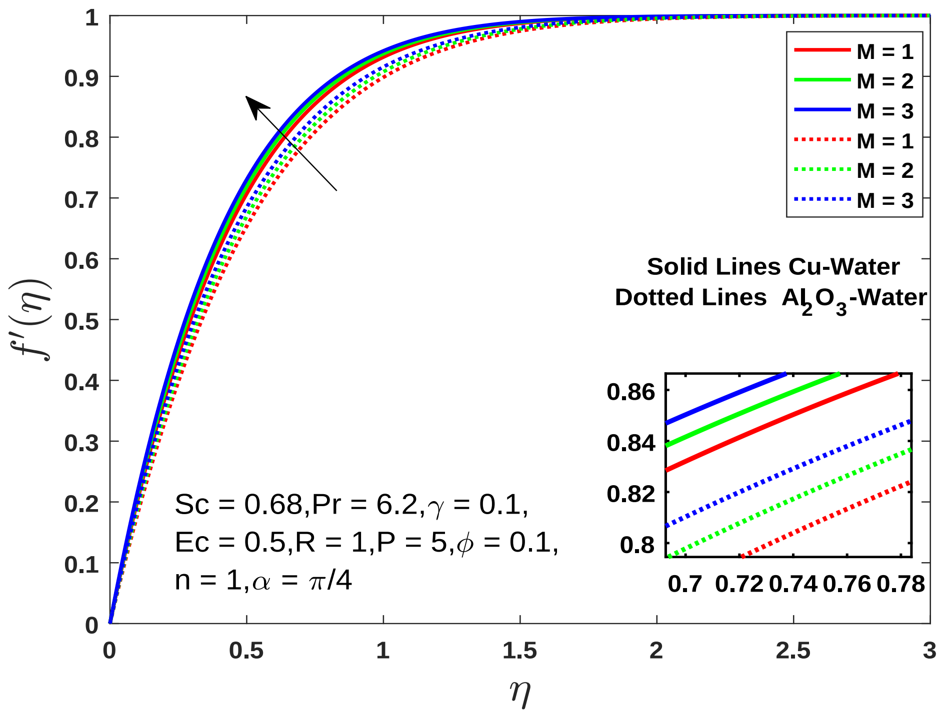

FIGURE 4.5: Impact of M on the dimensionless velocity f'

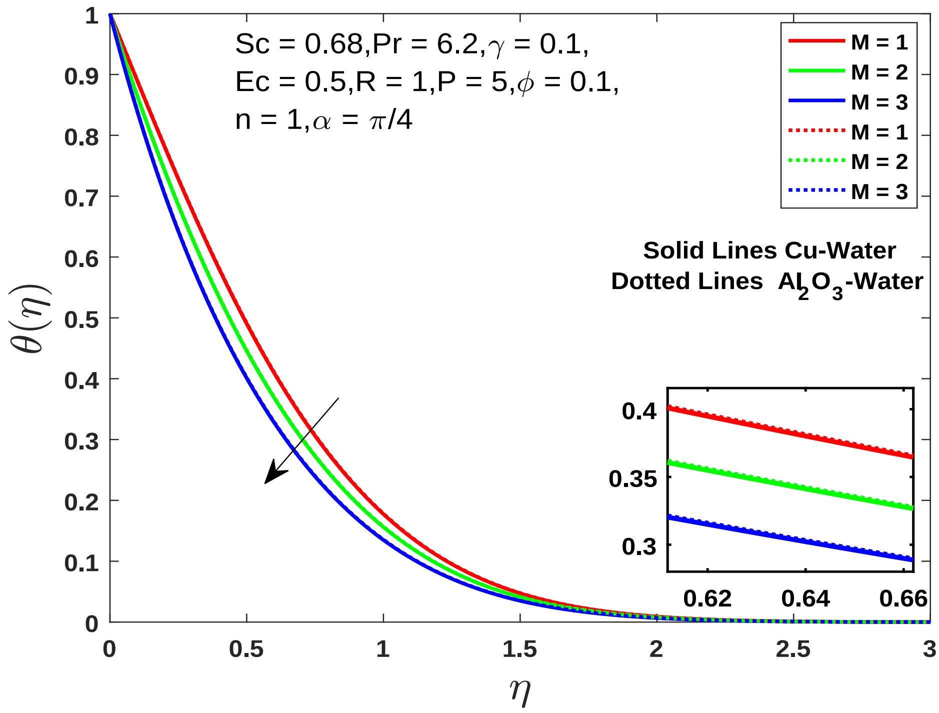

FIGURE 4.6: Impact of M on the dimensionless temperature θ

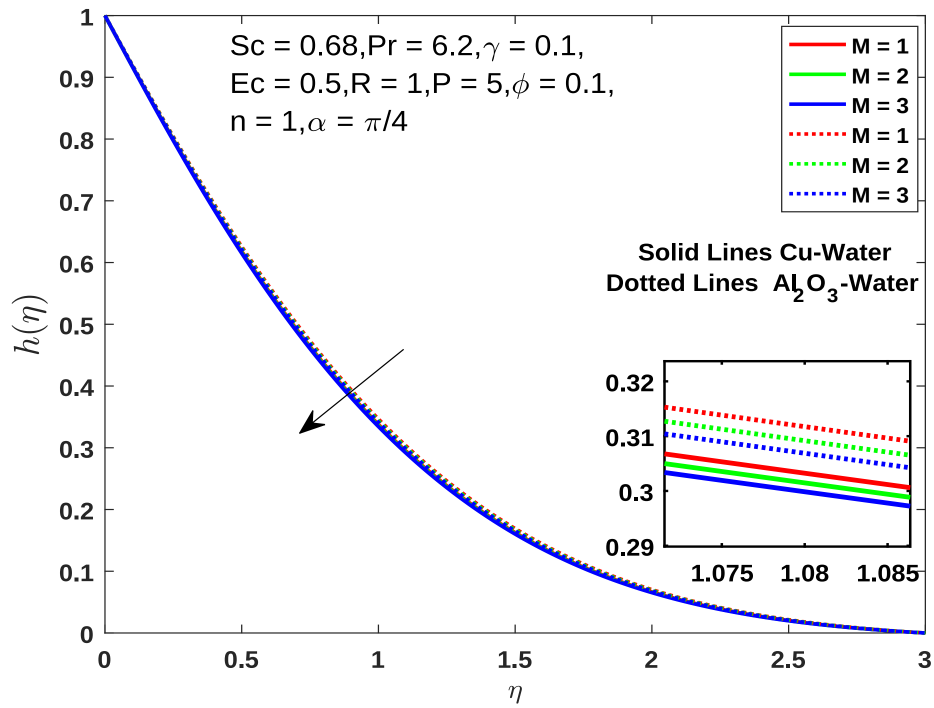

FIGURE 4.7: Impact of M on the dimensionless concentration h

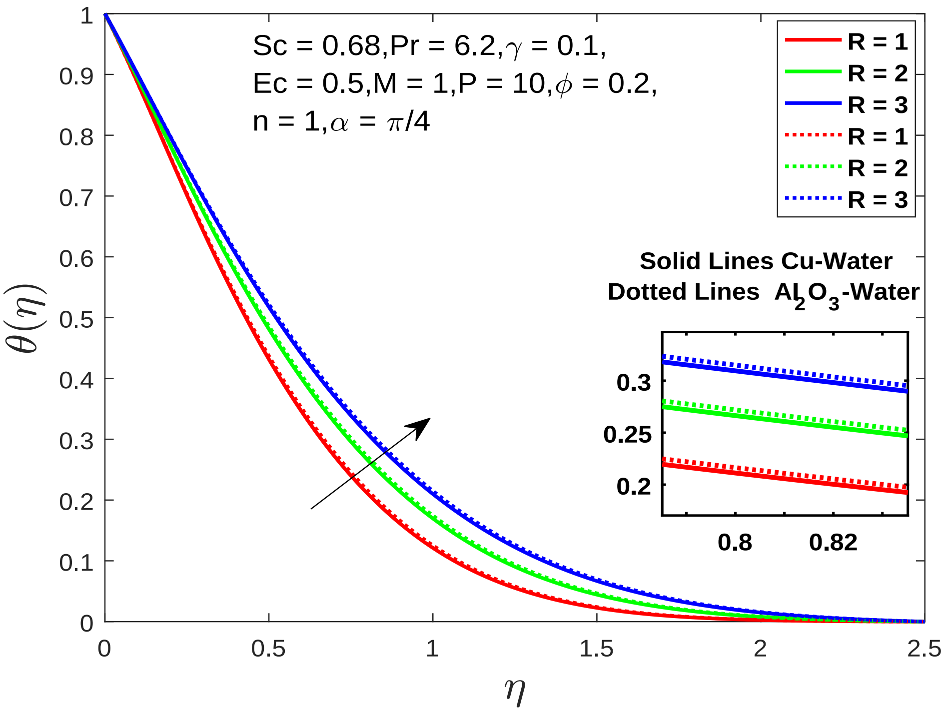

FIGURE 4.8: Impact of R on the dimensionless temperature θ

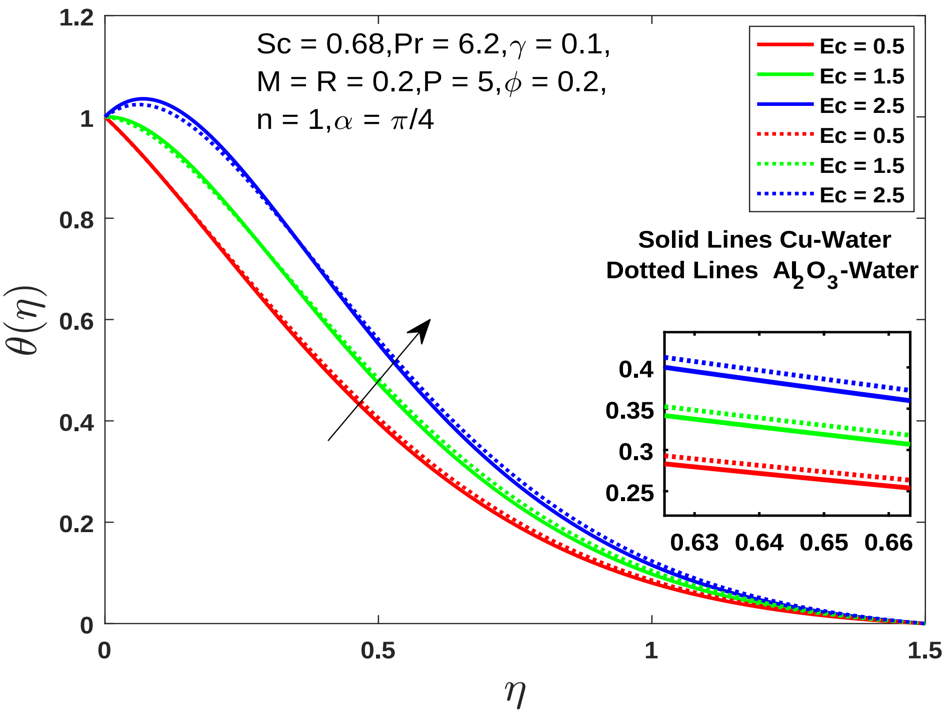

FIGURE 4.9: Impact of Ec on the dimensionless temperature θ

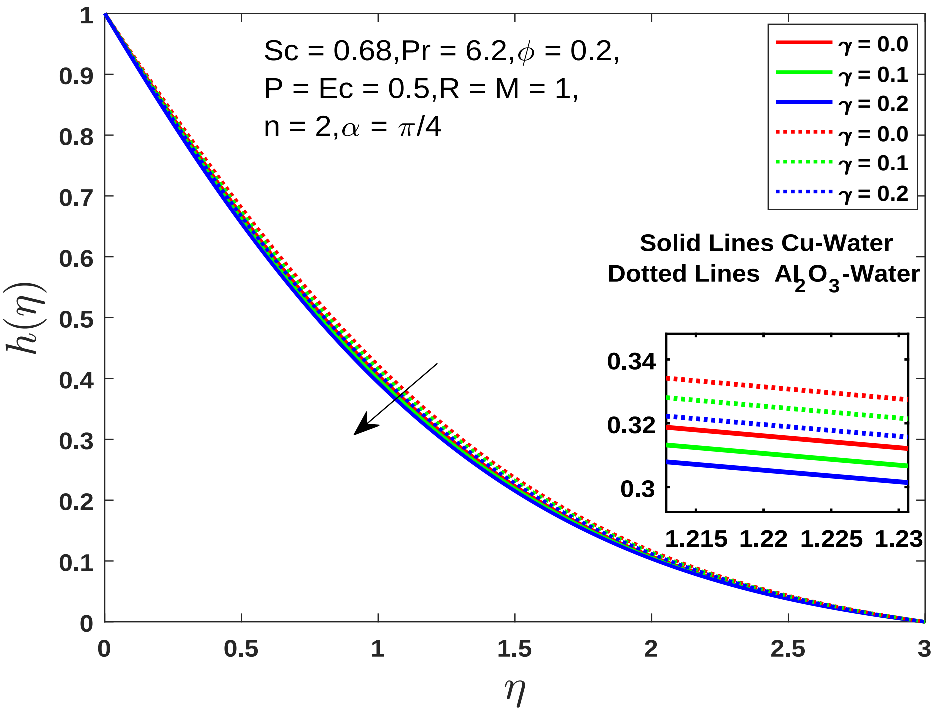

FIGURE 4.10: Impact of γ on the dimensionless concentration h

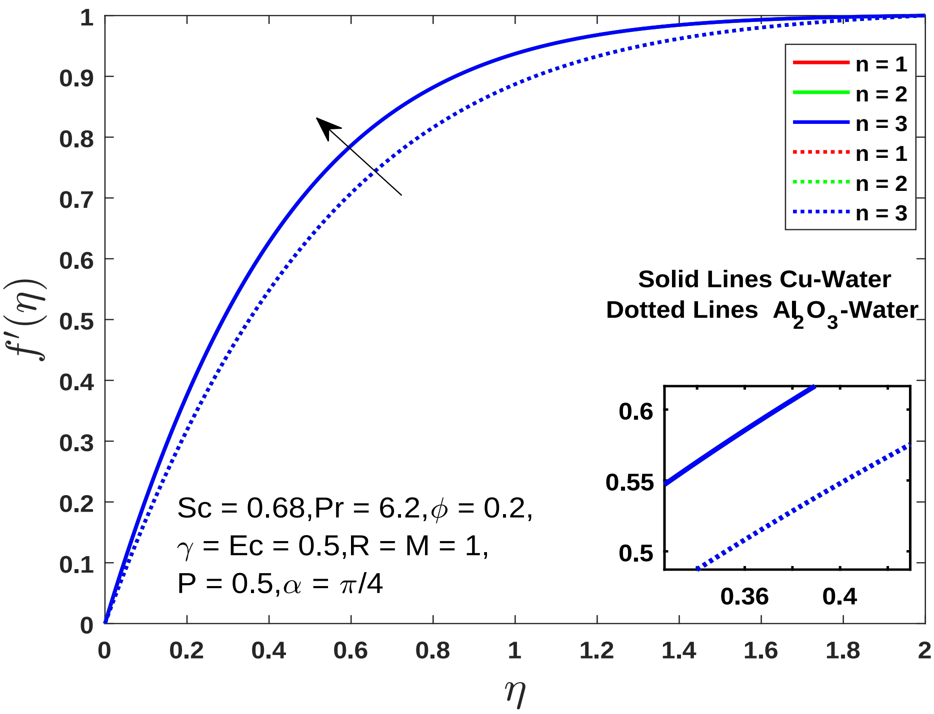

FIGURE 4.11: Impact of n on the dimensionless velocity f'

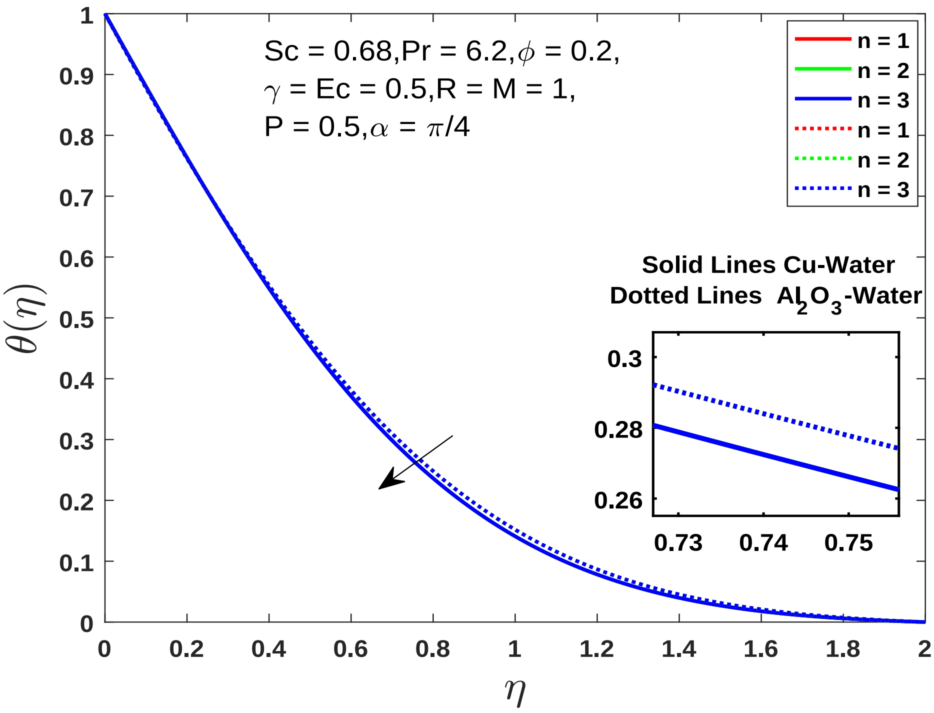

FIGURE 4.12: Impact of n on the dimensionless temperature θ

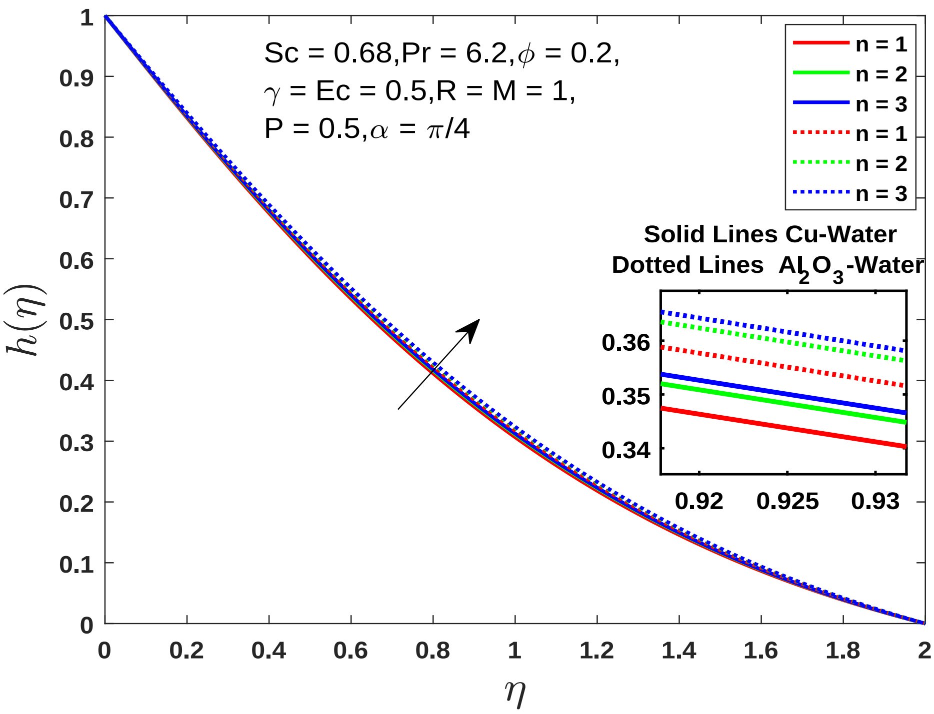

FIGURE 4.13: Impact of n on the dimensionless concentration h

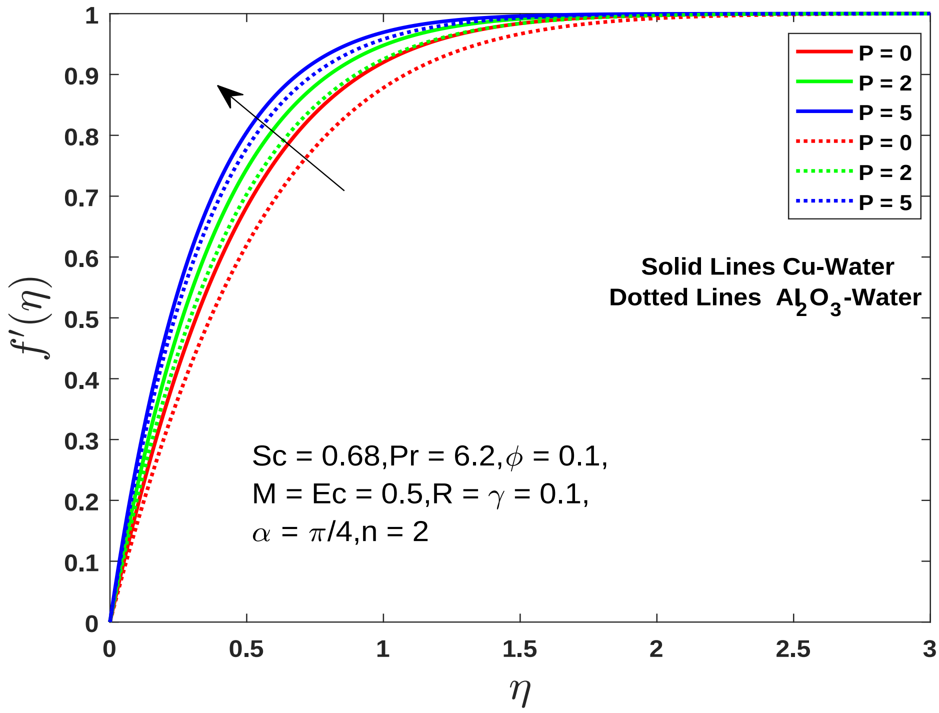

FIGURE 4.14: Impact of P on the dimensionless velocity f'

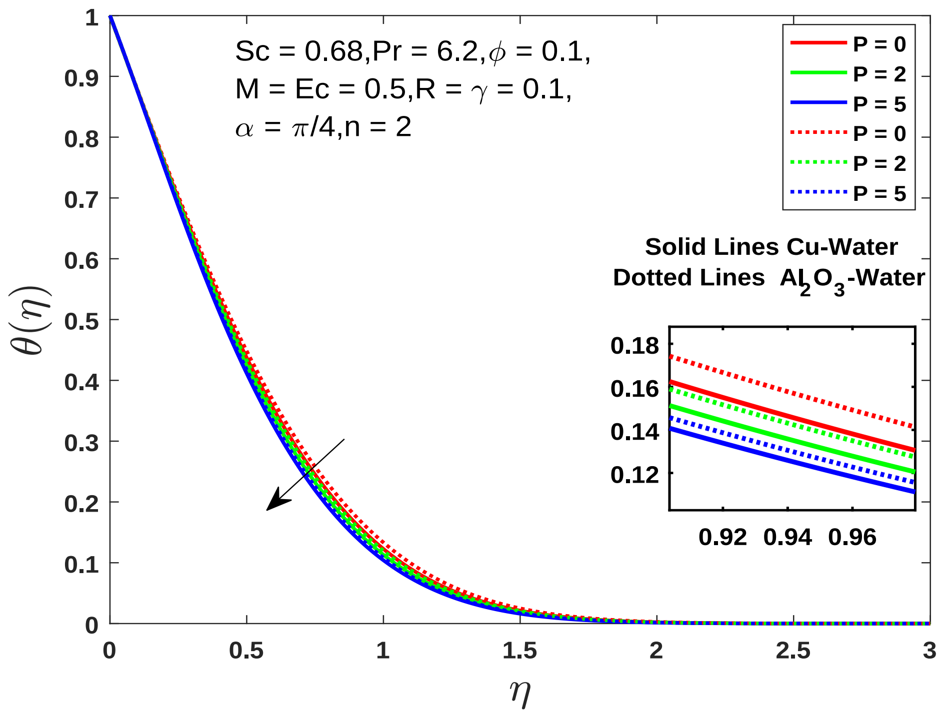

FIGURE 4.15: Impact of P on the dimensionless temperature θ

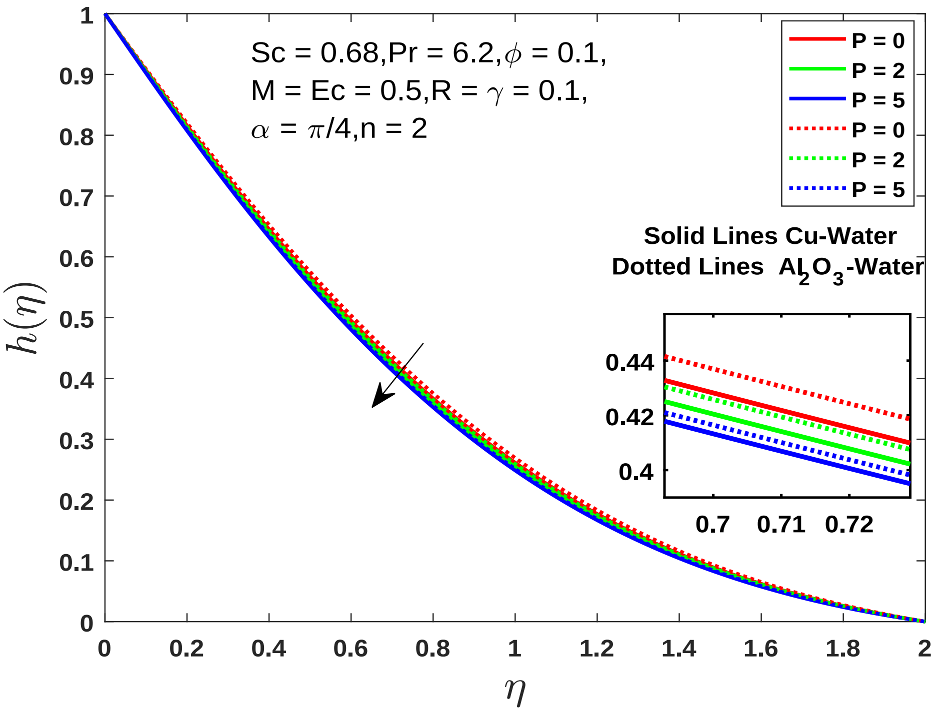

FIGURE 4.16: Impact of P on the dimensionless concentration h

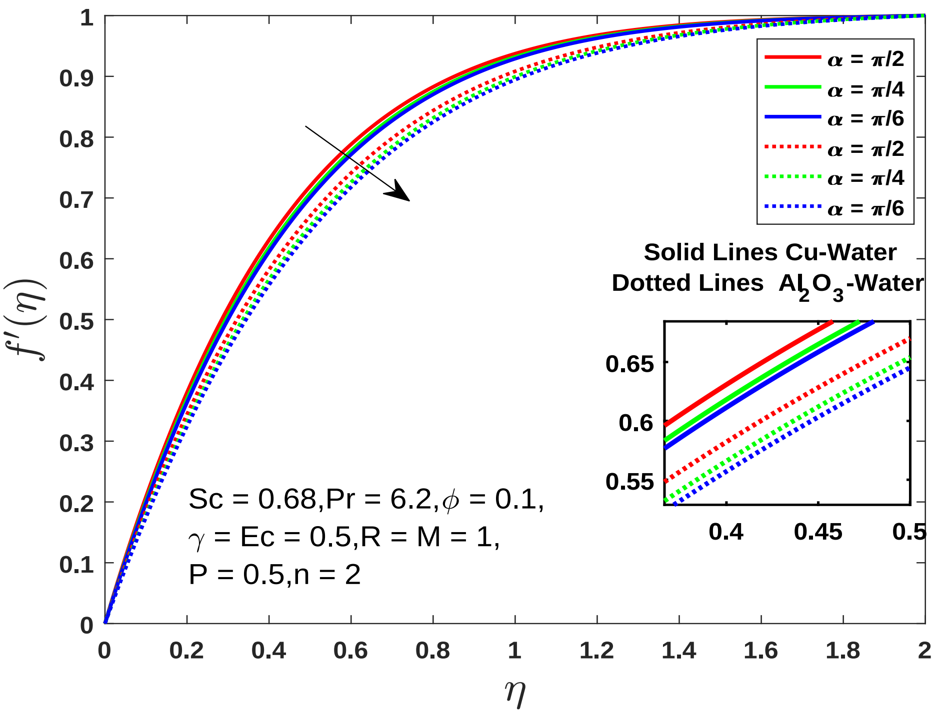

FIGURE 4.17: Impact of α on the dimensionless velocity f'

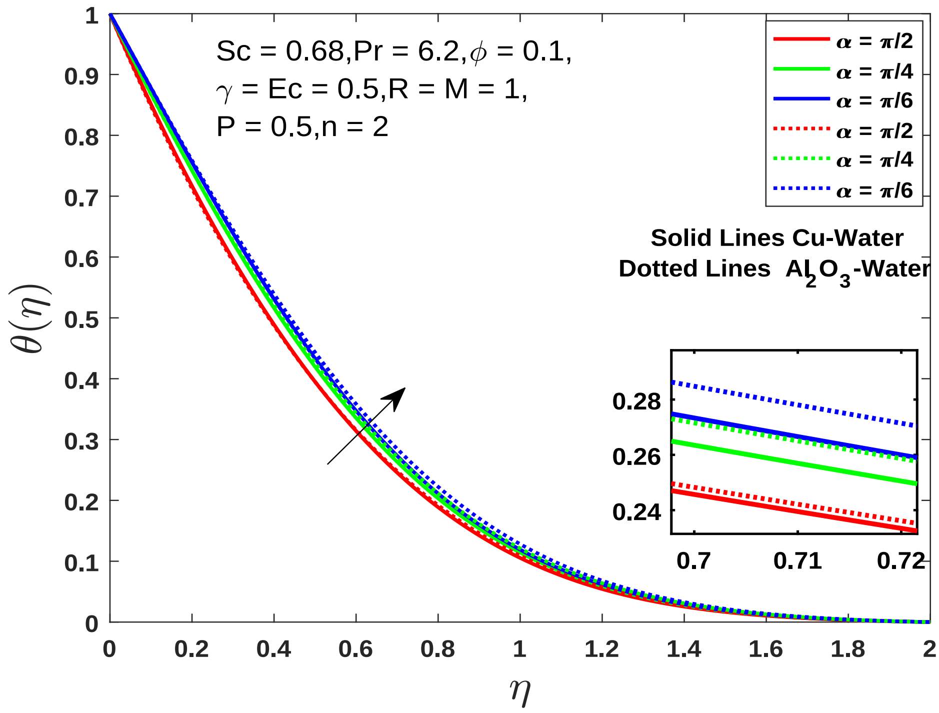

FIGURE 4.18: Impact of α on the dimensionless temperature θ

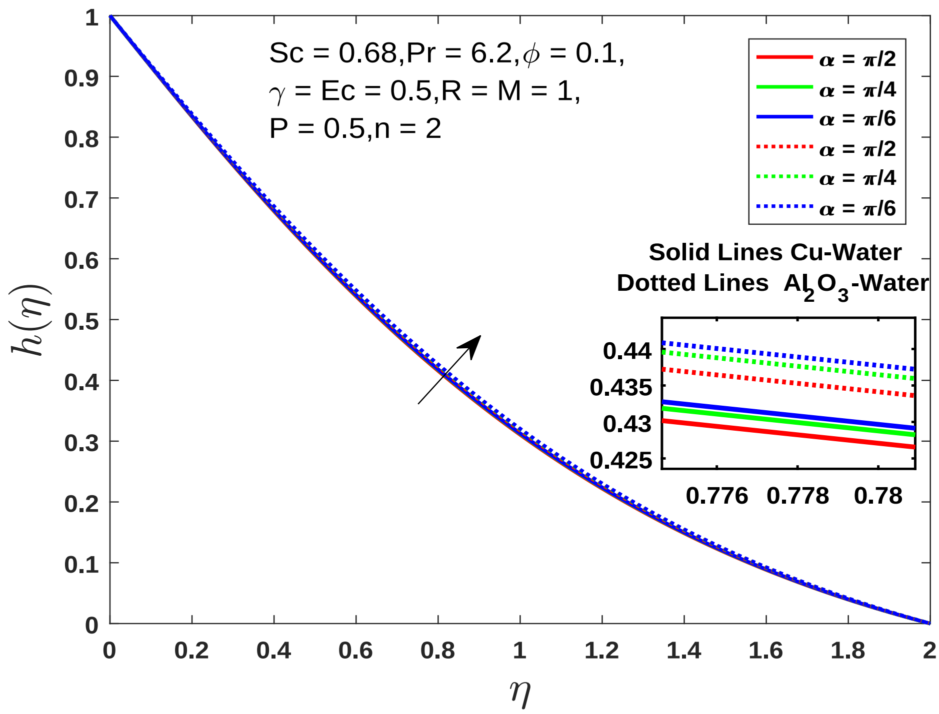

FIGURE 4.19: Impact of α on the dimensionless concentration h

Chapter 5

Conclusion

In this thesis, we reviewed the work of Mabood *et al.* [48] and extended with the effect of Joule heating and inclined magnetic field. First of all, momentum, energy and concentration equations are converted into the ODEs by using an appropriate transformation called similarity transformation. By using the shooting technique, numerical solution has been found for transformed ODEs. Using different values of governing physical parameters we presented the results in the form of tables and graphs for velocity, temperature and concentration profiles. Concluding all arguments and results we summarized our findings as follows:

- The volume fraction of nanoparticles decelerates the velocity for Al_2O_3–water nanofluid whereas an opposite trend has been observed for the Cu-water.
- The temperature escalates for both Cu-water and Al_2O_3–water whereas the concentration falls for Cu-water and climbs marginally for Al_2O_3–water for the larger values of the volume fraction of nanoparticles.
- The magnetic parameter increases the velocity whereas an opposite trend has been observed for the temperature and concentration profiles for both types of nanofluid Cu-water and Al_2O_3–water.
- The heat transfer rate escalates for the radiation paramter for both Cu-water and Al_2O_3–water.

- The Eckert number accelerates the temperature profile for both nanofluid Cu-water and Al_2O_3–water.
- The higher values of chemical reaction parameter escalates the concentration profiles.
- The temperature falls whereas the velocity and concentration escalates for the larger estimation of the higher order chemical reaction parameter n.
- The higher estimation of the permeability parameter escalates the velocity profile, but an opposite behaviour has been observed for the temperature and concentration profiles.
- The inclination angle α decelerates the velocity whereas an opposite trend has been observed for the temperature and concentration profiles.

Bibliography

[1] S. U. Choi and J. A. Eastman, "Enhancing thermal conductivity of fluids with nanoparticles," Argonne National Lab., IL (United States), Tech. Rep. 6, 1995.

[2] J. Buongiorno, "Convective transport in nanofluids," *Journal of heat transfer*, vol. 128, no. 3, pp. 240–250, 2006.

[3] M. Hashmi, N. Khan, T. Mahmood, and S. Shehzad, "Effect of magnetic field on mixed convection flow of Oldroyd-B nanofluid induced by two infinite isothermal stretching disks," *International Journal of Thermal Sciences*, vol. 111, pp. 463–474, 2017.

[4] I. Tlili, W. Khan, and I. Khan, "Multiple slips effects on MHD SA-Al_2O_3 and SA-Cu non-Newtonian nanofluids flow over a stretching cylinder in porous medium with radiation and chemical reaction," *Results in physics*, vol. 8, pp. 213–222, 2018.

[5] M. S. Anwar and A. Rasheed, "Simulations of a fractional rate type nanofluid flow with non-integer Caputo time derivatives," *Computers & Mathematics with Applications*, vol. 74, no. 10, pp. 2485–2502, 2017.

[6] T. Hayat, M. Rashid, and A. Alsaedi, "Three dimensional radiative flow of magnetite-nanofluid with homogeneous-heterogeneous reactions," *Results in physics*, vol. 8, pp. 268–275, 2018.

[7] M. Irfan, M. Khan, W. Khan, and M. Ayaz, "Modern development on the features of magnetic field and heat sink/source in Maxwell nanofluid subject

to convective heat transport," *Physics Letters A*, vol. 382, no. 30, pp. 1992–2002, 2018.

[8] T. Grosan, I. Pop, C. Revnic, and D. Ingham, "Magnetohydrodynamic oblique stagnation-point flow," *Meccanica*, vol. 44, no. 5, p. 565, 2009.

[9] F. Homann, "The influence of great toughness in the flow around the cylinder and around the ball," *ZAMM-Journal of Applied Mathematics and Mechanics*, vol. 16, no. 3, pp. 153–164, 1936.

[10] Y. Lok, A. Ishak, and I. Pop, "MHD stagnation-point flow towards a shrinking sheet," *International Journal of Numerical Methods for Heat & Fluid Flow*, 2011.

[11] J. Merkin and I. Pop, "Stagnation point flow past a stretching/shrinking sheet driven by Arrhenius kinetics," *Applied Mathematics and Computation*, vol. 337, pp. 583 – 590, 2018.

[12] P. Weidman, "Hiemenz stagnation-point flow impinging on a uniformly rotating plate," *European Journal of Mechanics - B/Fluids*, vol. 78, pp. 169 – 173, 2019.

[13] T. Mahapatra and S. Sidui, "Non-axisymmetric homann stagnation-point flow of a viscoelastic fluid towards a fixed plate," *European Journal of Mechanics - B/Fluids*, vol. 79, pp. 38 – 43, 2020.

[14] M. Ilbas, "The effect of thermal radiation and radiation models on hydrogen–hydrocarbon combustion modelling," *International Journal of Hydrogen Energy*, vol. 30, no. 10, pp. 1113 – 1126, 2005.

[15] M. Ghalambaz, M. Sabour, and I. Pop, "Free convection in a square cavity filled by a porous medium saturated by a nanofluid: Viscous dissipation and radiation effects," *Engineering Science and Technology, an International Journal*, vol. 19, no. 3, pp. 1244 – 1253, 2016.

[16] M. Sheikholeslami, T. Hayat, and A. Alsaedi, "On simulation of nanofluid radiation and natural convection in an enclosure with elliptical cylinders,"

International Journal of Heat and Mass Transfer, vol. 115, pp. 981 – 991, 2017.

[17] M. Waqas, M. I. Khan, T. Hayat, and A. Alsaedi, "Numerical simulation for magneto Carreau nanofluid model with thermal radiation: A revised model," *Computer Methods in Applied Mechanics and Engineering*, vol. 324, pp. 640 – 653, 2017.

[18] A. Chamkha, "Unsteady heat and mass transfer from a rotating vertical cone with a magnetic field and heat generation or absorption effects," *International Journal of Thermal Sciences*, vol. 44, pp. 267 – 276, 2005.

[19] D. Chatterjee, B. Mondal, and P. Halder, "Hydromagnetic mixed convective transport in a vertical lid-driven cavity including a heat conducting rotating circular cylinder," *Numerical Heat Transfer, Part A: Applications*, vol. 65, no. 1, pp. 48–65, 2014.

[20] U. Mahabaleshwar, I. Sarris, A. Hill, G. Lorenzini, and I. Pop, "An MHD couple stress fluid due to a perforated sheet undergoing linear stretching with heat transfer," *International Journal of Heat and Mass Transfer*, vol. 105, pp. 157 – 167, 2017.

[21] J. A. Khan and M. Mustafa, "A numerical analysis for non-linear radiation in MHD flow around a cylindrical surface with chemically reactive species," *Results in Physics*, vol. 8, pp. 963 – 970, 2018.

[22] M. Irfan, W. Khan, M. Khan, and M. M. Gulzar, "Influence of arrhenius activation energy in chemically reactive radiative flow of 3D Carreau nanofluid with nonlinear mixed convection," *Journal of Physics and Chemistry of Solids*, vol. 125, pp. 141 – 152, 2019.

[23] B. Mahanthesh, B. Gireesha, R. R. Gorla, F. Abbasi, and S. Shehzad, "Numerical solutions for magnetohydrodynamic flow of nanofluid over a bidirectional non-linear stretching surface with prescribed surface heat flux boundary," *Journal of Magnetism and Magnetic Materials*, vol. 417, pp. 189–196, 2016.

[24] Y. S. Daniel, Z. A. Aziz, Z. Ismail, and F. Salah, "Entropy analysis in electrical magnetohydrodynamic (MHD) flow of nanofluid with effects of thermal radiation, viscous dissipation, and chemical reaction," *Theoretical and Applied Mechanics Letters*, vol. 7, no. 4, pp. 235–242, 2017.

[25] K. Ramadan, "Effects of pressure work, viscous dissipation, shear work and axial conduction on convective heat transfer in a microtube," *Case Studies in Thermal Engineering*, vol. 10, pp. 370 – 381, 2017.

[26] S. Anjalidevi and R. Kandasamy, "Effects of chemical reaction, heat and mass transfer on laminar flow along a semi infinite horizontal plate," *Heat and Mass transfer*, vol. 35, no. 6, pp. 465–467, 1999.

[27] Y. Zhang and L. Zheng, "Analysis of MHD thermosolutal Marangoni convection with the heat generation and a first-order chemical reaction," *Chemical Engineering Science*, vol. 69, no. 1, pp. 449 – 455, 2012.

[28] K. Bhattacharyya and G. Layek, "Slip effect on diffusion of chemically reactive species in boundary layer flow over a vertical stretching sheet with suction or blowing," *Chemical Engineering Communications*, vol. 198, no. 11, pp. 1354–1365, 2011.

[29] F. Mabood, W. Khan, and A. Ismail, "MHD stagnation point flow and heat transfer impinging on stretching sheet with chemical reaction and transpiration," *Chemical Engineering Journal*, vol. 273, pp. 430 – 437, 2015.

[30] G. Swapna, L. Kumar, P. Rana, and B. Singh, "Finite element modeling of a double-diffusive mixed convection flow of a chemically-reacting magneto-micropolar fluid with convective boundary condition," *Journal of the Taiwan Institute of Chemical Engineers*, vol. 47, pp. 18 – 27, 2015.

[31] W. Khan, F. Sultan, M. Ali, M. Shahzad, M. Khan, and M. Irfan, "Consequences of activation energy and binary chemical reaction for 3D flow of Cross-nanofluid with radiative heat transfer," *Journal of the Brazilian Society of Mechanical Sciences and Engineering*, vol. 41, no. 1, p. 4, 2019.

[32] V. M. Starov and V. G. Zhdanov, "Effective viscosity and permeability of porous media," *Colloids and Surfaces A: Physicochemical and Engineering Aspects*, vol. 192, no. 1, pp. 363 – 375, 2001.

[33] F. Khani, A. Farmany, M. A. Raji, A. Aziz, and F. Samadi, "Analytic solution for heat transfer of a third grade viscoelastic fluid in non-Darcy porous media with thermophysical effects," *Communications in Nonlinear Science and Numerical Simulation*, vol. 14, no. 11, pp. 3867 – 3878, 2009.

[34] M. Kothandapani and J. Prakash, "Effect of radiation and magnetic field on peristaltic transport of nanofluids through a porous space in a tapered asymmetric channel," *Journal of Magnetism and Magnetic Materials*, vol. 378, pp. 152 – 163, 2015.

[35] M. G. Reddy, K. V. Reddy, and O. Makinde, "Hydromagnetic peristaltic motion of a reacting and radiating couple stress fluid in an inclined asymmetric channel filled with a porous medium," *Alexandria Engineering Journal*, vol. 55, no. 2, pp. 1841 – 1853, 2016.

[36] J. Lenz and S. Edelstein, "Magnetic sensors and their applications," *IEEE Sensors journal*, vol. 6, no. 3, pp. 631–649, 2006.

[37] L. Gilbert *et al.*, "One experiment, different uses: Floating magnetic bodies in peregrinus, norman and gilbert," *Journal of Early Modern Studies*, no. 1, pp. 81–103, 2013.

[38] N. Sandeep and V. Sugunamma, "Radiation and inclined magnetic field effects on unsteady hydromagnetic free convection flow past an impulsively moving vertical plate in a porous medium," *Journal of Applied Fluid Mechanics*, vol. 7, no. 2, pp. 275–286, 2014.

[39] A. J. Chamkha and R. A. Khaled, Abdul, "Similarity solutions for hydromagnetic simultaneous heat and mass transfer by natural convection from an inclined plate with internal heat generation or absorption," *Heat and Mass Transfer*, vol. 37, no. 2-3, pp. 117–123, 2001.

[40] K. Yih, "Uniform transpiration effect on coupled heat and mass transfer in mixed convection about inclined surfaces in porous media: the entire regime," *Acta Mechanica*, vol. 132, no. 1-4, pp. 229–240, 1999.

[41] M. Rahman, "Convective flows of micropolar fluids from radiate isothermal porous surfaces with viscous dissipation and Joule heating," *Communications in Nonlinear Science and Numerical Simulation*, vol. 14, no. 7, pp. 3018 – 3030, 2009.

[42] M. Sheikholeslami and D. Ganji, "Nanofluid hydrothermal behavior in existence of Lorentz forces considering Joule heating effect," *Journal of Molecular Liquids*, vol. 224, pp. 526 – 537, 2016.

[43] B. Mahanthesh, B. Gireesha, and R. S. R. Gorla, "Unsteady three-dimensional MHD flow of a nano Eyring-Powell fluid past a convectively heated stretching sheet in the presence of thermal radiation, viscous dissipation and Joule heating," *Journal of the Association of Arab Universities for Basic and Applied Sciences*, vol. 23, no. 1, pp. 75–84, 2017.

[44] M. I. Khan, M. Waqas, T. Hayat, and A. Alsaedi, "Chemically reactive flow of micropolar fluid accounting viscous dissipation and Joule heating," *Results in Physics*, vol. 7, pp. 3706 – 3715, 2017.

[45] O. D. Makinde, "MHD mixed-convection interaction with Thermal radiation and nth order Chemical reaction past a vertical porous plate embedded in a porous medium," *Chemical Engineering Communications*, vol. 198, no. 4, pp. 590–608, 2010.

[46] B. Van Den Bosch and D. Luss, "Uniqueness and multiplicity criteria for an nth order Chemical reaction," *Chemical Engineering Science*, vol. 32, no. 2, pp. 203–212, 1977.

[47] H.-C. Chang and J. M. Calo, "Exact criteria for uniqueness and multiplicity of an nth order Chemical reaction via a catastrophe theory approach," *Chemical Engineering Science*, vol. 34, no. 3, pp. 285–299, 1979.

[48] F. Mabood, S. Shateyi, M. Rashidi, E. Momoniat, and N. Freidoonimehr, "MHD stagnation point flow heat and mass transfer of nanofluids in porous medium with radiation, viscous dissipation and chemical reaction," *Advanced Powder Technology*, vol. 27, no. 2, pp. 742 – 749, 2016.

[49] F. M. White, *Fluid Mechanics Seventh Edition.* MC-Graw Hill, 2011.

[50] L. M. Jiji, *Heat Convection.* Springer, 2006.

[51] R. W. Fox, A. T.McDonald, and P. J.Pritchard, *Introduction to fluid mechanics sixth edition.* John Wiley & Sons,INC., 2003.

[52] Y. A.Cengel and J. M. Cimbala, *Fluid Mechanics.* McGraw Hill, 2006.

[53] S. Molokov, A. R. Moreau, and H. Moffatt, *Magnetohydrodynamics Historical Evolution and Trends.* Springer, 2007.

[54] F. Irgens, "Generalized newtonian fluids," in *Rheology and Non-Newtonian Fluids.* Springer, 2014, pp. 113–124.

[55] A. J. Smits, *A Physical Introduction to Fluid Mechanics.* A.J. Smits, 2019.

[56] R. Bansal, *A Textbook of Fluid Mechanics*, 1st ed. Firewall Media, 2005.

[57] P. M. Gerhart, A. L. Gerhart, and J. I. Hochstein, *Munson, Young and Okiishi's Fundamentals of Fluid Mechanics.* John Wiley & Sons, 2016.

[58] P. H. Oosthuizen and D. Naylor, *An introduction to convective heat transfer analysis.* MC-Graw Hill, 1999.

[59] J. N. Reddy and D. K. Gartling, *The Finite Element Method in Heat Transfer and Fluid Dynamics.* CRC Press, 2010.

[60] M. Pakdemirli, "The boundary layer equations of third-grade fluids," *International Journal of Non-Linear Mechanics*, vol. 27, no. 5, pp. 785–793, 1992.

[61] W. M. Rohsenow, J. P. Hartnett, Y. I. Cho *et al.*, *Handbook of heat transfer.* McGraw-Hill New York, 1998, vol. 3.

[62] A. Bejan, *Convection heat transfer.* John wiley & sons, 2013.

[63] T.Y.Na, *Computational methods in engineering boundary value problems.* Academic Press, 1979.

[64] N. C. Roşca and I. Pop, "Axisymmetric rotational stagnation point flow impinging radially a permeable stretching/shrinking surface in a nanofluid using tiwari and das model," *Scientific reports*, vol. 7, no. 1, pp. 1–11, 2017.